Prepared for:

ICF International
33 Hayden Avenue
Lexington, MA 02421

Results from Brine Discharge Modeling for the Proposed Strategic Petroleum Reserve Richton Expansion

Project 08–156 **Report** **3 June, 2009**

Prepared by:
Craig Swanson
Chris Galagan
Tatsu Isaji
David Stuebe
Yong Kim
Christin Reynolds
Lauren Decker

Applied Science Associates, Inc.
55 Village Square Drive
South Kingstown, RI 02879

science. services. solutions.

Executive Summary

The U.S. Department of Energy (DOE) is evaluating the development of new storage sites in the Gulf of Mexico region to increase the capacity of the Strategic Petroleum Reserve (SPR) under congressional directive. One of these sites is located at Richton, MS and is designed to store 160 million barrels of crude oil in underground caverns. The caverns are formed by controlled pumping of fresh water into salt domes to dissolve the salt. The byproduct of this process is a high salinity brine solution that is planned to be discharged in the Gulf of Mexico. Being of higher density than the surrounding Gulf water, the brine remains near the bottom as it dilutes with the ambient water in the vicinity of the discharge. A local area of higher salinity is created by this discharge which is ultimately transported away by ambient currents and further diluted.

The solution to the problem of determining the fate of high salinity discharges requires two modeling efforts, one to predict the currents in the area and a second to predict the transport of the brine as a result of the discharge itself and currents in the Gulf of Mexico. Currents were predicted from a previously applied and run hydrodynamic model of the area developed by the U.S. Army Corps of Engineers (USACE). The model output data were used in the second modeling effort. This effort consisted of two models – a near-field model to predict the local dynamics and initial dilution of the brine plume as it exited the discharge structure and a far-field model to predict the ultimate dilution as the plume was transported from the site by currents and density-driven flow.

A time series of velocity, salinity, and temperature fields from the USACE hydrodynamic model application was provided for this study by the USACE Engineer Research and Development Center (ERDC) so that both summer and winter hydrodynamic conditions could be utilized in the modeling. A time series of velocity, salinity, and temperature fields for the period 1 April through 30 September 1997 was used as input to define the summer conditions. A time series of velocity, salinity, and temperature fields for the period February 2001 was used to define the winter conditions for simulating the movement and dilution of the brine discharge.

The U.S. Environmental Protection Agency (USEPA) model UM3 (Visual Plumes model framework) was used to simulate discharge near field dynamics. Hydrodynamic data from the USACE/ERDC model were used as input for the UM3 modeling.

The ASA Lagrangian particle model was used to simulate the far-field transport of the discharge plume as it moved in response to ambient currents and differences in density between the discharge plume and surrounding water. The brine discharge plume transport case is more complex than a particle model calculation can perform because it does not account for the force of gravity acting on the density difference between the salty plume and the surrounding ocean, which pushes the dense fluid down slope into deeper water. The Lagrangian model was modified so that the motion of the plume responds to both ocean currents and density differences. The modified particle model was used to simulate plume dilution and movement away from the discharge using output from the USACE 3-dimensional (3-D) hydrodynamics model.

To assess the abilities of the models to predict the behavior of the brine plume, a data set developed from monitoring of a brine discharge from the Bryan Mound SPR facility in Freeport, Texas was used to compare with model predictions. Measurements of salinity at the active Bryan Mound discharge site during the 1980s provide horizontal and vertical dimensions of a brine discharge plume resulting from discharge rates similar to those proposed for the Richton site. Measurements of the vertical distribution of the brine plume collected directly over the

diffuser and at points surrounding the diffuser indicate that the excess salinity from the discharge extended up to 5.4 meters (17.7 feet) above the seafloor. The maximum excess salinity measured during the entire 1980–1981 monitoring period was 6.9 parts per thousand (ppt). The relatively low excess salinity maximums measured at Bryan Mound indicate that the brine is diluting rapidly at a short distance from the diffuser and/or that the vertical measurements never sampled the highest salinity portion of the discharge. Either way, the measurements indicate that excess salinities above 7 ppt exist within a small volume of water directly surrounding the diffuser.

There is generally good agreement between far-field model results and observation data from Bryan Mound. The area enclosed by the far-field model-predicted 2-ppt excess salinity contour compares well with the 2-ppt excess salinity contours defined from monitoring data collected on two separate dates in August 1981. The major axis of the 2-ppt excess salinity areas also compares well between the model prediction and the monitoring data at Bryan Mound.

The UM3 near-field model was run using a range of current speeds to simulate the near-field dynamics of the discharge plume at the Bryan Mound and Richton North and South discharge sites. Results of near-field modeling show that the discharge plume rises a few meters in the water column and then descends, making contact with the bottom within a few meters from the diffuser. UM3 predicts a rapid dilution (reduction of excess salinity) of approximately 85 percent of the 263-ppt concentration discharge within a few meters of the diffuser. The near-field model results suggest that salinity measurements taken at the Bryan Mound site were not of sufficient resolution to measure salinity in the brine jet.

Model simulations were run for the length of time simulated by the Curvilinear Hydrodynamics in 3-D (CH3D) model, which is sufficient time for the discharge plume simulations in the far-field model to demonstrate steady-state behavior. The summer model run was for 5 months, the winter simulation for 1 month.

The model predicts that at the Richton North discharge site the mean extent of the excess salinity for the 1- and 2-practical salinity unit (psu) concentrations will be 34.7 and 13.7 square kilometers (13.4 and 5.3 square miles) respectively. Using the 1-psu contour to define the footprint, the brine plumes from the north site are predicted to be narrow and long, typically 2 to 3 kilometers (1.2 to 1.9 miles) wide and between 10 and 15 kilometers (6.2 and 9.3 miles) long. The extent of the 2-psu contours is typically 1 to 1.2 kilometers (0.6 to 0.74 mile) wide and between 5.4 and 28 kilometers (3.4 and 17.4 miles) long. The major direction of plume dispersion is toward the south or southwest for most of the simulation period. Discharge plume vertical thickness at the Richton North site averages 5 meters (16 feet) with a maximum of 10 meters (33 feet). Figure 4.2.2-7 shows the plan view of the discharge plume during the winter simulation period (mid-February). The brine plume dispersion during the winter is similar to that during the summer period, which implies that the seasonal effect is minimal.

The model predicts that at the Richton South discharge site the mean extent of the excess salinity for 1- and 2-psu concentrations will be 18.9 and 7.6 square kilometers (7.3 and 2.9 square miles), respectively, which is 45 percent smaller than that predicted at the north site. Using the 1-psu contour to define the footprint, the brine plumes from the Richton South site are predicted to be smaller compared to those of the Richton North site, typically 2 to 3 kilometers (1.2 to 1.9 miles) wide and between 5 and 10 kilometers (6.2 and 9.3 miles) long. The major direction of plume dispersion is toward the south for the period when the shape of the contour is elongate. Discharge plume vertical thickness at the Richton South site averages 5 meters (16 feet) and has a maximum of 10 meters (33 feet), which is similar to the north site. The brine

plume dispersion during the winter is similar to that during the summer period, which implies that the seasonal effect is minimal.

The small variability in the flow direction of the plume to the west and south is a response to the general northwest-southeast flowing tidal currents, but the model shows that the plume generally flows down slope, perpendicular to the depth contours, into deeper water.

Table of Contents

List of Figures

List of Tables

List of Acronyms

3-D	three-dimensional
CH3D	Curvilinear Hydrodynamics in 3-D
DOE	U.S. Department of Energy
ERDC	Engineer Research and Development Center
NOAA	National Oceanic and Atmospheric Administration
NOS	National Ocean Service
ODE	ordinary differential equation
ppt	parts per thousand
psu	practical salinity unit
SPR	Strategic Petroleum Reserve
USACE	U.S. Army Corps of Engineers
USEPA	U.S. Environmental Protection Agency

1.0 Introduction

The U.S. Department of Energy (DOE) is evaluating the development of new storage sites in the Gulf of Mexico region to increase the capacity of the Strategic Petroleum Reserve (SPR) under congressional directive. One of these sites is located at Richton, MS and is designed to store 160 million barrels of petroleum (crude oil) in underground caverns (DOE, 2006). The caverns are formed by controlled pumping of fresh water into salt domes to dissolve the salt. The byproduct of this process is a high salinity brine solution that is planned to be discharged in the Gulf of Mexico. Being of higher density than the surrounding Gulf water, the brine remains near the bottom and moves down slope as it dilutes with the ambient water. The dense plume is also transported away by ambient currents and further diluted.

A Final Environmental Impact Statement was prepared (DOE, 2006) that evaluated the Richton site. Comments were received about the potential environmental effects, particularly on the Mississippi Sound, landward of the proposed discharge site, among other issues. In response, DOE contracted with ICF International (ICF) to prepare a Supplemental EIS for the proposed project. ICF in turn contracted with Applied Science Associates, Inc. (ASA) to analyze the fate and transport of the discharged brine in the Gulf. This report discusses the methods and results of computer modeling used to perform this analysis.

The solution to the problem of determining the transport fate of high salinity discharges requires two modeling efforts, one to predict the currents in the area and a second to predict the transport of the brine as a result of the currents. Currents were predicted from a previously applied and run hydrodynamic model of the area developed by the U.S. Army Corps of Engineers (USACE) (Bunch et al., 2005). The model output data were used as input in the second modeling effort. This effort consisted of two models – a near-field model to predict the local dynamics and initial dilution of the brine plume as it exited the discharge structure, and a far-field model to predict the ultimate dilution as the plume was transported from the site.

The report is divided into sections that document the study performed by ASA. Section 1 provides an introduction while Section 2 describes each of the model systems used in the analysis. Section 3 presents descriptions of the models applied and the results from a field monitoring study of an existing brine discharge off the Texas coast with characteristics similar to those proposed at the Richton site. The model results are presented and discussed in Section 4. Section 5 contains the conclusions draw from the modeling study. Attachment A to this report contains a detailed discussion of an enhanced velocity formulation implemented in the Lagrangian particle model applied to estimate the transport and dilution of the brine discharge. The results from a series of model sensitivity simulations using ambient flow without gravity-enhanced flow at the Richton North site are presented in Attachment B.

2.0 Description of Models

This section of the report describes the models used to analyze the fate of the brine discharge. A number of models were used in the analysis:

- A hydrodynamic model previously applied to Mississippi Sound and the surrounding region by the USACE was used to define the circulation.
- The UM3 model from the U.S. Environmental Protection Agency (USEPA) was used to determine the near-field dynamics of the brine discharge plume.

- A Lagrangian particle model was used to simulate the far-field movement of the brine discharge.

2.1 Hydrodynamic Model

The three-dimensional (3-D) baroclinic hydrodynamic model used to supply currents for the brine discharge modeling was originally developed by the USACE for the area surrounding and including Mississippi Sound to support a proposed project to deepen the channels and port area of Pascagoula, MS (Bunch, et al., 2003). A description of the model is repeated here from the Bunch et al. (2003) report:

> …the sigma-stretched version of Curvilinear Hydrodynamics in 3-D model (CH3D) was applied. The goal of the modeling work was to represent 3-D hydrodynamics, temperature, and salinity during a period of poor water quality for evaluating the effects of three alternatives for placement of dredged material islands.
>
> CH3D was developed by Sheng (1986), but has been modified to implement different basic numerical formulations of the governing equations and to provide more efficient computing. A description of modifications to the model is provided in Chapman, Johnson, and Vemulakonda (1996). Physical processes impacting circulation and vertical mixing that are modeled include tides, wind, density effects (salinity and temperature), freshwater inflows, turbulence, and the effect of the earth's rotation.
>
> The boundary-fitted coordinate feature of the model provides grid resolution enhancement necessary to adequately represent deep navigation channels and irregular shoreline configurations of the flow system, important factors for the present study. The curvilinear grid also permits adoption of accurate and external mode, consisting of vertically averaged equations, which provides a solution for the free surface displacement for input to the internal mode, which contains the full 3-D equations.

Bunch et al. (2003) describe the model application and data on currents and waves that were collected as part of this study, and the model calibration to field data for the periods February to March 2001 and April through September in 1997. Section 3.2.2 contains additional discussion of the application of the CH3D hydrodynamic model for use in simulating the transport of the brine discharge.

2.2 Near Field Discharge Model

A near-field model simulates the movement of the brine plume based on the dynamics of the discharge itself. Output from a near-field model provides an estimate of the evolving dimensions of the brine jet as it exits the diffuser port, rises into the water column, descends back down, and encounters the bottom. The near-field model also calculates the dilution achieved within the near-field area, typically a few meters to tens of meters from the discharge device. In the near-field, the effluent discharged through nozzles or diffuser ports is dominated by both the momentum of the discharge flow and by buoyancy forces resulting from the difference in density between the discharge and the surrounding water.

The first phase of the discharge stream (initial jet) is primarily driven by the momentum of the fluid exiting the diffuser port. As the fluid moves away from the port, it loses momentum and its

motion becomes dominated by buoyancy forces which are positive if the discharge is less dense than surrounding water or negative if the discharge is denser (as is the case here) than surrounding water. Characteristics of the receiving fluid, such as its density and stratification, as well as ambient currents, further affect the shape and dimensions of the discharge jet as it traverses the water column and entrains ambient fluid, aiding dilution.

The USEPA model UM3 (Visual Plumes model framework) (Frick et al., 2003) is a near field model based on the UM model described by Baumgartner, et al. (1994). Visual Plumes is a model framework containing several models for simulating discharges in fresh and marine waters. For negatively buoyant plumes such as a brine discharge, the UM3 model is appropriate for calculating initial dilution and near-field discharge jet dimensions.

UM3 is a 3-D Lagrangian entrainment model which solves the equations for conservation of mass, momentum, and energy at a series of simulation time steps as the discharge rises and falls in the water column. The UM3 model uses the projected area entrainment hypothesis to calculate dilution of the discharge plume by the forced entrainment of ambient water. The UM3 model is well suited for dense brine discharges because it is not constrained by the Boussinesq approximations and can simulate negatively buoyant flows (Baumgartner et al., 1994).

UM3 requires the definition of the diffuser geometry used to discharge the fluid, the discharge characteristics, and the ambient current, temperature, and salinity conditions. Model output defines the discharge plume centerline, the plume diameter, and the discharge dilution along the centerline.

2.3 Far Field Brine Transport Model

The far-field model simulates the flow of the discharge plume as it spreads in response to ambient currents and differences in density between the brine plume and surrounding water. A Lagrangian particle model is used in the far-field simulation of plume dilution and movement. The model predicts the movement of particles which, in aggregate, represent the plume. The Lagrangian particle velocity is calculated using a combination of ambient currents (from either hydrodynamic model results or observations) and a parameterization of the behavior of the dense brine plume. The hydrodynamic model used is the USACE CH3D model described in Section 2.1. The enhanced velocity parameterization is described in the following sections. The resulting plume motion is the linear combination of the background (ambient) flow field and the gravity-enhanced flow resulting from the brine plume.

Many physical, chemical, and biological processes can be accurately modeled using a Lagrangian-based particle approach where each particle represents some chemical or biological constituent that is advected and dispersed in response to various physical processes. ASA originally applied this approach to the simulation of oil spills (Spaulding et al., 1993; Spaulding et al., 1994) and subsequently to spills and the resultant biological effects (French McCay, 2003). It was also applied to transport and fate of sewage sludge from offshore dumping (Isaji et al., 1996), produced water discharged from offshore platforms (Burns et al., 1999), and to search and rescue (Spaulding and Howlett, 1996).

The basic concept of a Lagrangian particle model is to simulate the transport and fate of some material released into the environment using a series of particles that are advected (transported) by the ambient currents and dispersed by turbulent mixing. For this application, the discharge is represented by a number of particles, each of which initially represents an equal fraction of the salt mass discharged. Particles are advected in response to currents with random turbulent dispersion superimposed. Advection and diffusion are physical processes

which move and diffuse mass from one location to another. The advection process is modeled using a Lagrangian formulation. The diffusion process is modeled using a random walk formulation.

The dense brine plume is not a passive tracer responding to the ambient currents. The dissolved salt in the plume significantly increases the density of the plume relative to ambient ocean water. This plume cannot be adequately simulated by the advection and diffusion processes alone. The density difference between the discharge and the ambient waters will exert forces on the discharged brine, which tend to reduce the potential energy of the system. These baroclinic forces (due to sloping pressure surfaces) reduce the potential energy by lowering the center of mass of the water column. Just as water on land seeks the lowest level, the brine discharge will flow down slope displacing less dense ambient fluid. This enhanced velocity effect of the dense brine plume must be accounted for to adequately simulate the advection of the plume. Thus the modeling approach applied here is a combination of the advection and diffusion processes of the basic Lagrangian particle model to which we have added the enhanced velocity effects of the baroclinic flow, both of which are described below.

The brine discharge problem is well suited to a Lagrangian approach. The exact mass conservation and scalable resolution of the particles in the plume make the Lagrangian approach ideal. In the Lagrangian model the total mass of salt is exactly conserved because it is represented by an integer number of particles of known mass. In an Eulerian model of the plume, the bottom boundary condition requires no normal flux of salt, but the numerical method may introduce mass conservation errors due to the strong gradients normal to the bottom that exist in the plume. By adjusting the number of particles released in the Lagrangian model, the numerical resolution of the plume can be increased very efficiently (linear computation time). However, in an Eulerian gridded model, increasing the grid resolution dramatically increases computer time (generally, doubling the horizontal grid resolution increases the computer time by a factor of 8). The details of the dynamics applied to the Lagrangian model for the brine discharge flow are developed in the next four sections.

2.3.1 Lagrangian Particle Model

The advection and diffusion of the Lagrangian particles in the ambient current field is solved using a time stepping method. The position of a particle at time n+1 is equal to its location at the present time step, n, plus the change in position in one time step due to advection and dispersion:

$$X^{n+1} = X^{n} + \Delta X$$

$$Y^{n+1} = Y^{n} + \Delta Y$$

$$Z^{n+1} = Z^{n} + \Delta Z$$

where

$$\Delta X = U\Delta T + L_x$$

$$\Delta Y = V\Delta T + L_y$$

$$\Delta Z = W\Delta T + L_z$$

where

X, Y, Z = location of particle in the horizontal (x, y) and vertical (z) directions, respectively.

U, V, W = ambient plus enhanced velocity in the horizontal (x, y) and vertical (z) directions, respectively. U,V,W are functions of space and time.

ΔT = time step

L_x, L_y, L_z = particle diffusion distances in the horizontal (x, y) and vertical (z) directions, respectively.

Particle diffusion is assumed to follow a simple random walk process. A diffusion distance, defined as the square root of the product of an input diffusion coefficient and the time step, is decomposed into X and Y displacements via a random direction function. The Z diffusion distance is scaled by a random positive or negative direction. The equations for the horizontal and vertical diffusion displacements are written as:

$$L_x = \sqrt{cD_h\Delta \mathrm{T}} \quad 0.5 - R$$

$$L_y = \sqrt{c\,D_h\Delta T} \quad 0.5 - R$$

$$L_z = \sqrt{c\,D_v\Delta T} \quad 0.5 - R$$

where

D_{xx}, D_{zz} = horizontal and vertical diffusion coefficients, respectively.

R = random real number between 0 and 1.

c = 2 or 6 for normal or uniform random number distribution, respectively.

The vertical diffusivity D_v is determined from the characteristics of the flow. The critical parameter that characterizes the stability of the plume interface is the Richardson number. Large density gradients tend to reduce the mixing and large current shear tends to increase the mixing.

$$Ri = \frac{-g}{\rho}\left(\frac{\frac{\partial \rho}{\partial z}}{\frac{\partial u^2}{\partial z}}\right)$$

where

g = acceleration due to gravity.

ρ = density.

u = horizontal velocity.

The density is calculated from the plume's salinity distribution described below. The ratio of the terms in the Richardson number expresses the stability of the plume interface due to stratification (density gradient) versus the instability due to shear (velocity gradient). Small

Richardson number flows (less the ¼) are considered super critical and highly unstable resulting in large diffusivities. Values greater than 1 represent subcritical flow where the interface is very stable and diffusion is retarded. The formula used in the model (Munk and Anderson, 1948) to calculate diffusivity is as follows:

$$D_{zz} = D_0(1.0 + 3.33Ri)^{-3/2}$$

where

D_0 = 10, the maximum diffusivity.

The sensitivity of the model results to the use of this formulation will be examined in Chapter 4. There is a detailed discussion on the use of the diffusivity and its role in the plume dynamics in Section 2.3.4.

All of the plume characteristics are calculated from the Lagrangian particles on a fixed square grid covering the model domain. The Lagrangian model and the enhanced velocity calculation require the plume salinity (density) and plume thickness be calculated at a fine resolution for each time step in the model. The bottom slope, also needed for the enhanced velocity, is also calculated on the same fixed grid from National Ocean Service (NOS) bathymetry data (Divins and Metzger, 2009)

In order to determine the salinity of the plume from the particle distribution, a 3-D square grid is overlain on the model domain and the concentration is calculated in each grid cell. The salinity of each cell is determined from the mass of salt, represented by the sum of the number of particles in the cell (each with equal salt mass) divided by the cell volume. This excess salinity is added to the background ambient salinity in the model. The calculation is repeated for all grid cells at each time step and the resulting spatial salinity distribution is used to calculate the density, stratification, and Richardson number.

The thickness of the plume is calculated from the vertical distribution of particles in each vertical column of grid cells. Taking the mean position of the particles in the water column, the distance between the bottom and the mean is doubled to get the thickness. Where this value is greater than the water depth, the plume thickness is set equal to the water depth.

The Lagrangian particle-based approach is robust and independent of an Eulerian approach, which is dependent on grid resolution. In contrast to an Eulerian approach, the Lagrangian method is not subject to artificial diffusion near sharp concentration gradients and retains exact mass conservation. The linear method of the Lagrangian model permits the superposition of multiple influences on the motion of the particles. The combination of advection and diffusion is a well accepted example. In biological models, the particles which may represent groups of living organisms are often given a behavior which is added in linear superposition to the ambient currents. To model the brine discharge, we have added an additional velocity to the particle motion based on a diagnostic equation for the velocity of the plume as a function of local parameters.

2.3.2 Dynamics of Dense Plumes

The motion of dense plumes in a fluid medium is a persistently challenging problem in fluid dynamics. There are many terms in the Navier-Stokes (fluid momentum) equations each of which represent physical processes that play a role in the evolution of a dense plume. Through insight about the relative size of these terms under different circumstances, the dynamics of a particular problem can be simplified. The importance of each term in the solution depends on

the parameters of the flow. Dynamics which may be very important over short distances, a few centimeters (inches), can be neglected or simplified over several kilometers (miles) where the balance of forces may be different. The length scale is just one factor which must be considered. The speed of the flow may also dramatically change the dynamics of its motion. Forces which are critical at low speeds may no longer be the dominant terms when the flow speed increases. Correctly identifying the forces which control the motion of the brine plume allows the intractable dynamics of the momentum equations to be simplified but accurately model the particulars of the specific problem. All numerical ocean models, Eulerian and Lagrangian, require assumptions of this kind, based on scientific insight about the dynamics of the problem. The discussion in this section focuses on the enhanced gravity flow velocity developed by ASA for the brine discharge model. Attachment A presents the details of the derivation of the equations used while the discussion here reviews the relevant scientific literature concerning dense bottom plumes.

The model of dense brine discharge from an oceanic bottom diffuser, developed by ASA, started from a rich literature of models and analysis from other dense plume studies. Determining which of these is most applicable was a critical step in the analysis. Starting from Randall's previous observations of the brine discharge at Bryan Mound (Hann and Randall, 1982), key characteristics of the flow were identified. The brine plume was observed to form a layer on the bottom a few meters (feet) thick. The water column remained highly stratified in all the observed profiles. The lateral extent of the plume spread up to 3 kilometers (2 miles) from the discharge site. The direction of the plume reflected the integrated current history at the discharge site. Based on these characteristics, ASA reviewed the scientific literature on dense bottom plumes as a foundation to model the effects of baroclinic forces on the plume. Our Lagrangian model can predict the motion of a passive tracer discharge, but a model of the dense plume requires additional terms because the plume's density can drive flow as described in numerous scientific journal articles for example Ozgokmen et. al., 2002, Scully et. al., 2003.

In reviewing the literature, the bottom slope was identified by scaling analysis as an important term which drives bottom plumes over long distances. Parker et al., (1986) developed a vertically integrated set of equations for the dynamics of a dense plume in a rotated reference frame relative to the sloping bottom. While the bottom slope at the proposed Richton site is small, these equations are equally valid as the bottom slope goes to zero (with a flat bottom the un-rotated equations of motion are recovered). From Parker's analysis, it was clear that a wide range of dynamics is still possible. Depending on the conditions at the discharge, baroclinic forces due to either the bottom slope or the shape of the plume surface could force the plume. Parker's theory has been applied to both turbidity currents and dense overflows. Using scaling analysis, the relative importance of the terms in the equations and the dynamics of the plume are analyzed in Attachment A. The diagnostic equation for the enhanced velocity used in the Lagrangian model was developed through a combination of scaling analysis, numerical experiments, and review of papers on turbidity currents and dense overflows. These flows are discussed below.

Turbidity currents occur in the ocean where the load of suspended sediment in the water column is so large that the density is significantly higher than the surrounding water. These currents often occur where strong currents, breaking waves, or a river outflow create large, turbulently suspended sediment loads which can travel several kilometers (miles) due to the baroclinic forces acting on the dense plume. Wright (1985) and Wright et al. (2001) identify many instances where turbulent gravity currents have been observed. Turbidity currents have a complex interaction with the sea floor below and the ambient water above. To keep sediment in suspension, the turbidity current must move fast and remain highly turbulent within the plume to

counteract the sinking rate of the sediment particles. The plume can accelerate if the turbulence is strong enough to resuspend sediment as it passes over the sea floor. However, the more turbulent the plume is the more energy is lost to bottom drag, which slows the plume. The entrainment of ambient water from above is another consideration, which also depends on the speed of the current and the strength of the turbulence in the plume. The basic equations for the momentum of the plume described by Parker et al. (1986) still apply to these complex systems. It is the boundary conditions and conservation equations for the mass of sediment that become complex when considering the turbidity currents.

Dense overflows are a critical area of study in physical oceanography. Much of the water mass in the ocean interior originated in high latitude marginal seas (Cenedese et al., 2004; Ozgokmen et al., 2002). The cold, salty water which forms there at the sea surface sinks to the bottom and fills the marginal sea until it overflows into the deeper ocean basin. The overflow passes over the lowest sill (a pass between underwater mountains) of the marginal sea and down the slope into the deep ocean basins to form the water which occupies most of the ocean interior. These dense overflow plumes may travel hundreds of kilometers (miles) as they move down the slope into the deep ocean slowly entraining ocean water as they go. In spite of the entrainment, the net buoyancy forcing is fixed at the sill as the water leaves the marginal sea. There is no other source or sink for density as the flow moves down slope. Entrainment of ambient water into the plume reduces the average density but also makes it proportionally thicker. There is no change in the density anomaly integrated over the plume thickness. The dense overflow plume shares this trait with the brine discharge plume where the forcing is set at the discharge diffuser.

The single source of buoyancy forcing for the brine discharge plume greatly simplifies the dynamics of the plume relative to studies of turbidity currents. The highly turbulent turbidity currents which can accelerate as they go are much more complex than the brine plume problem. The interaction with the upper boundary and entrainment of overlying fluid in the brine discharge is dynamically less complicated. There is still a critical value for the speed of the plume above which it will entrain fluid quickly due to shear instability and below which entrainment of water into the plume is slow. However entrainment of fluid from above is not a first-order forcing term because the buoyancy anomaly of the plume is fixed at the source. The details of the entrainment parameterization in the Lagrangian model are explained in Section 2.3.4.

The ASA Lagrangian brine plume model development is focused on the speed and direction of the plume due to baroclinic forces. Starting from the momentum equations derived by Parker et al. (1986), ASA used scaling analysis to determine the dynamic balance of forces given the parameters of the brine plume (details presented in Attachment A). The system of equations derived from this process is very similar to that used by Cenedese (pers. comm., 2009).

Enhanced Plume Velocity Equation

The diagnostic equation (Equation 1) determines the equilibrium velocity defined in terms of the down slope (v) and across slope (u) components. The equation has five parameters. The linear bottom drag coefficient C_f, and the Coriolis parameter f are constants. The thickness, h and the reduced gravity, R_g are determined from the current spatial distribution of particles in the Lagrangian model. Finally, the bottom slope, s is calculated locally for each particle from bottom bathymetry data. From these coefficients the enhanced velocity of the plume can be determined at any point. The dynamic effects of entrainment on the plume velocity are fully described by these equations, changing the local velocity as entrainment thickens the plume. The thickness of the plume is determined from the vertical distribution of particles as described

in Section 2.3.1. The entrainment process is modeled by the vertical diffusivity of the Lagrangian particles.

$$\text{Across slope}: 0 \approx fvh - C_f u$$

$$\text{Down slope}: 0 \approx -fuh - C_f v + R_g hs$$

$$v = \frac{R_g hsC_f}{(C_f)^2 + (fh)^2}$$

$$u = \frac{fvh}{C_f}$$

Equation 1 Diagnostic equation for steady state linear plume velocity

2.3.3 Entrainment

In the Lagrangian plume model the thickness of the plume is evaluated on a high resolution grid covering the model domain. Within each grid cell, the vertical distribution of particles determines the thickness. This method makes it impossible to apply the canonical formulation for the entrainment of ambient water. It is not possible to impose the change in thickness with time on the Lagrangian model. The change in thickness must be a result of the collective particle motion. This is accomplished through the vertical diffusion coefficient. The numerical method implemented in the Lagrangian model is described in Section 2.3.1. In this section the relationship between diffusivity and entrainment velocity is discussed.

Ellison and Turner (1959) describe entrainment in a dense plume, $We = EU$. We is the rate of change of thickness, while E, the entrainment coefficient is a function of the parameters of the flow, usually Richardson number. U is the speed of the plume. This formulation, often referred to as an entrainment velocity, describes the speed at which the upper edge of the plume moves upward. Numerous laboratory studies and field experiments have tried to find the correct formula for the entrainment coefficient. The Richardson number is the key parameter in this kind of two-layer flow. It expresses the stability of the flow due to stratification of the layers which prevents mixing compared to the instability caused by shear between the layers which tends to mix the fluids. The Richardson number has a critical value behavior. Near the critical value the rate of entrainment is extremely sensitive as the flow transitions from stable to unstable. Ellison and Turner (1959) and Turner (1986) approximated the entrainment rate as zero for stable flows with Richardson number greater than 0.8.

Cenedese (pers. comm., 2009) has developed a new parameterization which takes the Reynolds number as well as the Richardson number into account in determining the value. The new formulation is more nuanced as it is designed for application to subcritical geophysical flows such as dense overflows. Dense overflows occur in most of the world's oceans where cold salty water is formed in high latitude marginal seas. This dense water fills the marginal sea and overflows into the deep ocean basins. As the water flows down the slope, the flow is usually subcritical and the entrainment rate is small, but over long distances, entrainment may significantly alter the water properties. To validate the formulation, Cenedese used estimates of diapycnal diffusivity from tracer experiments in oceanic dense overflows.

Cenedese relates the entrainment velocity of the plume to the diapycnal diffusivity, K_ρ of the tracer experiment using the steady-state advection diffusion equation.

$$w\frac{\partial T}{\partial z} = K_\rho \frac{\partial^2 T}{\partial z^2}$$

The horizontal gradients in the plume are much smaller than the vertical gradients and can be ignored. Based on dimensional analysis of this equation we arrive at a simple expression for the entrainment velocity in terms of the diffusivity, We = K_ρ/H where H is the thickness of the plume. This formula allows comparison of the effective entrainment rate in the Lagrangian model's diffusive parameterization with the canonical entrainment velocity used in analytic models. The vertical diffusivity in the Lagrangian model is function of Richardson number. Sensitivity analysis to the parameterization used is presented in Section 4.3 along with the equivalent entrainment velocity using the vertical advection diffusion equation described here.

3.0 Application of Models

The models described in Section 2 were applied to simulate a brine discharge at the existing Bryan Mound site off the coast of Freeport, Texas and at the proposed Richton North and South sites south of Mississippi Sound. Section 3 of this report begins with a description of the field program undertaken by researchers at Texas A & M University in the early 1980s at the Bryan Mound discharge site. Data collected at the Bryan Mound site provide a relatively complete observational data set of the excess salinity plume in the area of a brine discharge with a flow rate and concentration similar to that proposed at the Richton sites. The data from Bryan Mound are important in validating the far-field model used to simulate the brine discharge.

Subsequent discussion in this section includes a description of the application of the UM3 near-field model and the Lagrangian particle far-field model to brine discharges at Bryan Mound and at the north and south Richton discharge sites.

3.1 Bryan Mound Site

3.1.1 Study Area

The Bryan Mound brine discharge site is located in the northwestern Gulf of Mexico, off the coast of Freeport, Texas. A 0.9-meter (2.95-foot) diameter pipeline is buried beneath the sea floor from Bryan Mound to a point 20 kilometers (11.2 nautical miles) off the Texas coast where the depth is 21.6 meters (71 feet) (Figure 3.1.1-1; Hann and Randall, 1982). Tides in this area are of mixed type with a 10- to 15-centimeter (4- to 6-inch) tidal range. The tidal components of the bottom current measured at the discharge site were found to be small (i.e., K1 and M2 tidal constituents of 2 to 4 centimeters per second (0.04 to 0.08 knots) compared to the mean and residual components of bottom current (Hann and Randall, 1982). Spectral analysis of wind and current data by Hann and Randall (1982) showed a strong coherence between the alongshore component of wind stress and alongshore components of surface and bottom currents.

Figure 3.1.1-1 is a map of the Bryan Mound region in the northwestern Gulf of Mexico. Figure 3.1.1-2 shows the Bryan Mound discharge site on a map with water depths. The seafloor slopes away from the discharge site toward the southeast.

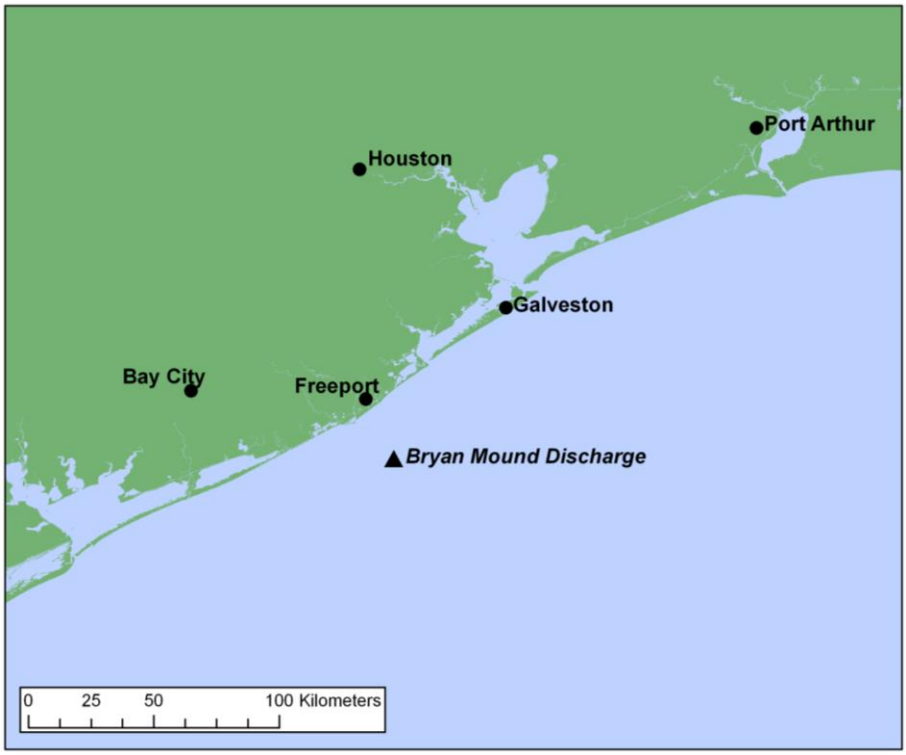

Figure 3.1.1-1. Region of the Bryan Mound discharge site in the northwestern Gulf of Mexico.

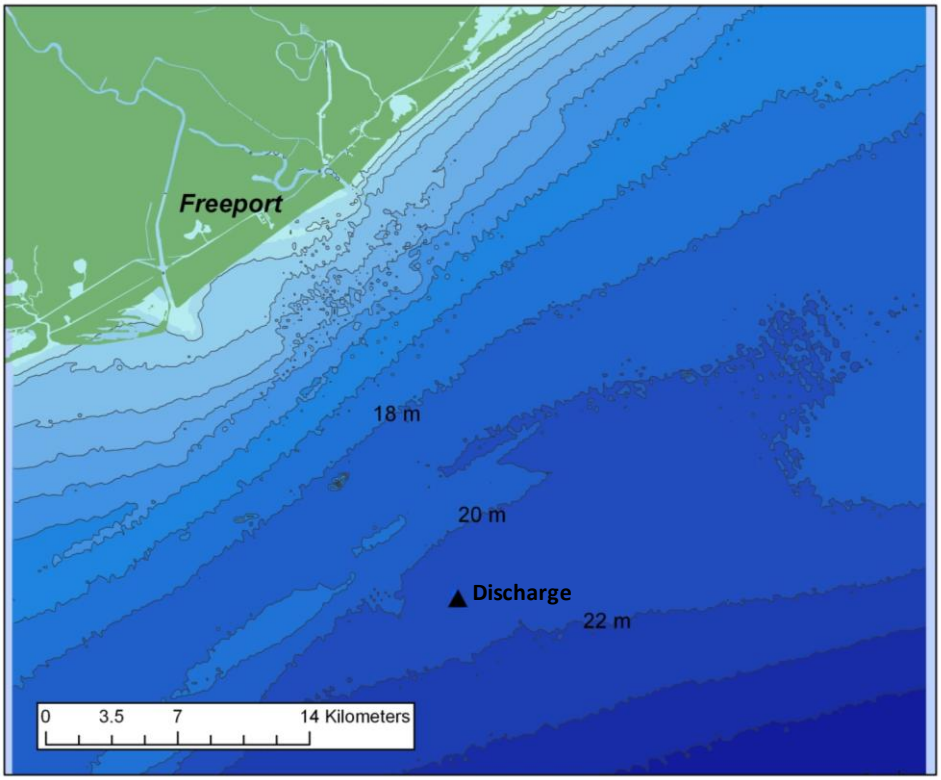

Figure 3.1.1-2. Bathymetry in the area of the Bryan Mound discharge site off the coast of Freeport, TX. Depth contours are shown at a 2-meter interval. Depths are in meters below mean sea level.

3.1.2 Historical Data

A series of surveys was conducted in the early 1980s at the brine discharge site associated with the Bryan Mound SPR facility in Freeport, Texas. During multiple field surveys, salinity was measured in the waters around the site and reported in a series of publications (Randall, 1982; Hann and Randall, 1982). Surveys were performed from March 1980 through August 1981. Each survey was performed by towing a sled mounted with instruments along the seabed to measure salinity. The salinity measurements were then contoured with lines of equal excess salinity (salinity above ambient) and published as a series of maps. The results of the surveys are useful for comparison with the plumes simulated with the near-field and far-field models at the Bryan Mound discharge site.

Even though the Bryan Mound and Richton discharge sites are at different depths and have different current speeds, it is useful to compare the observed dimensions of the Bryan Mound discharge plume with the results of near-field and far-field model results to determine the predictive success of the models. Although one could expect that the dimensions of the Richton discharge plume would be similar to those measured at Bryan Mound due to the similar discharge rates and brine salinity, the comparison is only approximate because the Bryan Mound discharge is in an area with deeper water than the Richton North site and faster current speed at both the Richton sites so the plume will behave somewhat differently.

A time series of velocity, salinity, and temperature fields from Hann and Randall (1982) was re-analyzed for this study so that a total 2 months of hydrodynamic conditions (July through August of 1981) could be utilized in modeling the brine discharge at Bryan Mound. Figure 3.1.2-1 shows a time series of salinity, temperature, current speed, and direction for July at three

depths: surface (18.2 meters above the bed), middle (8.2 meters above the bed) and bottom (1.8 meters above the bed). The difference in temperature and salinity are relatively significant during the July period (2–3 degrees different between layers) indicating a stratified condition. Currents in the surface layer show a strong tidal influence with both diurnal and neap-spring variability. In the middle layer, this tidal signal is reduced significantly and the bottom layer currents show almost no tidal variability. The data show an increase of current velocity with the depth.

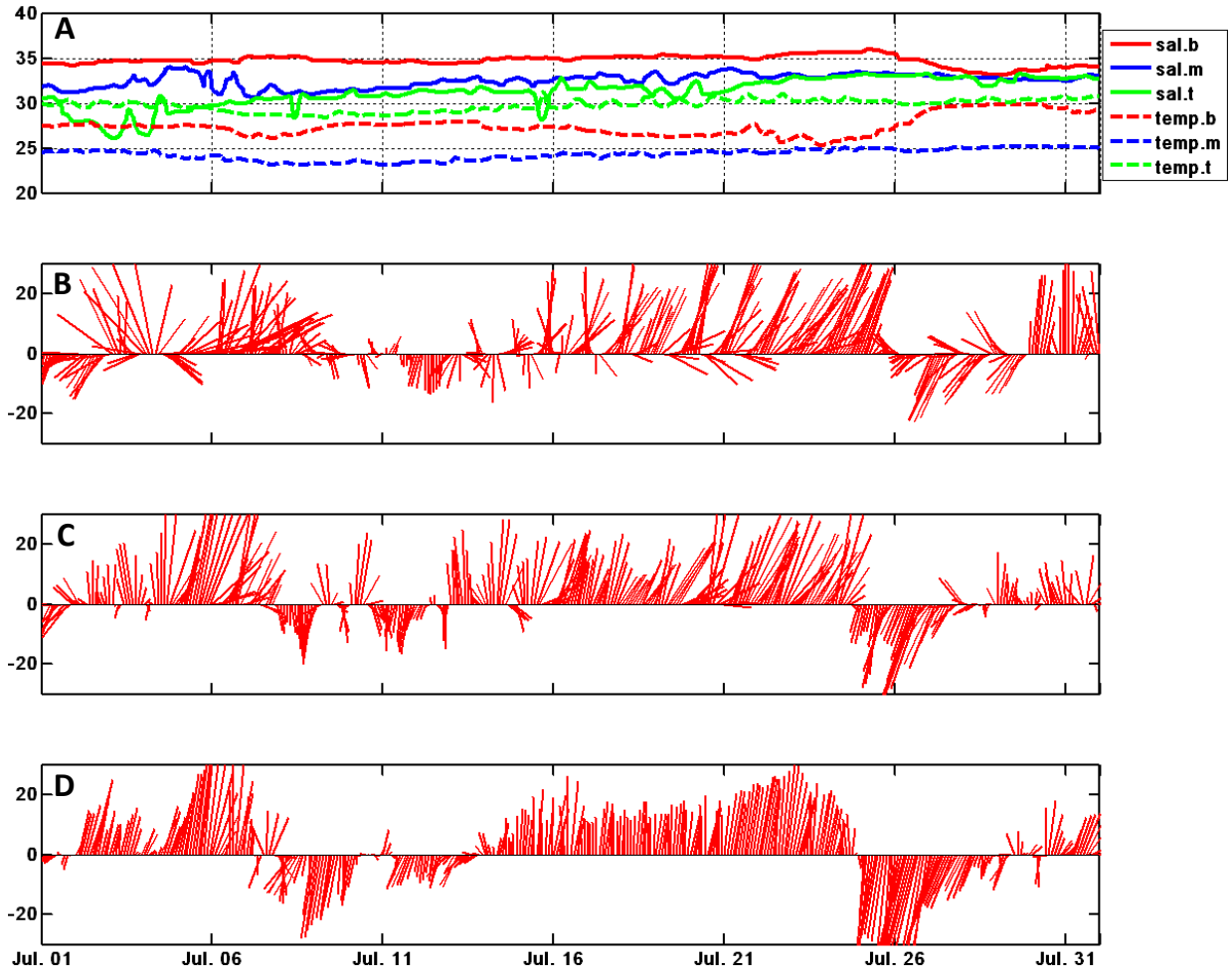

Figure 3.1.2-1. Data collected in July, 1981 and reported by Hann and Randall (1982). Panel A shows temperature (degrees Celsius) and salinity (ppt) variation at three water depths. Surface, mid-depth and bottom current speed (cm/s) and direction are shown in panels B, C, and D, respectively.

Figure 3.1.2-2 shows a time series of salinity, temperature, current speed, and direction for August 1981 reported by Hann and Randall (1982) at three depths: surface (18.2 meters above the bed), middle (8.2 meters above the bed) and bottom (1.8 meters above the bed). The differences in temperature and salinity through the water column are significantly less compared to those during July, which indicates a relatively well-mixed condition during most of this period. The current directions are more or less the same for of all three layers. The vertical current distribution is characterized by a decrease in current velocity with depth.

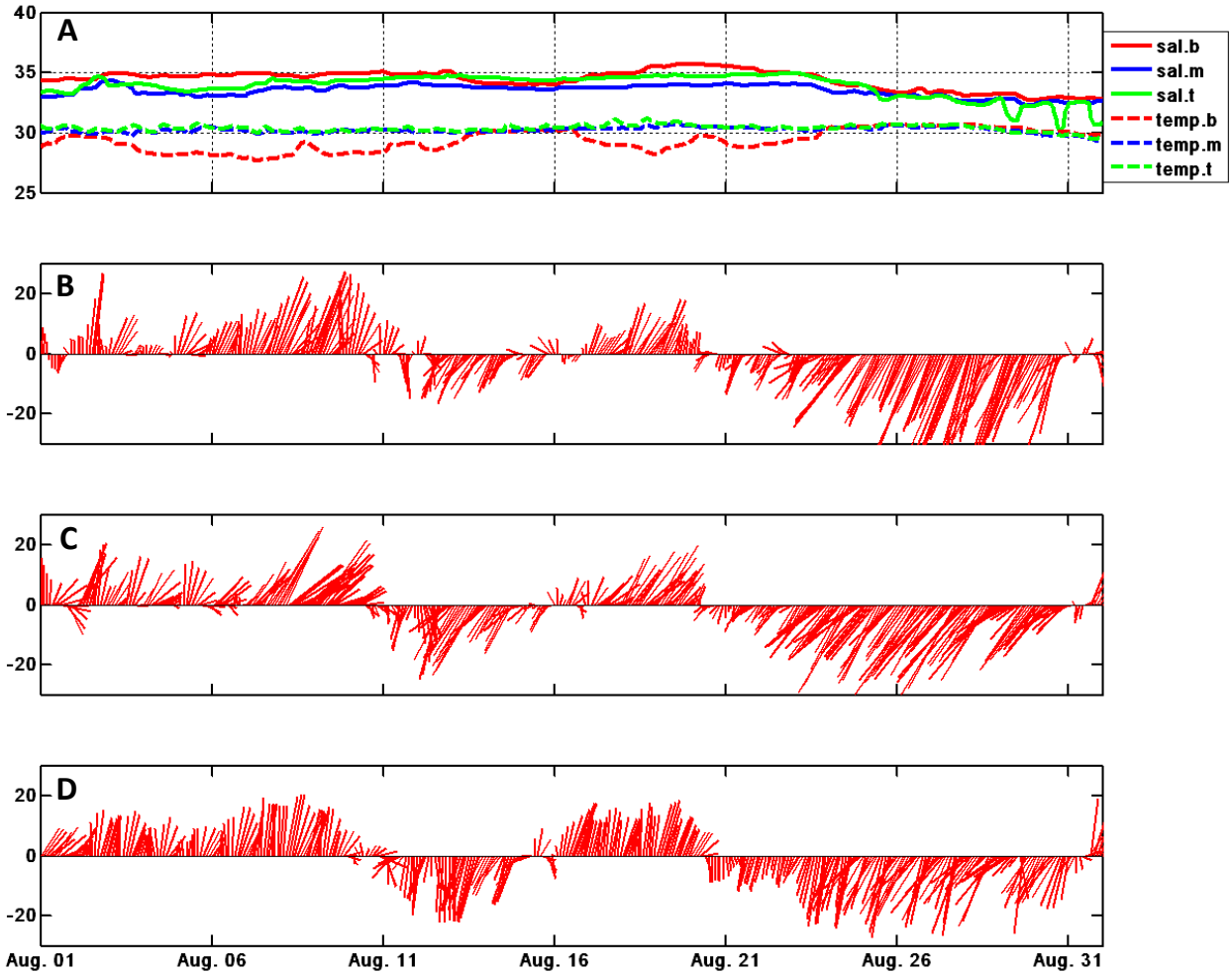

Figure 3.1.2-2. Data collected in August, 1981 and reported by Hann and Randall (1982). Panel A shows temperature (degrees Celsius) and salinity (ppt) variation at three water depths. Surface, mid-depth and bottom current speed (cm/s) and direction are shown in panels B, C and D, respectively.

Figure 3.1.2-3 shows the time series of salinity, temperature, current speed and direction for the period August 8 through 24, 1981 at two depths: bottom (1.8 meters [6 feet] above the bed) and very near the bed (0.5 meter [1.6 feet] above the bed). The very near-bed data came from a location south (offshore) of the diffuser, and the bottom observations were collected at a location west of the diffuser. Even though these two data sets were collected at sites approximately 200 meters (660 feet) apart, it is still valid to compare the data in order to discuss the vertical variability in flow within the brine plume.

The difference in salinity at the two depths is negligible for the first couple of days and during the period 17–23 August (Panel A in Figure 3.1.2-3). During the rest of this 17-day period the salinity was 3–4 practical salinity units (psu) higher at the near bed layer which is 1.3 meters (4.3 feet) above the bottom layer. This strong salinity stratification implies the existence of the brine plume very near the bed during August 10–17 and 23–25 and is also supported by the temperature which shows no difference between the two layers.

From the temperature and salinity measurements it can be assumed that the current velocity recorded at 1.8 meters above the bottom (panel B) represents the flow of the ambient water mass, and that the velocity recorded at 0.5 meter (1.6 feet) above the bottom (panel C) can be regarded as the movement of the brine plume layer, so that an understanding of the brine plume dynamics in response to ambient currents can be gained. When the ambient current was relatively slow (e.g., August 10 and 11 and August 15 and 16), the direction of the brine plume flow was directed to the southeast, which is the down-slope direction. This down-slope flow seen in the very near-bed data was consistent in spite of variable direction of the currents recorded 1.8 meters (5.9 feet) above the bottom. In addition to the period of slow bottom flows, the direction of the very near-bed plume flow was in the down-slope direction during the period when the ambient current flowed toward the southwest or south (e.g., Aug 11–15). This indicates that the brine plume is mainly controlled by the down-slope forcing. The coherence of this down-slope flow with higher salinity at the near-bed layer provides strong evidence that supports the hypothesis of the gravity-induced density flow discussed in Section 2.3.2 in this report.

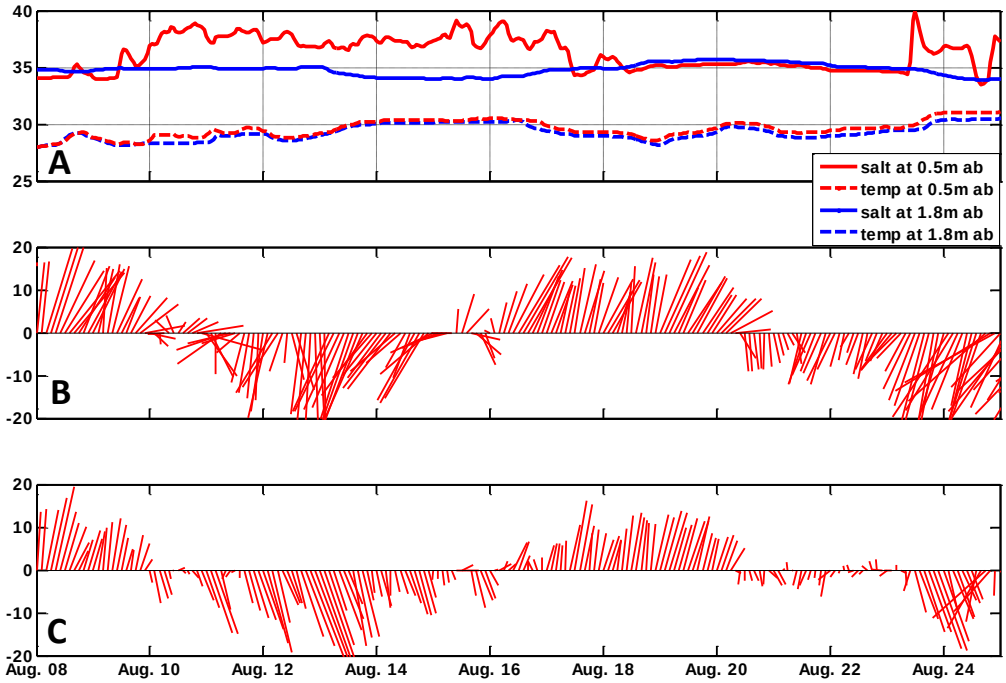

Figure 3.1.2-3. Data collected in August, 1981 and reported by Hann and Randall (1982). Panel A shows temperature (dashed lines, degrees Celsius) and salinity (solid lines, ppt) variation at 0.5 and 1.8 m (5.9 ft) above the bottom. Panel B shows current speed (cm/s) and direction at 1.8 m (5.9 ft) above the bottom, Panel C shows current speed and direction at 0.5 m (1.6 ft) above the bed.

3.1.3 Near Field Model Application

The UM3 model was used to simulate the near-field behavior of the brine discharge plume for the Bryan Mound site. A series of simulations was performed using data describing the discharge diffuser geometry, discharge rate, and discharge salinity reported by Hann and Randall (1982) and listed in Table 3.1.3-1.

Table 3.1.3-1. Characterization of the discharge used in the UM3 near-field model simulations at Bryan Mound. Data from Hann and Randall (1982).

Port Diameter	Vert. Angle	Horiz. Angle (relative to current)	Number of Ports	Port Spacing	Discharge Rate	Discharge Salinity	Temp
(m)	(deg)	(deg)		(m)	(m^3/s)	(psu)	(C)
0.076	90	90	31	18	1.17	257	20

A series of simulations was run using the UM3 model to characterize plume behavior and dilution under varying current speeds present at the Bryan Mound discharge site. Three constant currents based on the 5th, 50th, and 95th percentile speed recorded at the site (Hann and Randall, 1982) were used to simulate discharge from the diffusers. Currents for the Bryan Mound simulations were taken from data collected at the site on June 25, 1981 (Hann and Randall, 1982). Current direction is the angle of the oncoming current relative to the diffuser orientation.

Table 3.1.3-2. Characterization of ambient conditions used in the UM3 near-field model simulations at Bryan Mound. Current speeds are 5th, 50th, and 95th percentile speeds. Current direction is the angle of the oncoming current relative to the orientation of the diffuser. Data from Hann and Randall (1982).

Depth	Current Speed	Current Direction	Ambient Salinity	Ambient Temperature
m	cm/s	deg	psu	C
	0.84	0		
	10.34	45		
21.6	21.64	90	35.6	20

3.1.4 Far Field Brine Transport Model Application

The Lagrangian particle model was applied at the Bryan Mound discharge site using data from Hann and Randall (1982) to describe the discharge and ambient parameters. The goal was to use the monitoring data collected at Bryan Mound to validate the far-field model approach. The far-field model was used to simulate the period of August 1981 because the salinity of the brine discharge at that time (257 parts per thousand [ppt]) was close to the discharge salinity proposed for the Richton sites (263 ppt), and because monitoring was conducted on multiple occasions during this time, providing data on the extent of the brine plume during a variety of oceanographic conditions.

For application of the far-field model, the initial distribution of salt from the brine discharge was defined based on monitoring data collected at the Bryan Mound site by Hann and Randall (1982). Measurements of the vertical distribution of the brine plume collected directly over the diffuser and at points surrounding the diffuser during August 1981 indicate that the excess salinity from the discharge extended up to a maximum of 5.4 meters (17.7 feet) above the seafloor. The majority of this excess salinity was seen within 3 meters (9.8 feet) of the bottom. The maximum excess salinities measured during two monitoring events in August 1981 were 3.8 and 4.2 ppt. The maximum excess salinity measured during the entire 1980–1981

monitoring period was 6.9 ppt. The relatively low excess salinity maximums mean that either the brine is diluting rapidly and at a short distance from the diffuser ports or that the vertical measurements never sampled the highest salinity portion of the discharge. Either way, the measurements indicate that excess salinities above 4–7 ppt exist within a small volume of water just above the diffuser.

The diffuser at Bryan Mound during August 1981 consisted of a 933-meter (3060-foot) long pipeline section with 52 ports extending vertically to a height of 1.2 meters (3.9 feet) above the bottom. Each port was 7.6 centimeters (3 inches) in diameter with an18-meter (59-foot) horizontal spacing. During August 1981, a brine solution was discharged from the Bryan Mound diffuser 24 hours per day from 31 to 34 of the 52 ports.

The far-field model simulates the discharge of the brine from the diffuser by releasing a mass of salt at a constant rate equal to the known discharge rate. The salt is represented by particles of equal mass. Consistent with the results of the Bryan Mound monitoring data, the initial salt particle release in the far-field model occurs within a volume of water 558 meters (1831 feet) long (31 ports x 18-meter spacing), 3 meters (9.8 feet) high, and 100 meters (328 feet) wide. Once released, the particles are advected by the far-field model.

In addition to the ambient currents from the Bryan Mound observations, the enhanced velocity of the plume due to baroclinic forces is used in the Lagrangian model. The method described in Section 2 requires the bottom slope at the particle location. At the Bryan Mound site, the model uses bathymetry data from the National Oceanic and Atmospheric Administration (NOAA) Coastal Relief Model (Divins and Metzger, 2009). The 3-arc-second grid data were derived from the U.S. National Oceanographic Survey hydrographic database. Consistent with the model derivation, the bathymetry data have been smoothed because the plume velocity is the result of the bottom slopes over distances of a kilometer or more.

The plume model also depends on the estimated Richardson number, which is a combination of the ambient conditions and values calculated dynamically from the plume. Using the available time series profile from the Bryan Mound study, the shear and stratification between the plume and the ambient water column is calculated in each grid cell of the model domain. Combining these values, the Richardson number is used to calculate the vertical diffusivity required for the model. While it is an approximation to apply the mooring data profile uniformly to the model domain, generally regions with small bottom slope result in regionally uniform flow.

The Richardson number calculated in the model is always subcritical (RI>1). In this range, the diffusivity tends to be low, closer to open-ocean levels.

3.2 Richton Site

3.2.1 Study Area

The proposed Richton brine discharge area is located in the northern Gulf of Mexico east of Chandeleur Sound and south of Mississippi Sound. Figure 3.2.1-1 is a map of the region with the locations of the proposed discharge sites shown. Mississippi Sound is bounded to the north by the coasts of Mississippi and Alabama and by Mobile Bay, to the west by the Mississippi delta and to the south by barrier islands of the Gulf Islands National Seashore. Freshwater flow to the Sound comes from eight rivers that enter from the north. Tidal exchange with the Gulf of Mexico occurs through passes between the barrier islands along the southern margin of the Sound. The sound is approximately 145 kilometers (90 miles) long east-to-west with an average depth of 3 meters (10 feet).

Figure 3.2.1-1. Map showing Mississippi Sound and the region of the proposed Richton North and South discharge sites in the northern Gulf of Mexico.

Currents in the discharge area are typically dominated by tides, but tidal currents are periodically overridden by wind-generated currents from passing tropical storms and hurricanes (Johnson, 2008). The north brine discharge diffuser site is located 6 kilometers (3.2 nautical miles) south of Horn Island in 14 meters (45 feet) water depth. The south brine discharge diffuser site is approximately 15 kilometers (8.1 nautical miles) south of Horn Island (Figure 3.2.1-2) in a water depth of 16.8 meters (55 feet). The area of the traffic fairway shown in Figure 3.2.1-2 is excluded as a potential site for the discharge.

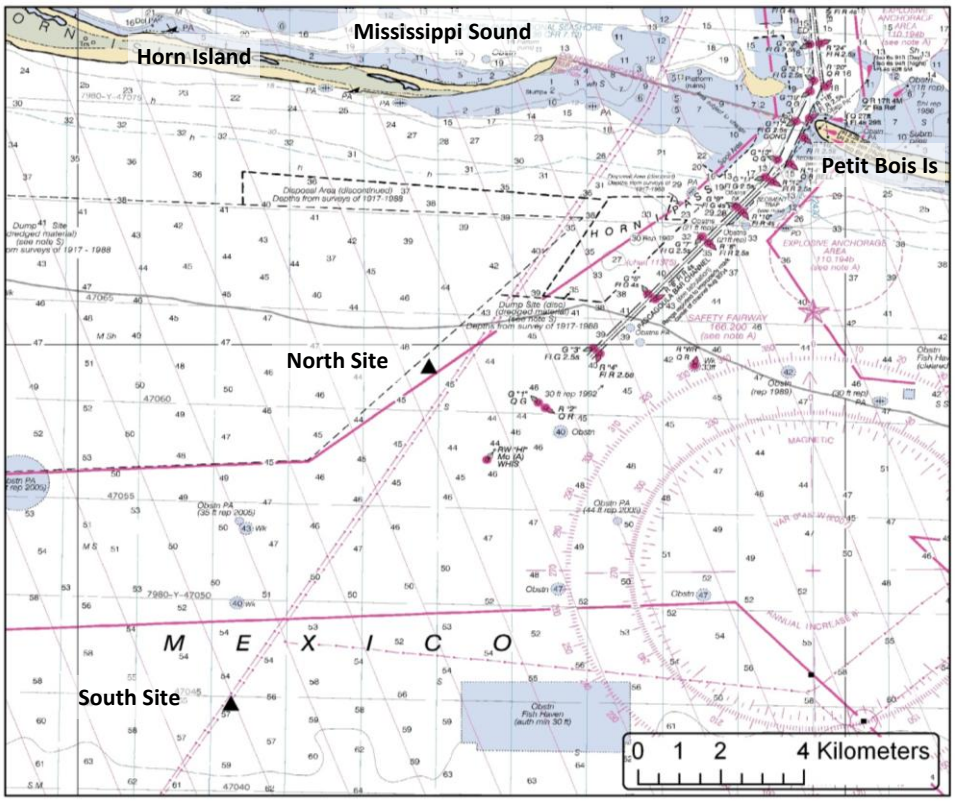

Figure 3.2.1-2. Chart of the area around the proposed north and south Richton discharge sites in the northern Gulf of Mexico.

3.2.2 Hydrodynamic Model Application

The CH3D hydrodynamic model, described in Section 3 of this report, was used to provide currents for the brine discharge modeling. The model used five sigma layers in the vertical to resolve the vertical structure of horizontal currents. Figure 3.2.2.-1 shows the hydrodynamic model grid provided by the USACE Engineer Research and Development Center (ERDC). Grid sizes ranged from 300 to 2,500 meters (1,000 to 8,200 feet).

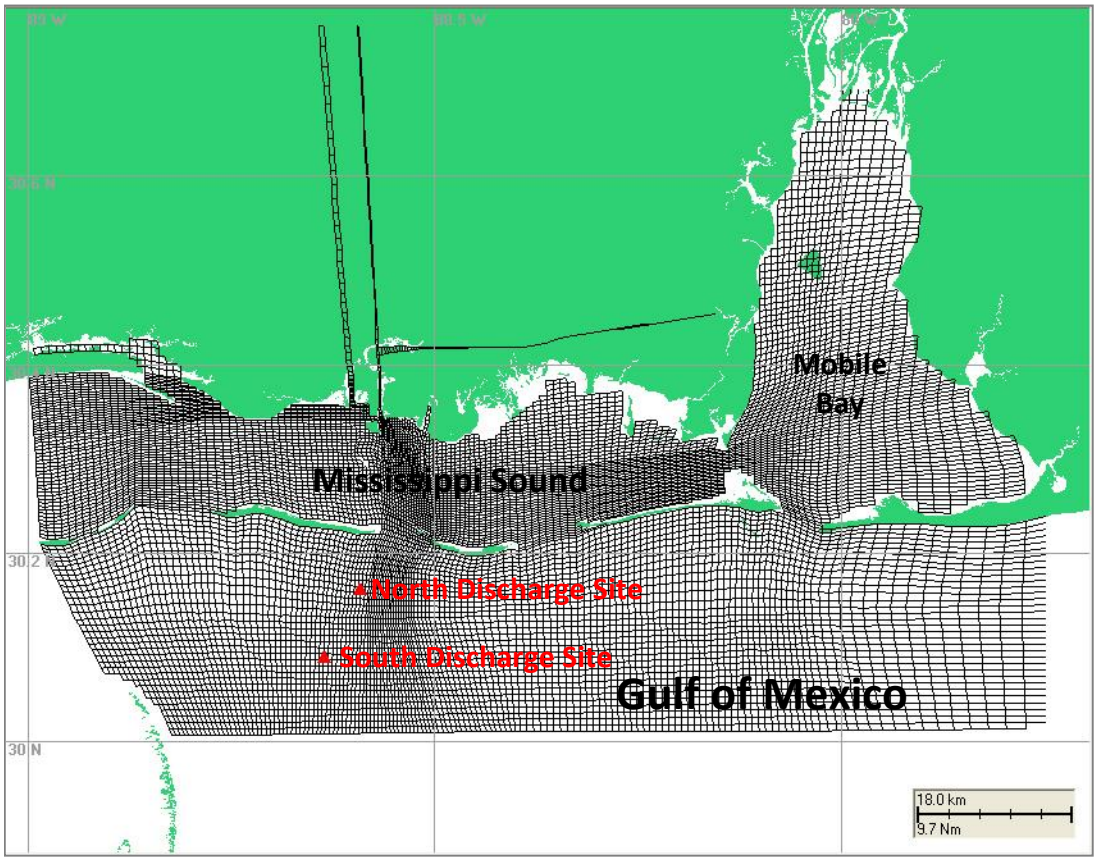

Figure 3.2.2-1. USACE CH3D hydrodynamic model grid.

The east, south, and west boundary conditions of ocean hydrodynamics (water surface and velocity) for the CH3D model were developed from larger domain ADCIRC model simulations. ADCIRC uses Garatt's (1977) wind drag formula for computing wind shear stress, which is based on an empirical relationship between wind speed and resulting shear stress. Because the wind fields extracted from the NOAA National Centers for Environmental Prediction database and used to force the CH3D hydrodynamic model were of relatively coarse resolution in both temporal and spatial domains (e.g., 6-hour intervals for 1.9 degrees in latitude and longitude), the model accuracy was decreased during periods of rapidly changing wind directions (Bunch et al., 2003). Although the CH3D model was then calibrated to the observed water surface, current, temperature, and salinity data, most of these available data sets were limited to areas within or in the vicinity of Mississippi Sound (Bunch et al., 2003).

Two sets of time series of velocity, salinity, and temperature fields from the USACE/ERDC model application (Bunch, et al. 2003; 2005) were provided for this study so that both summer and winter hydrodynamic conditions could be utilized in the modeling. A time series of velocity, salinity, and temperature fields over the model domain for the period April 1 through September 30, 1997 was used as input to define the summer conditions for the far-field model. Figure 3.2.2-2 shows a time series of surface elevation, salinity, and current speed and direction for three sites: in the channel at Horn Pass between Horn and Petit Bois Islands, at the Richton North discharge site, and at the Richton South discharge site. The differences in water elevation, and salinity at the two sites are insignificant. However, the currents are dramatically different. The Horn Pass site shows strong tidal currents with maximum speeds up to 40

centimeters per second (0.8 knot) while the Richton discharge sites show much weaker tidal currents with maximum speeds up to 21 centimeters per second (0.4 knot). The orientation of the currents at Horn Pass are primarily north-northeast on flood and southwest on ebb while at the Richton discharge sites they are primarily northwest on flood and south-southeast on ebb. Currents at the south discharge site are of almost identical speed and direction as those at the north site.

A time series of velocity, salinity, and temperature fields over the model domain for the period February 2001 was used to define the winter conditions for simulating the movement and dilution of the brine discharge in the far-field model. Figure 3.2.2-3 shows similar results for winter compared to the summer results shown in Figure 3.2.2-2 indicating that the current regime does not show strong seasonality.

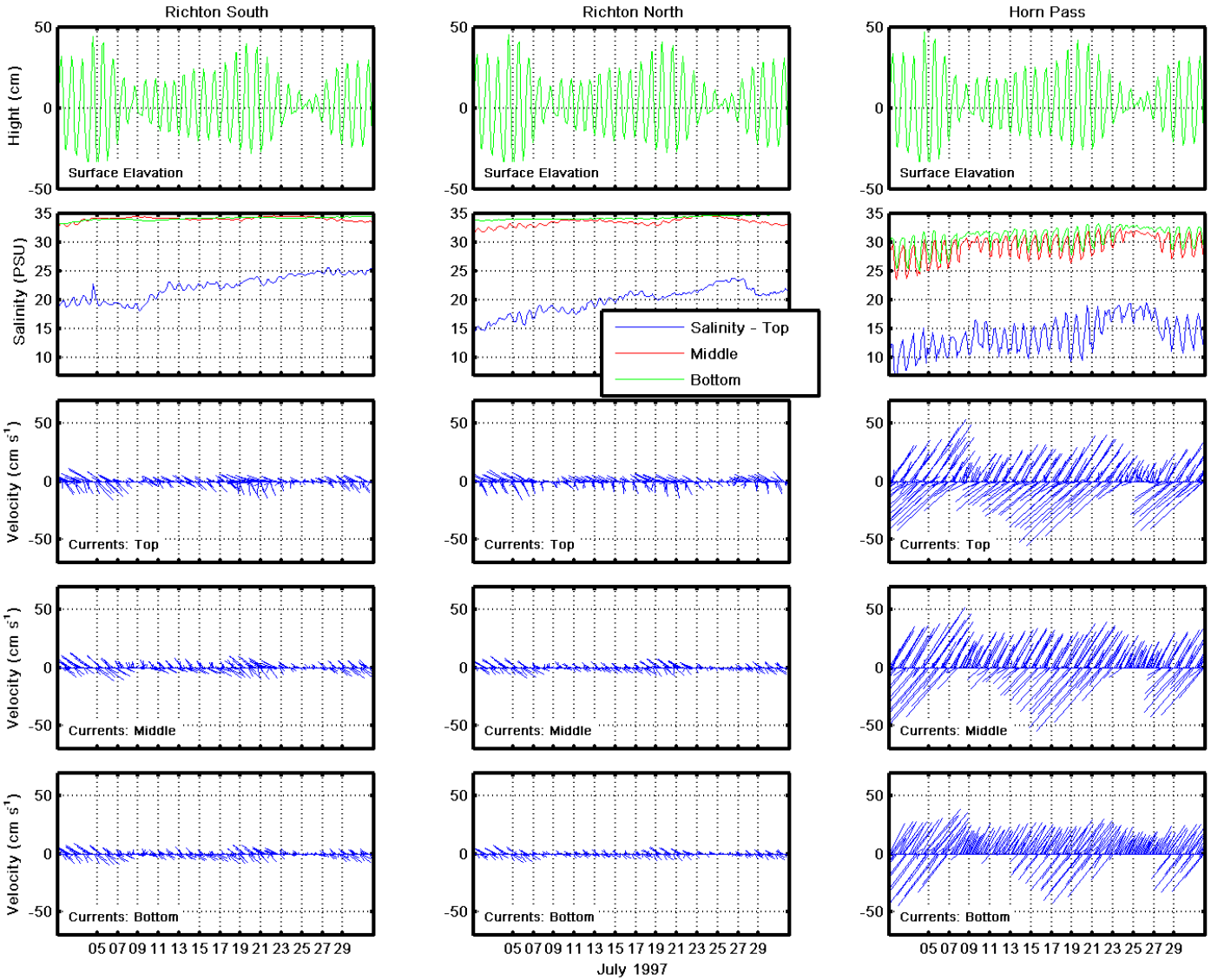

Figure 3.2.2-2. Example USACE CH3D model output for Richton South (left panel), Richton North (middle panel) and Horn Pass (right panel) during the summer period (July 1997).

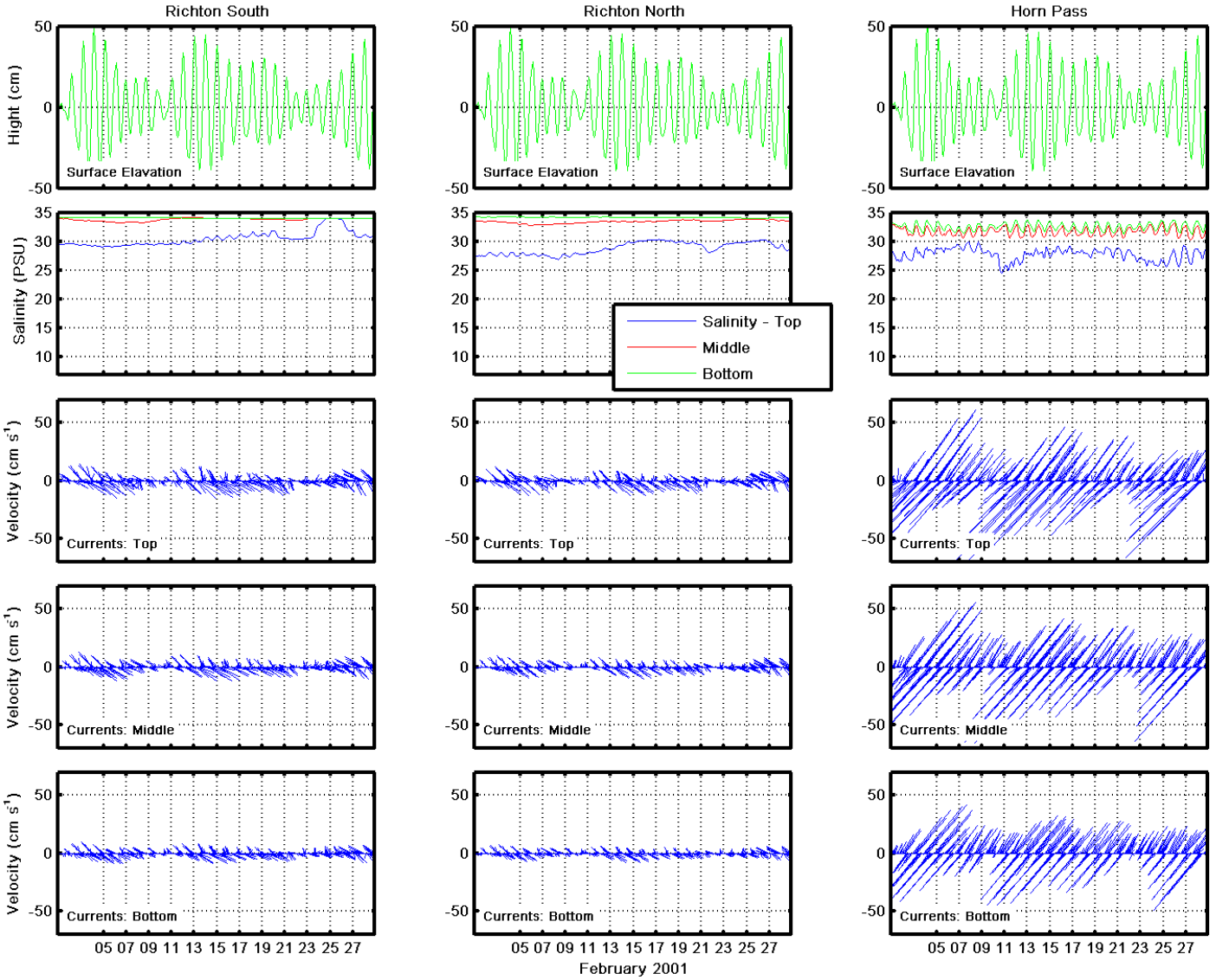

Figure 3.2.2-3. Example USACE CH3D model output for Richton South (left panel), Richton North (middle panel) and Horn Pass (right panel) during the winter period (February 2001).

3.2.3 Near Field Model Application

The UM3 model was used to simulate the near-field behavior of the brine discharge plume from the north and south Richton discharge sites. A series of simulations was completed using data describing the discharge diffuser geometry, discharge rate, and discharge salinity listed in Table 3.2.3-1 and the ambient conditions listed in Table 3.2.3-2.

Table 3.2.3-1. Characterization of the discharge used in the UM3 near-field model at the Richton North and Richton South sites.

Port Diameter	Vert. Angle	Horiz. Angle (relative to current)	Number of Ports	Port Spacing	Discharge Rate	Discharge Salinity	Temp
(m)	(deg)	(deg)		(m)	(m^3/s)	(psu)	(C)
0.076	90	90	53	20	2.208	263	20

A series of simulations was run using the UM3 model to characterize plume behavior and dilution under varying current speeds present at the Richton discharge sites. Three constant currents based on the 5th, 50th, and 95th percentile speed at each site were used to simulate discharge from the diffusers. Currents for the Richton sites were extracted from the CH3D model.

Table 3.2.3-2. Characterization of ambient conditions used in the UM3 near-field model simulations at the Richton North and Richton South discharge sites. Current speeds are 5th, 50th, and 95th percentile speeds. Current direction is the angle of the oncoming current relative to the line of the diffuser.

Depth	Current Speed	Current Direction	Ambient Salinity	Ambient Temperature
m	cm/s	deg	psu	C
Richton North				
13.8	1.24 5.53 12.87	0 45 90	31	20
Richton South				
16.8	1.10 3.23 7.38	0 45 90	31	20

3.2.4 Far Field Brine Transport Model Application

The Lagrangian particle model was applied at the Richton North and Richton South discharge sites using the CH3D hydrodynamic model results of Bunch, et al. (2003, 2005) to describe the ambient parameters. The discharge parameters used at the Richton sites are listed in Table 3.2.4-1. The far-field brine transport model was used to simulate the summer and winter periods based on the period covered by the CH3D hydrodynamic data provided.

Table 3.2.4-1. Characteristics of the brine discharge at the Richton North and South sites.

Location	Diffuser Orientation	Port Diameter	Vert. Angle	Number of Ports	Port Spacing	Discharge Rate	Discharge Salinity	Temp
	(deg)	(m)	(deg)		(m)	(m^3/s)	(psu)	(C)
North	59	0.076	90	53	20	2.208	263	20
South	45	0.076	90	53	20	2.208	263	20

The proposed diffuser at the Richton discharge sites consists of a 1,060-meter (3,478-foot) long pipeline section with 53 ports extending vertically to a height of 1.2 meters (3.9 feet) above the bottom. Each port will have a 7.6-centimeter (3-inch) diameter opening with a 20-meter (66-foot) horizontal spacing. A brine solution would be discharged from the diffuser 24 hours per day from all of the 53 ports.

The far-field model simulates the discharge of the brine from the diffuser by releasing a mass of salt at a constant rate equal to the known discharge rate. The salt is represented by particles of equal mass. Consistent with the specification of the proposed discharge at the Richton sites, the initial salt particle release in the far-field model occurs within a volume of water 1,060 meters (1,831 feet) long (53 ports x 20-meter spacing), 3 meters (9.8 feet) high, and 100 meters (328 feet) wide.

The far-field model uses a concentration grid to calculate the resulting brine salinity from the Lagrangian particles such that each represents the same mass of salt. The concentrations are used in the particle transport calculation to define the spatial extent of the brine plume. The extent of the far-field model concentration grid is shown on the map in Figure 3.2.4-1.

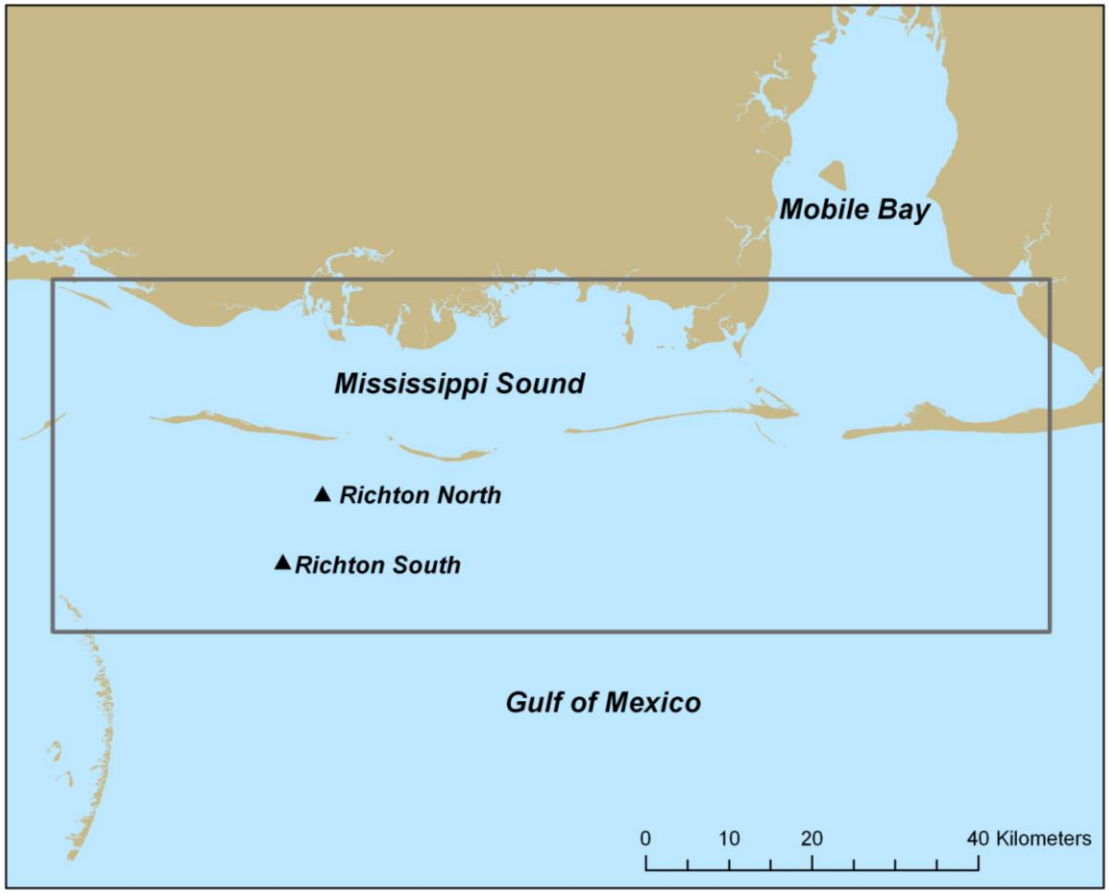

Figure 3.2.4-1. Area of the far-field model computational grid for calculating brine concentrations.

The bathymetry used in the far-field model was taken from the CH3D hydrodynamic model and is shown in Figure 3.2.4-2. Calculations encompass the water column from the surface to a variable depth across the grid in layers 1 meter (3.3 feet) thick. Particles moving through the three open (water) boundaries (edges of the grid) are assumed not to return. Particles cannot cross over land.

Bathymetry for the CH3D hydrodynamic model was obtained primarily from the Northern Gulf Littoral Initiative as 3-arc-sec (approximately 90 meters [295.27 feet]) resolution gridded bathymetry (Bunch et al., 2003). Local corrections to the navigation channel depths were obtained from authorized depths published on NOS navigation charts, and the Pascagoula River navigation channel was assumed to have a uniform depth of 12 meters (39.37 feet). Bathymetry in the Naval turning basin north of Singing River Island was modified according to information published in the NOS 1:40000 nautical chart. This chart was also utilized in the specification of channel depths near the mouths of rivers. The maximum grid depth was 27.0 meters (88.6 feet) at the offshore boundary and the minimum depth was restricted to 1.5 meters (4.9 feet) in shallow flats.

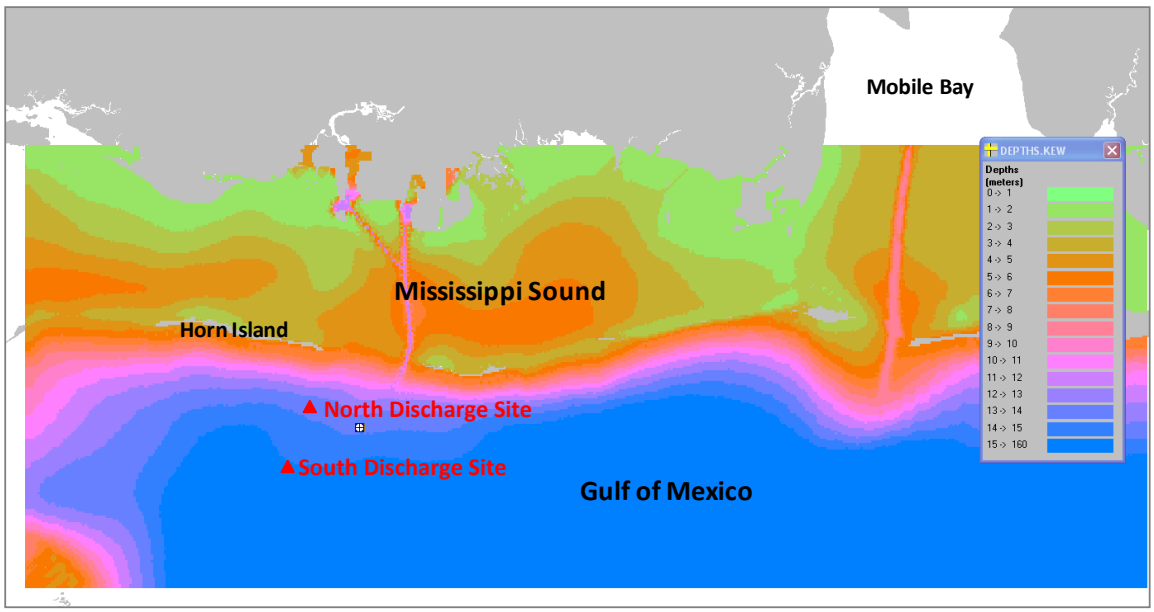

Figure 3.2.4-2. Bathymetry used in far-field model calculations. Depths are in meters as indicated by the color key.

Particle Release

The diffuser at both Richton discharge sites would consist of a 1060-meter (3478-foot) long pipeline section with 53 ports extending vertically to a height of 1.2 meters (3.9 feet) above the bottom. Each port opening would be 7.6 centimeters (3 inches) in diameter with a 20-meter (65.6-foot) horizontal spacing. Brine solution would be discharged from the diffuser 24 hours per day from all 53 ports.

The far-field model simulates the discharge of the brine from the diffuser by releasing a mass of salt at a constant rate equal to the proposed discharge rate. The salt is represented by particles of equal mass. Consistent with the results of the Bryan Mound monitoring data, the initial salt particle release in the far-field model occurs within a volume of water 1,060 meters (3,478 feet) long (53 ports x 20-meter spacing), 3 meters (9.8 feet) high, and 100 meters (328 feet) wide. The north discharge site is located in approximately 14.1 meters (46 feet) of water, while the south site is located in 16.8 meters (55 feet) water depth.

Diffusivity

Diffusivity is a measure of the turbulent mixing and controls the horizontal and vertical spread of the brine plume. The horizontal turbulent mixing controls the width of the brine plume as it is transported from the discharge site in the far field. It is defined as a function of the local current speed, water depth and bottom friction coefficient, C_f,

$$Dxx = speed*depth*7.1sqrt(C_f)$$

Table 4.3-1shows example horizontal diffusivity values for both the preferred and alternative sites using a bottom friction C_f of 0.003.

Table 3.2.4-1. Range of horizontal diffusivity values.

Site	Depth (m) [ft]	Dxx based on mean ambient velocity (m^2/s)	Dxx based on 95th percentile ambient velocity (m^2/s)
North Site	14.1 [46]	0.28	0.56
South Site	16.8 [55]	0.35	0.70

The vertical diffusivity is defined as a function of the Richardson number as described in Chapter 2. At the Richton site, stratification and shear between the plume model and the ambient flow results from the CH3D model are calculated at each time step. The Richardson number in the Richton plume model is always subcritical (RI>1), reflecting the large density gradients between the plume and the sea water above it. The resulting vertical diffusivity is generally between 0.01 and 1.0 centimeters squared per second. The sensitivity analysis of the model to the vertical diffusivity and the Richardson number calculation is described in the next section.

3.3 Model Sensitivity

In developing the dense brine plume model, several sensitivity studies were performed to ensure that the model parameterizations are robust with regard to the assumptions made. A series of model simulations was completed to determine the effect of applying different vertical diffusivity values and by running model simulations with ambient currents only, with enhanced flow only, and with both ambient and enhanced flow together.

Model results for Bryan Mound and Richton are presented in Section 4. Each case is presented using the full enhanced velocity model, the ambient currents only, and the enhanced flow only. By deconstructing the components of the flow in this way, it is easier to see how each contributes to the solution and to compare the effects of the components between the Bryan Mound and Richton sites. To further examine the plume model sensitivity to entrainment, the vertical diffusivity parameterization used in the far-field model simulations was compared with model runs using three different constant values (0.1, 1, and 10 centimeters squared per second) and a Richardson number formulation. These sensitivity experiments provide an assessment of the key parameters on which the model results depend.

4.0 Model Results

Application of the models as described in Section 3 generated a range of model results. This section presents the model results grouped by location, starting with Bryan Mound and then moving to the Richton North and South sites. For each location, near-field model results are presented first, followed by the far-field results. The final section in Section 4 contains the results from the model runs completed to assess model sensitivity.

4.1 Bryan Mound Site

Because the Richton SPR facility has only been proposed there are no field data to use for comparison with model results to evaluate how well the models predict the resulting transport and dilution of the brine plume. Therefore, to assess the abilities of the models, a data set developed from actual monitoring of a brine discharge from the Bryan Mound SPR facility was used for comparison to model predictions at this location.

4.1.1 Near Field Model Results

The UM3 model was used to model the near-field discharge plume behavior and calculate the initial dilution of the brine at the existing Bryan Mound site. Figure 4.1.1-1 shows the results from the UM3 near-field model simulations. The plot shows a vertical cross-section view of the model-predicted discharge plume centerlines from simulations using the 5th, 50th, and 95th percentile observed ambient current velocities. The discharge parameters and the ambient conditions used for the near-field simulations at Bryan Mound are listed in the tables in Section 3.1.3.

UM3 predicts that the plumes will rise a few meters (few feet) in the water column and then descend, making contact with the bottom within a few meters (few feet) from the diffuser. The higher current speeds slightly reduce the height of the plume and push the seafloor contact point of the plume farther away from the diffuser. The model predicts that the discharge plume has a diameter between 2 and 3 meters (6.6 and 9.8 feet) centered about the plume centerlines. With a port-to-port spacing of 20 meters (66 feet), UM3 predicts no adjacent plume interactions will occur in the near field.

Figure 4.1.1-2 shows the model-predicted dilution of the brine discharge in terms of excess salinity, or salinity above ambient, for each of the plumes simulated under the three constant current speeds. The salinity values plotted are the average excess salinity within the plume and it can be seen that salinity drops very rapidly within a short horizontal distance (less than 0.5 meter [1.6 feet]) from the diffuser and then decreases more gradually with distance. Excess salinity is predicted to drop below 40 ppt under the three current speeds simulated.

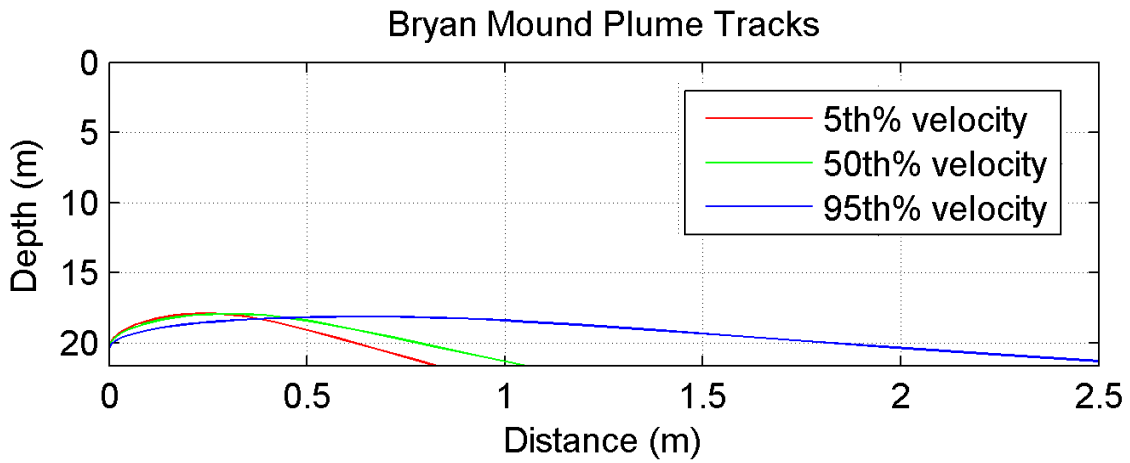

Figure 4.1.1-1. Results from UM3 model simulations at the Bryan Mound site. The red, green, and blue curves show the discharge plume centerline in cross-section for current speeds of 0.84, 10.34, and 21.64 cm/s, respectively. The x axis indicates the distance downstream from the diffuser port. Water depth is displayed on the vertical axis.

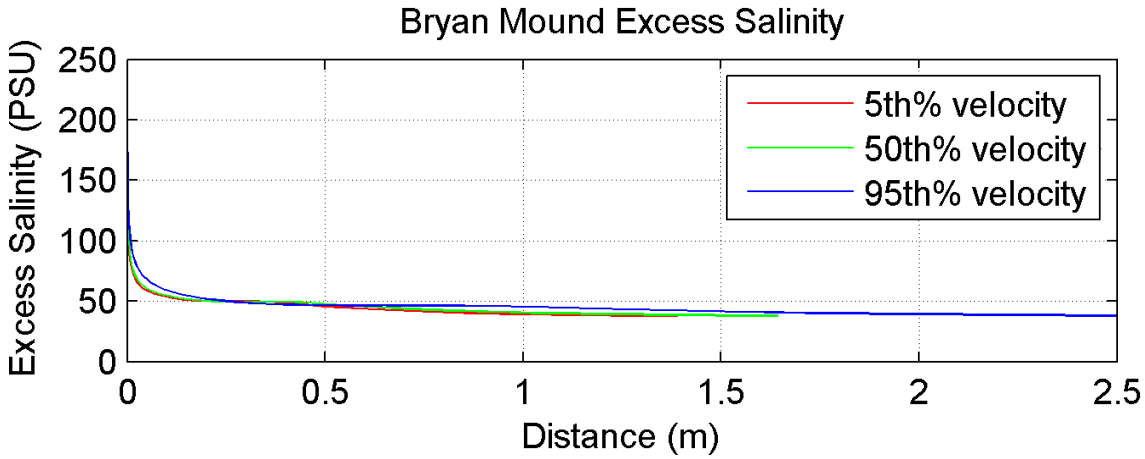

Figure 4.1.1-2. Results from UM3 model simulations at the Bryan Mound site. The red, green, and blue curves show the predicted excess salinity, or rate of dilution, for current speeds of 0.84, 10.34, and 21.64 cm/s, respectively. The x axis is horizontal distance downstream from the diffuser port.

4.1.2 Far Field Model Results

A six-week-long model simulation was performed using the observed current, salinity, and temperature data collected at the Bryan Mound site in July and August of 1981 (Hann and Randall, 1982) at three levels in the water column (see Section 3.1.2 for details). In order to validate the Lagrangian modeling approach using the enhanced velocity, a comparison was made of the area covered by the excess salinity plume predicted by the model with the area of excess salinity observed at the Bryan Mound brine discharge site and reported by Hann and Randall (1982) during August 1981. Two monitoring surveys were completed at the Bryan Mound site during August 3 and 27, 1981. Northeast (i.e., on-shore) directed currents prevailed on August 3, while southwest (i.e., off-shore) directed flow dominated on August 27.

The results of the model-data comparison are presented in Figure 4.1.2-1 as a temporal change of the extent of excess salinity at the 1-, 2-, and 3-psu concentration levels. The plot in the top panel of Figure 4.1.2-1 shows the current speed and direction recorded at the Bryan Mound discharge site at 1.8 meters (6 feet) above the bottom. The bottom panel in the figure shows the model-predicted area of the excess salinity plume at the specified concentrations (continuous solid lines) and the area of excess salinity of 1, 2, and 3 psu measured at the site during the monitoring surveys on August 3 and 27 (short horizontal lines). The model results show very good agreement when compared with the observed data.

Figure 4.1.2-1 shows that the model-predicted 1-psu contour encloses an area ranging from 3 to 25 square kilometers (1.2 to 9.7 square miles), which is approximately an order of magnitude in variability. The trend of this temporal variability is consistent across the other excess salinity concentrations. The variability seen in the area of the excess salinity is likely controlled by the combined effect of horizontal advection and vertical and horizontal diffusion, both of which are dominated by the ambient flow conditions. Because the model used a variable diffusivity, which is based on the gradient Richardson number, the vertical diffusion is mainly dependent on the stratification pattern in the water column.

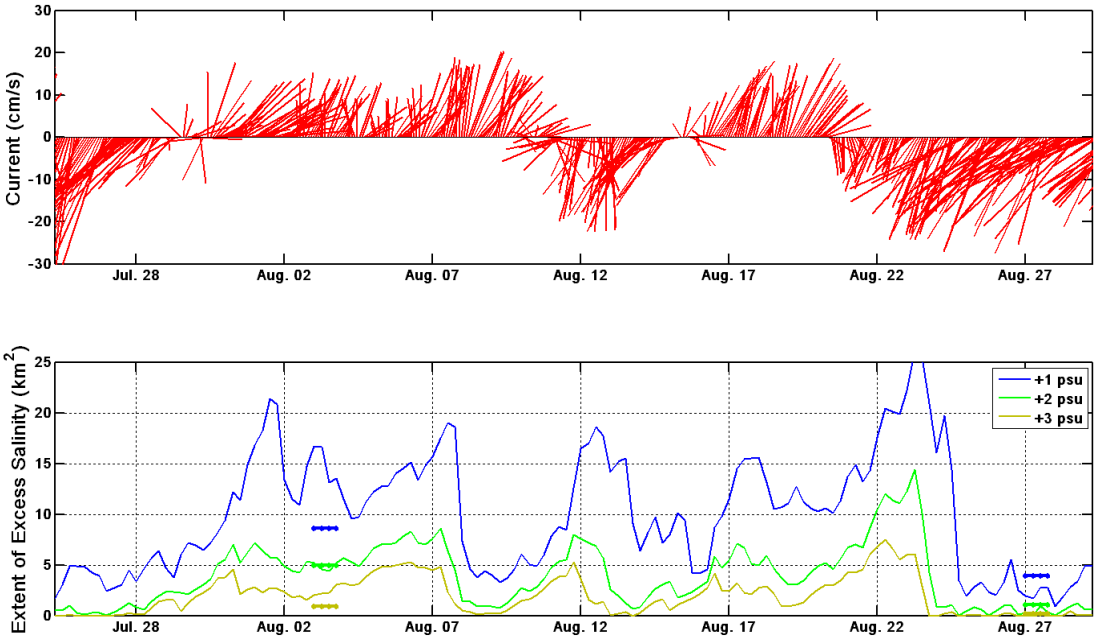

Figure 4.1.2-1. Stick plot (top panel) of current speed and direction recorded at the Bryan Mound discharge site at 1.8 m above the bottom during July and August 1981 (Hann and Randall, 1982). The bottom panel shows the variability of the area of excess salinity of 1-, 2-, and 3-psu concentrations as predicted by the model (continuous solid lines). Thick horizontal lines represent the observed area of excess salinity of 1, 2, and 3 psu from data by Hann and Randall (1982) on August 3 and 27.

Figure 4.1.2-2 shows the plan view of the excess salinity on August 3, 1981 as measured by Hann and Randall (1982) and as predicted by the far-field model. The current direction on this date as shown in Figure 4.1.2-1 was toward the north to north-northeast. The current observations by Hann and Randall (1982) show that the ambient flow during this period reached a maximum of 18.3 centimeters per second (0.35 knot), which is approximately three-to-four times larger than the CH3D-predicted currents at the proposed diffuser sites at Richton. In spite of the dominance of this generally north-directed flow, the observed salt distribution showed that the brine plume was dispersed mainly toward the east-northeast direction with minor dispersion toward the north.

The observations by Hann and Randall (1982) show that the major dispersion direction was parallel to the bathymetry, which implies that the forcing from the north-directed (i.e., up-slope) ambient flow might be balanced with other down-slope forcing such as gravity. To quantitatively compare the model results to the observations, the 2-psu contour line of excess salinity from the observation data was digitized from a plan view map and the orientation of the major axis of the closed contour was determined using the Image Processing Toolbox in Matlab™. The major dispersion axis of the 2-psu concentration contour predicted by the model shows that the brine plume dispersed toward 44 degrees east of north, which shows excellent agreement with the observed data (44 degrees).

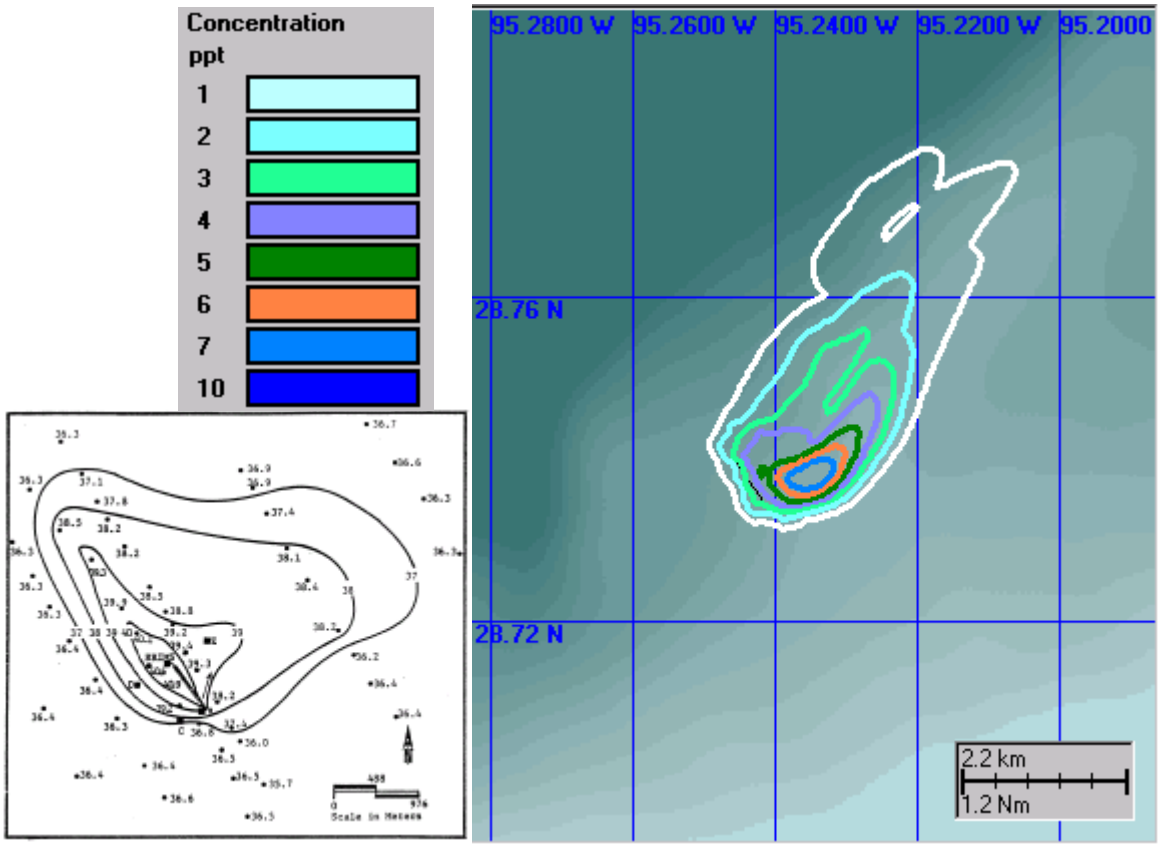

Figure 4.1.2-2. Observation data (reproduced from Hann and Randall, 1982) (left map) and simulation results for the distribution of the excess salinity at Bryan Mound site during August 3, 1981 (right map). The arrow next to the diffuser in the left-hand map represents the average direction of bottom flow (1.8 m [6 ft] above the bed).

Figure 4.1.2-3 shows the plan view of the excess salinity on August 27, 1981 as measured by Hann and Randall (1982) and as predicted by the far-field model. The bottom flow on this date as shown in Figure 4.1.2-1 was directed toward the southwest. The current observations by Hann and Randall (1982) show that the ambient flow during this period reached a maximum of 25 centimeters per second (0.49 knot), which is approximately five-to-six times larger than the CH3D-predicted currents at the proposed diffuser site at Richton. In spite of the dominance of this southwest-directed flow, the observed salt distribution showed that the excess salinity plume was dispersed mainly toward the south or even southeast in the observations.

The major dispersion axis in the observed data is perpendicular to the bathymetry, which implies that the gravity-enhanced forcing in the down-slope direction is dominant during this period. Although the gravity-enhanced flow is included in the model, the entrainment effect considered by the vertical diffusivity was strong enough to reduce the down-slope forcing. This result is less significant in the south- or southwest-directed forcing in the simulation results (see Figure 4.1.2-3) when compared to the observed results. The entrainment effect is kept as large as possible in the simulations at both Bryan Mound and the Richton North and South sites in order to simulate the most conservative estimate for the horizontal dispersion of the brine plume.

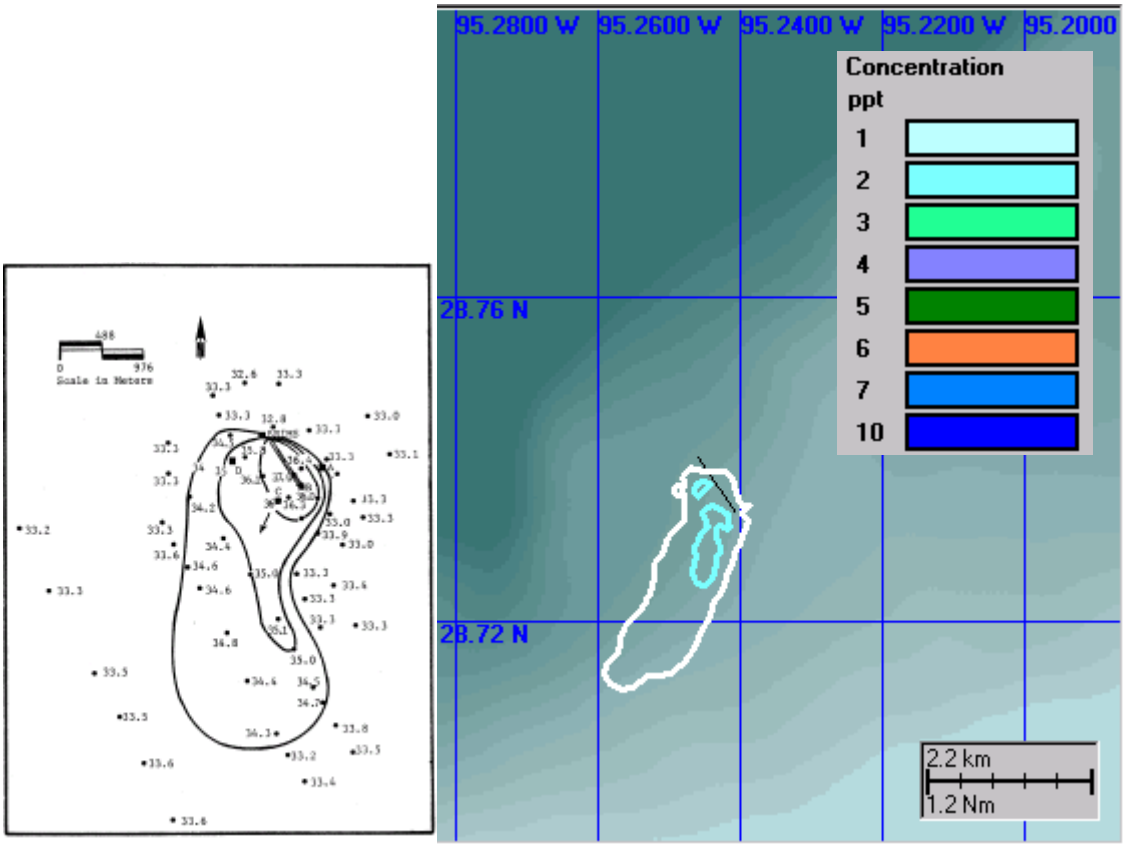

Figure 4.1.2-3. Observation data (reproduced from Hann and Randall, 1981) (left map) and simulation results for the distribution of the excess salinity at Bryan Mound site during August 27, 1981 (right map). The arrow next to the diffuser in the left-hand map represents the direction of average bottom flow (1.8 m [6 ft] above the bed).

4.2 Richton Site

4.2.1 Near Field Model Results

The UM3 model was used to model the near-field discharge plume behavior and calculate the initial dilution of the brine with ambient water. Figure 4.2.1-1 shows the results from the UM3 near-field model simulations of brine discharge at the proposed north (top panel) and south (bottom panel) Richton discharge sites. The plots show a vertical cross-section view of the model-predicted discharge plume centerlines from simulations using three ambient constant current velocities corresponding to the 5th, 50th, and 95th percentile current speeds at each site. The discharge parameters and ambient conditions used in the UM3 simulations at the Richton sites are listed in the tables in Section 3.2.3.

At the Richton North discharge site, the model predicts that the plume centerline rises a few meters in the water column under all three current speeds and then descends, making contact with the bottom within a few meters from the diffuser (top plot in Figure 4.2.1-1). The higher current speeds push the seafloor contact point of the discharge plume farther away from the diffuser. The plume centerline of the 5th percentile current speed (1.24 centimeters per second) is predicted to hit the bottom at less than 0.2 meter (0.66 foot) from the diffuser and have a plume diameter of 2.7 meters (8.9 feet). The plume centerline of the 95th percentile current

(12.87 centimeters per second) is predicted to hit the bottom at approximately 1.5 meters (4.9 feet) from the diffuser and have a plume diameter of 2.1 meters (6.9 feet).

At the Richton South discharge site, the model predicts that the plume centerline again rises a few meters in the water column under all three current speeds and then descends, making contact with the bottom within a meter from the diffuser (bottom plot in Figure 4.2.1-1). The plume centerline of the 5th percentile current speed (1.10 centimeters per second) is predicted to hit the bottom at less than 0.2 meter (0.66 foot) from the diffuser and have a plume diameter of 2.1 meters (6.9 feet). The plume centerline of the 95th percentile current (7.38 centimeters per second) is predicted to hit the bottom at approximately 0.7 meter (2.3 feet) from the diffuser and have a plume diameter of 2.2 meters (7.2 feet).

The plot in Figure 4.2.1-2 shows the model-predicted average excess salinity within the plume using three ambient constant current velocities corresponding to the 5th, 50th, and 95th percentile current speeds at each site. The plot shows that excess salinity drops rapidly within 0.5 meter (1.6 feet) of the diffuser and then decreases more gradually with distance. At the Richton North and South discharge sites, the model predicts that excess salinity will be 40 ppt or less in the near field.

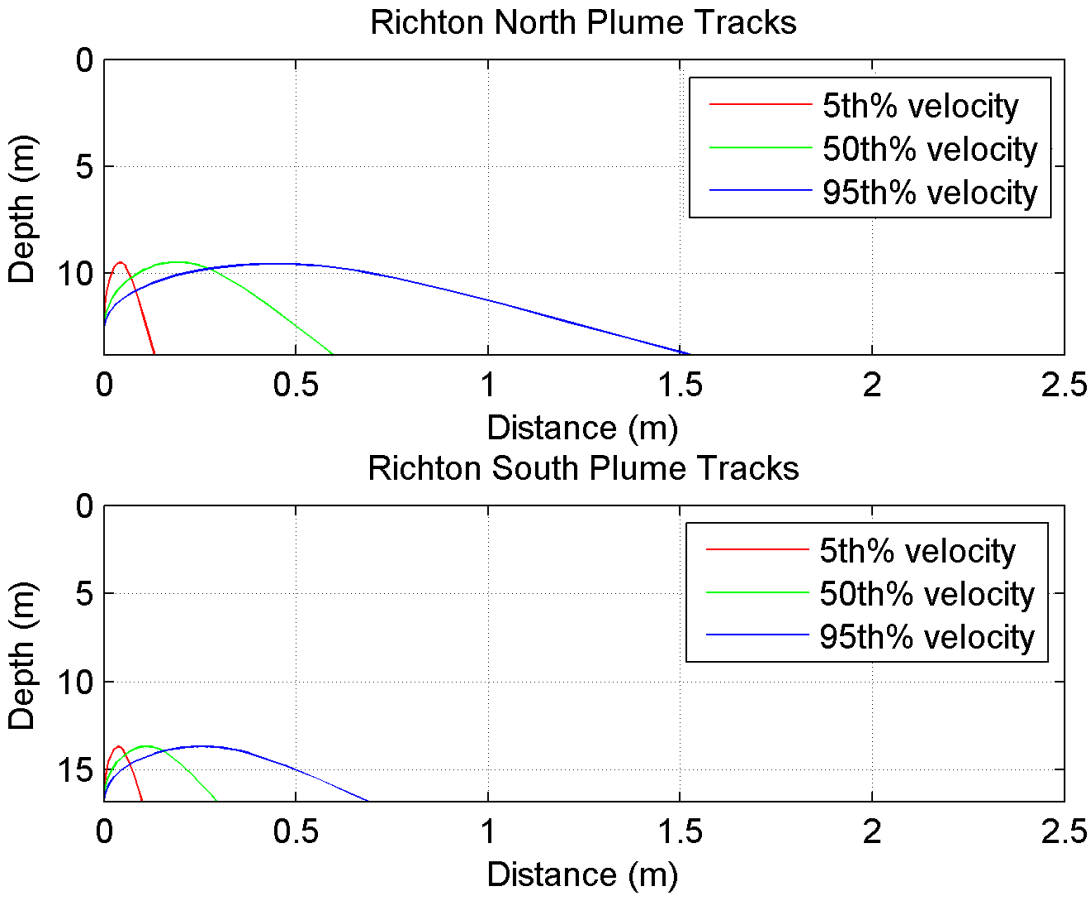

Figure 4.2.1-1. UM3 model predicted discharge plume centerlines at the Richton North (top panel) and Richton South (bottom panel) sites. The red, green, blue, and curves show the discharge plume centerline in cross-section for currents corresponding to the 5th, 50th, and 95th percentile

speeds at the sites. The horizontal axis indicates distance from the discharge. The vertical axis is water depth.

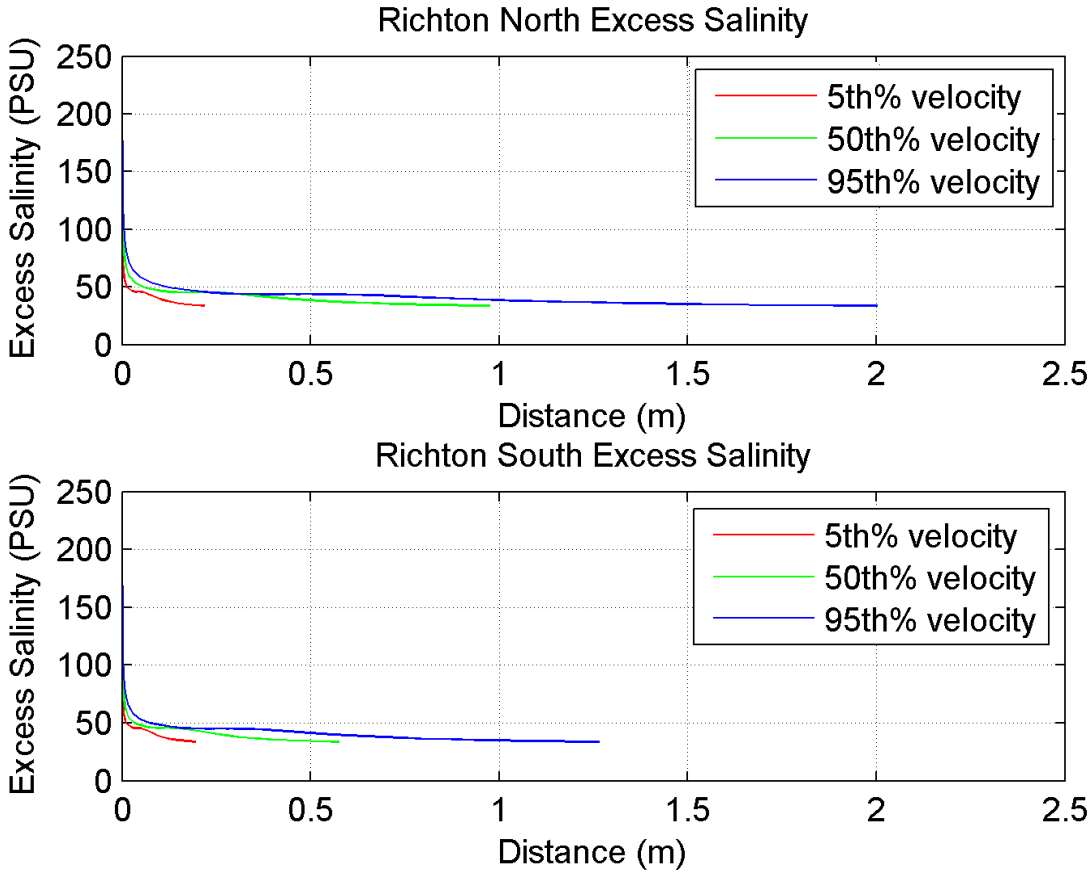

Figure 4.2.1-2. UM3 model predicted average excess salinity at the Richton North (top panel) and Richton South (bottom panel) sites. The red, green, and blue curves show the discharge plume excess salinity for currents corresponding to the 5th, 50th, and 95th percentile speeds at the sites. The horizontal axis indicates horizontal distance from the diffuser. The vertical axis is excess salinity.

4.2.2 Far Field Model Results

The results from a series of model simulations at the Richton North and South sites using the Lagrangian particle model are presented in this section of the report. The model was run to simulate the movement of the brine plume at the Richton discharge sites under both summer (5 months) and winter (1 month) current conditions. The results are presented as a time series of the extent of the excess 1- to 10-psu salinity that represents the temporal variability of the brine plume dispersion pattern. A series of maps showing a plan view snapshot of the brine plume as contours of excess salinity (salinity above ambient) between 1 and 10 psu is included. The snapshots were selected to show the excursion of the discharge plume as it moves in response to tidal currents, as well as the gravity-enhanced flow. Model simulations were run for the length of time simulated by the CH3D hydrodynamic model, which is sufficient time for the discharge plume simulations in the far-field model to demonstrate steady-state behavior. The summer model run was for 5 months, the winter simulation for 1 month.

Figure 4.2.2-1 shows a time series of the areal extent of the excess salinity at the Richton North site during summer and winter simulation periods. After approximately 2 weeks of spin-up time, the areal extent reaches a quasi-steady state. The mean extent of the excess salinity for the 1- and 2-psu concentrations is 34.7 and 13.7 square kilometers (13.4 and 5.3 square miles), respectively. Using the 1-psu contour to define the footprint, the brine plumes from the Richton North site are predicted to be narrow and long, typically 2 to 3 kilometers (1.2 to 1.9 miles) wide and between 10 and 15 kilometers (6.2 and 9.3 miles) long (Figures 4.2.2-2 to 6 are mid-month plan views of the plumes). The extent of the 2-psu contours is typically 1 to 1.2 kilometers (0.6 to 0.74 mile) wide and between 5.4 and 28 kilometers (3.4 and 17.4 miles) long. The major direction of plume dispersion is toward the south or southwest for most of the simulation period. Discharge plume vertical thickness at the Richton site averages 5 meters (16 feet) with a maximum of 10 meters (33 feet). Figure 4.2.2-7 shows the plan view of the discharge plume during the winter simulation period (end of February). The major direction of the plume dispersion at the end of simulation period is toward the west-southwest. Based on the shape and extent of dimension analysis, the brine plume dispersion during the winter is more or less similar to that during the summer period, which implies that the seasonal effect is minimal.

Figure 4.2.2-8 shows a time series of the extent of the excess salinity at the Richton South site during summer and winter simulation periods. After several weeks of spin-up time, the extent reaches a quasi-steady state around the end of May 1997. The mean extent of the excess salinity for 1- and 2-psu concentrations is 18.9 and 7.6 square kilometers (7.3 and 2.9 square miles), respectively, which is 45 percent smaller than that predicted at the north site. Using the 1-psu contour to define the footprint, the brine plumes from the Richton South site are predicted to be smaller compared to those of the Richton North site, typically 2 to 3 kilometers (1.2 to 1.9 miles) wide and between 5 and 10 kilometers (6.2 and 9.3 miles) long (Figures 4.2.2-9 to 13). When compared to the north site, the extent of the plume at the south site is rounder (see Figure 4.2.2-13). The major direction of plume dispersion is toward the south for the period when the shape of the contour is elongate. It should be noted that some of the excess salinity contours from the Richton South site are truncated along the southern edge because they reach the edge of the hydrodynamic grid used in the model simulations. Discharge plume vertical thickness at the Richton South site averages 5 meters (16 feet) and has a maximum of 10 meters (33 feet), which is similar to the north site. Figure 4.2.3-14 shows the plan view of the discharge plume under winter conditions. The shape of the plume extent at the end of the simulation period is toward the south, similar to the September simulation.

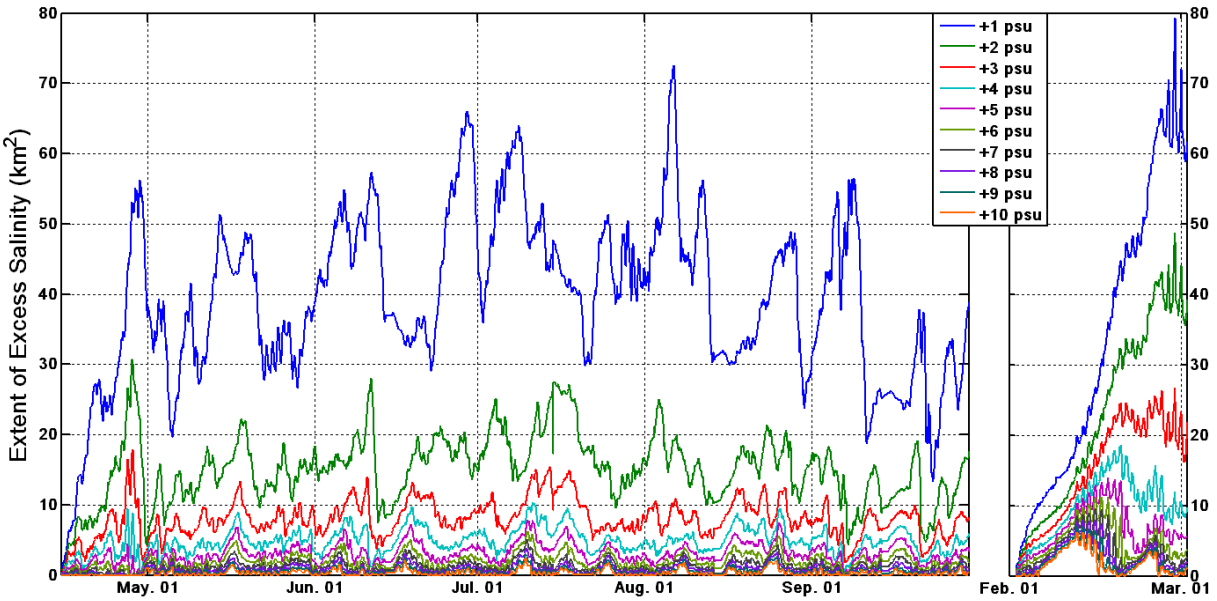

Figure 4.2.2-1. Variability of the area enclosed by contours of excess salinity of 1 to 10 psu from the simulation at the Richton North discharge site. Data from the entire summer and winter periods are shown.

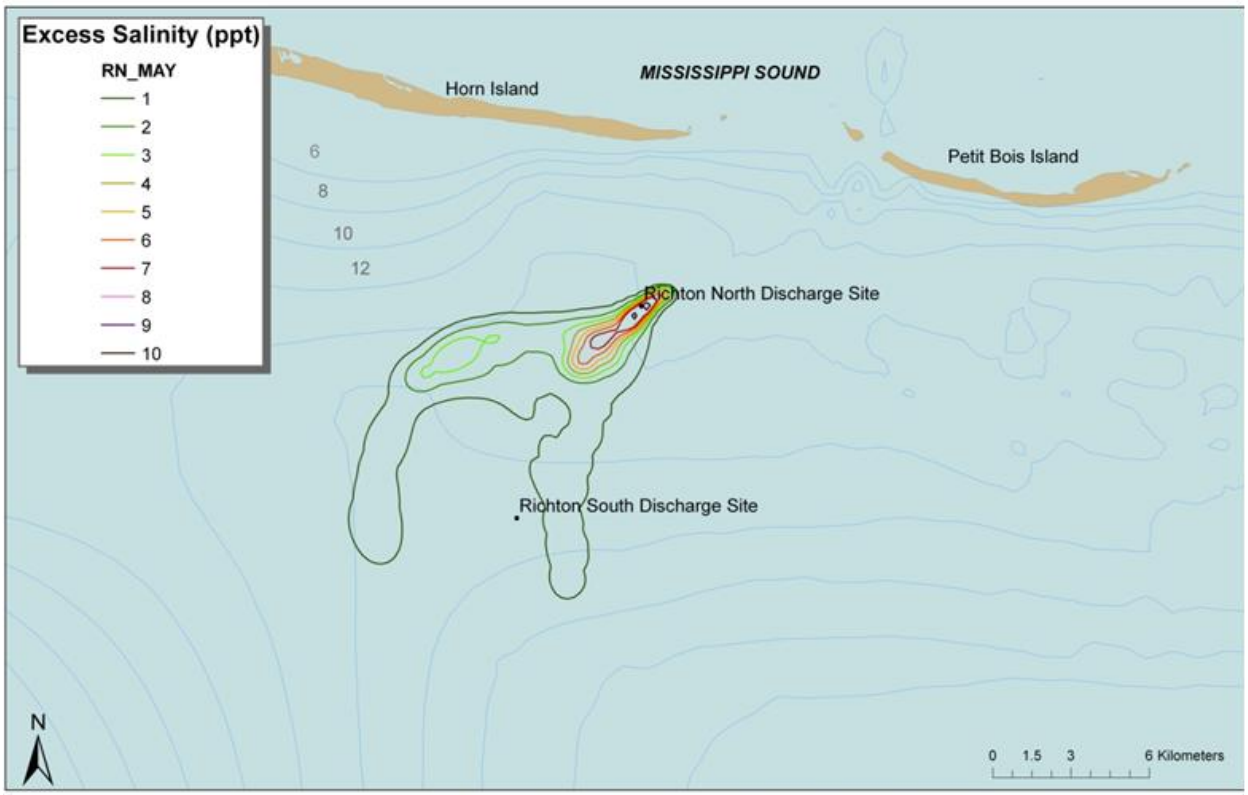

Figure 4.2.2-2. Model-predicted excess salinity of the brine discharge plume from the north discharge site during May 1997. Contours enclose areas of excess salinity.

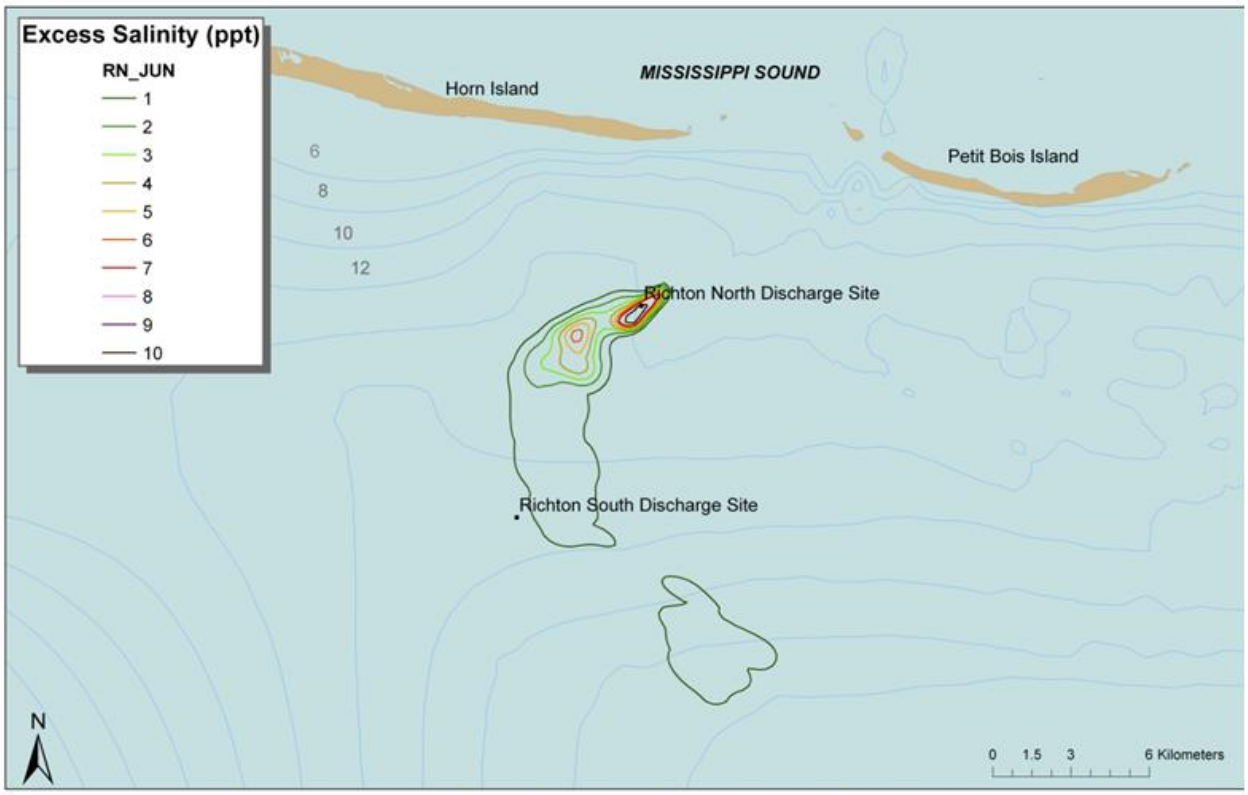

Figure 4.2.2-3. Model-predicted excess salinity of the brine discharge plume from the north discharge site during June 1997. Contours enclose areas of excess salinity.

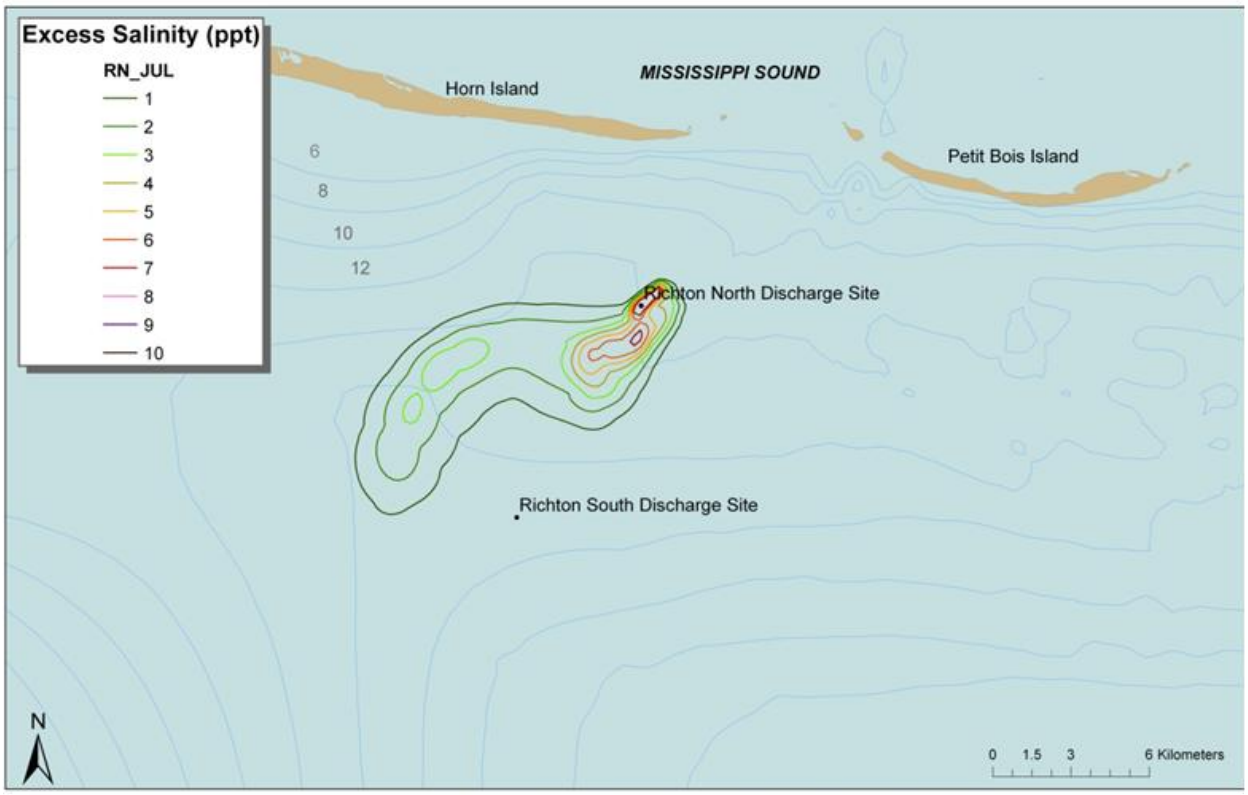

Figure 4.2.2-4. Model-predicted excess salinity of the brine discharge plume from the north discharge site during July 1997. Contours enclose areas of excess salinity.

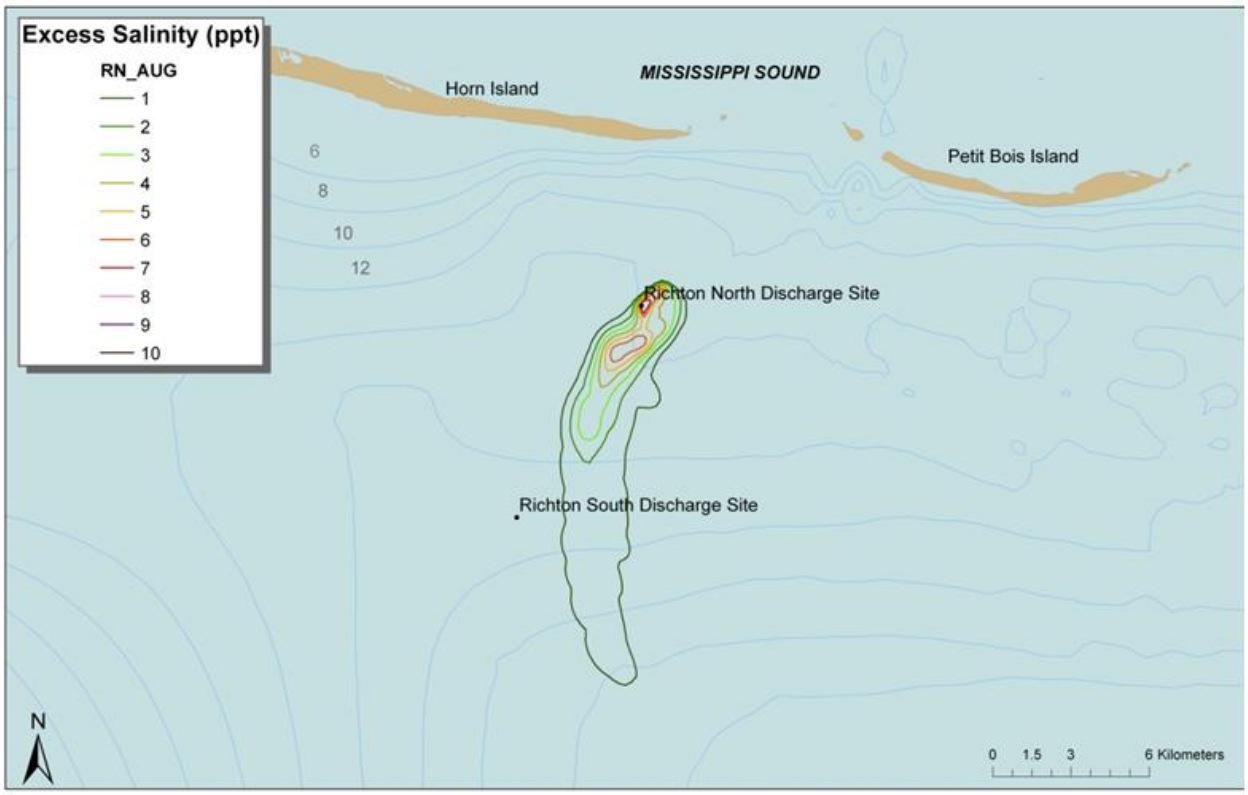

Figure 4.2.2-5. Model-predicted excess salinity of the brine discharge plume from the north discharge site during August 1997. Contours enclose areas of excess salinity.

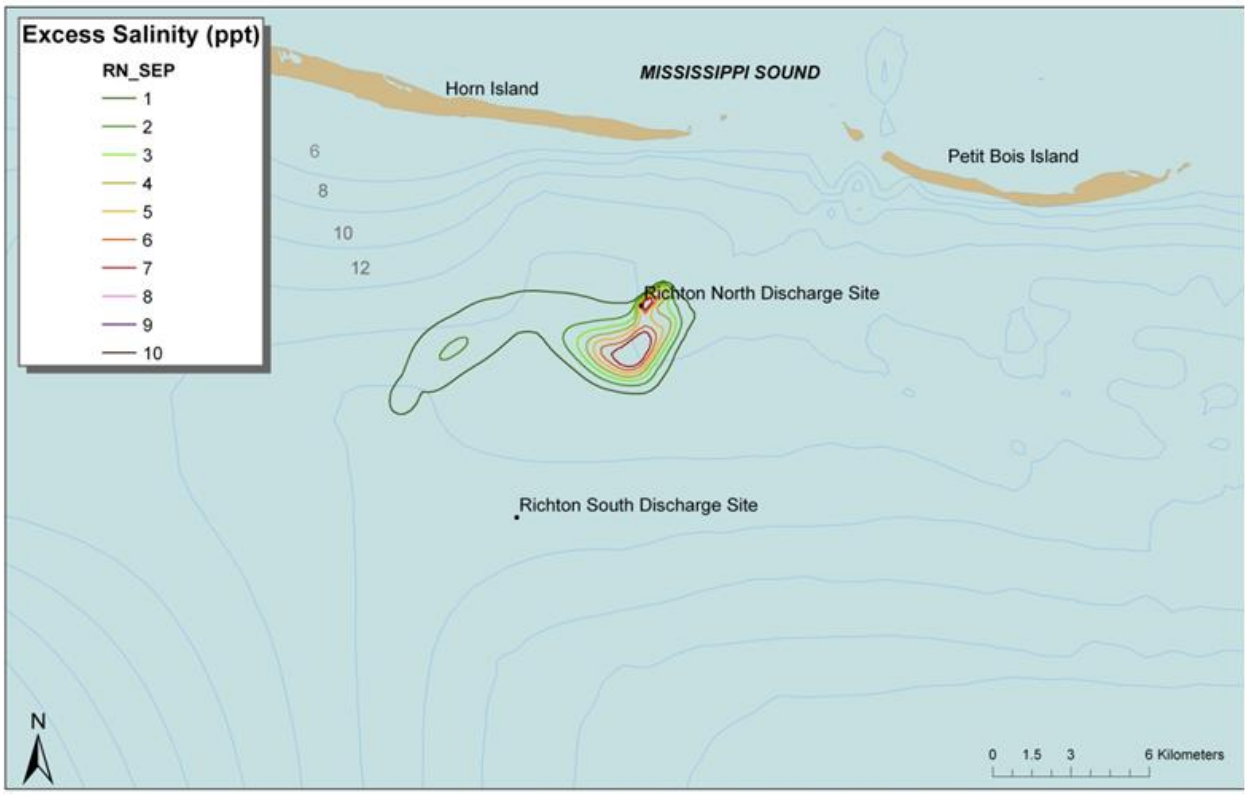

Figure 4.2.2-6. Model-predicted excess salinity of the brine discharge plume from the north discharge site during September 1997. Contours enclose areas of excess salinity.

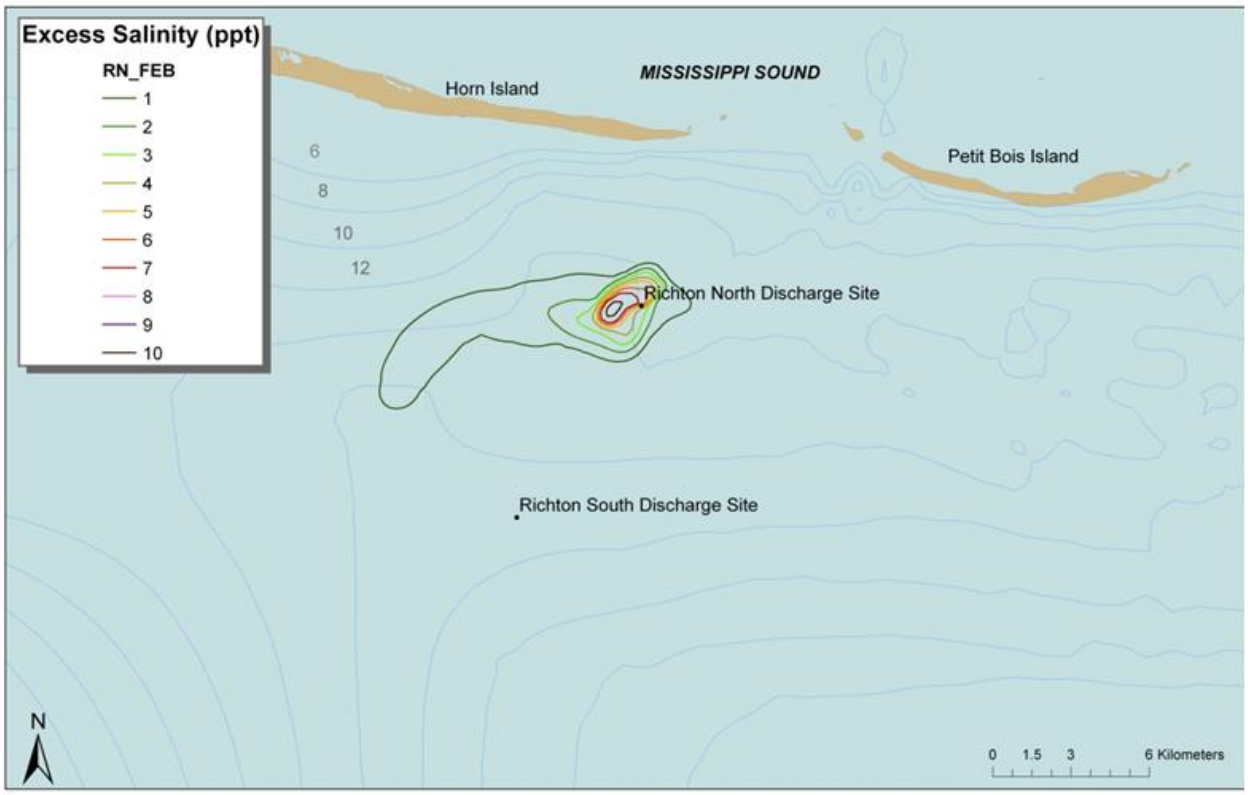

Figure 4.2.2-7. Model-predicted excess salinity of the brine discharge plume from the north discharge site during February 2001. Contours enclose areas of excess salinity.

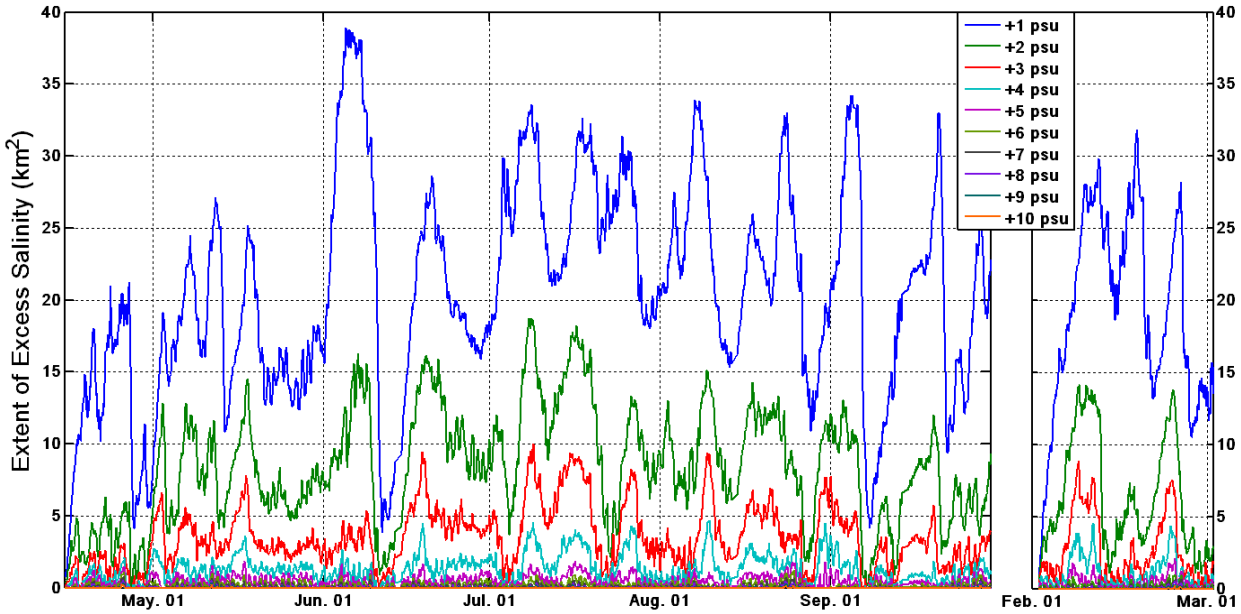

Figure 4.2.2-8. Variability of the area enclosed by contours of excess salinity of 1 to 10 psu from the simulation at the Richton South discharge site. Data from the entire summer and winter periods are shown.

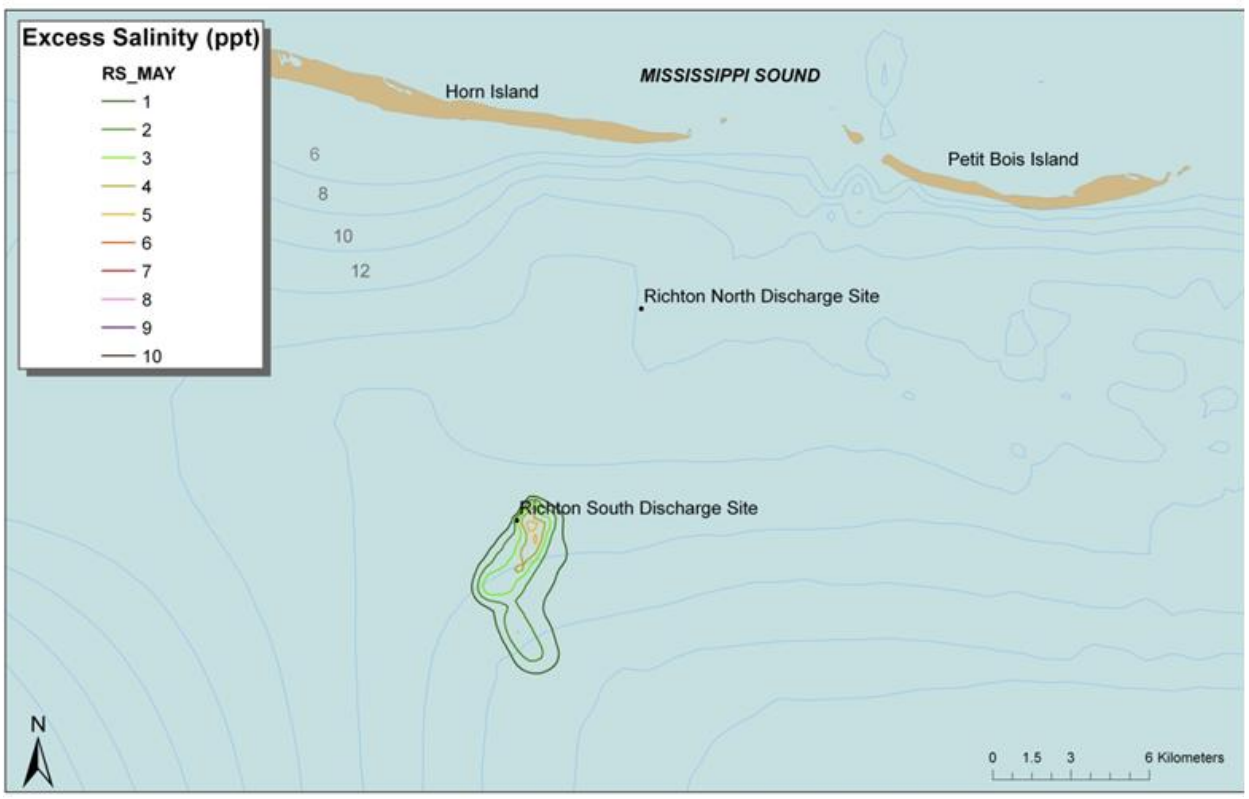

Figure 4.2.2-9. Model-predicted excess salinity of the brine discharge plume from the south discharge site during May 1997. Contours enclose areas of excess salinity.

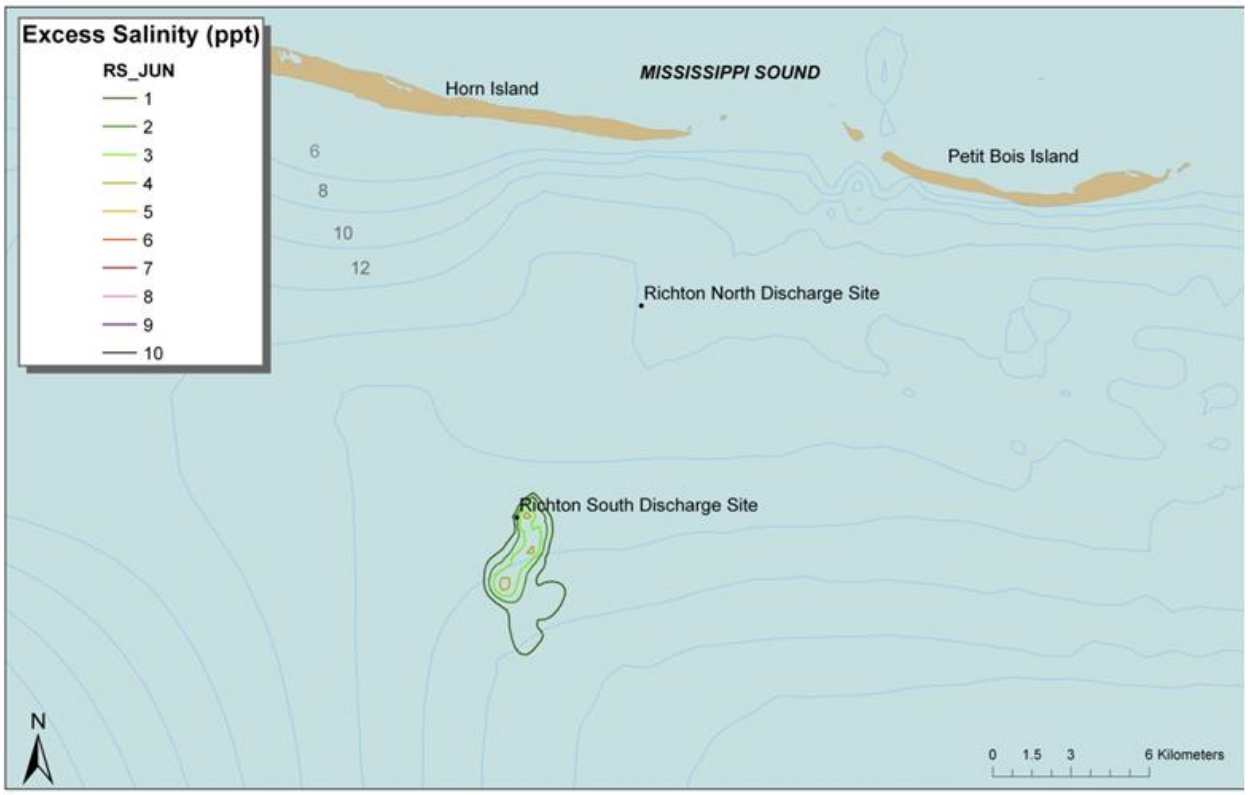

Figure 4.2.2-10. Model-predicted excess salinity of the brine discharge plume from the south discharge site during June 1997. Contours enclose areas of excess salinity.

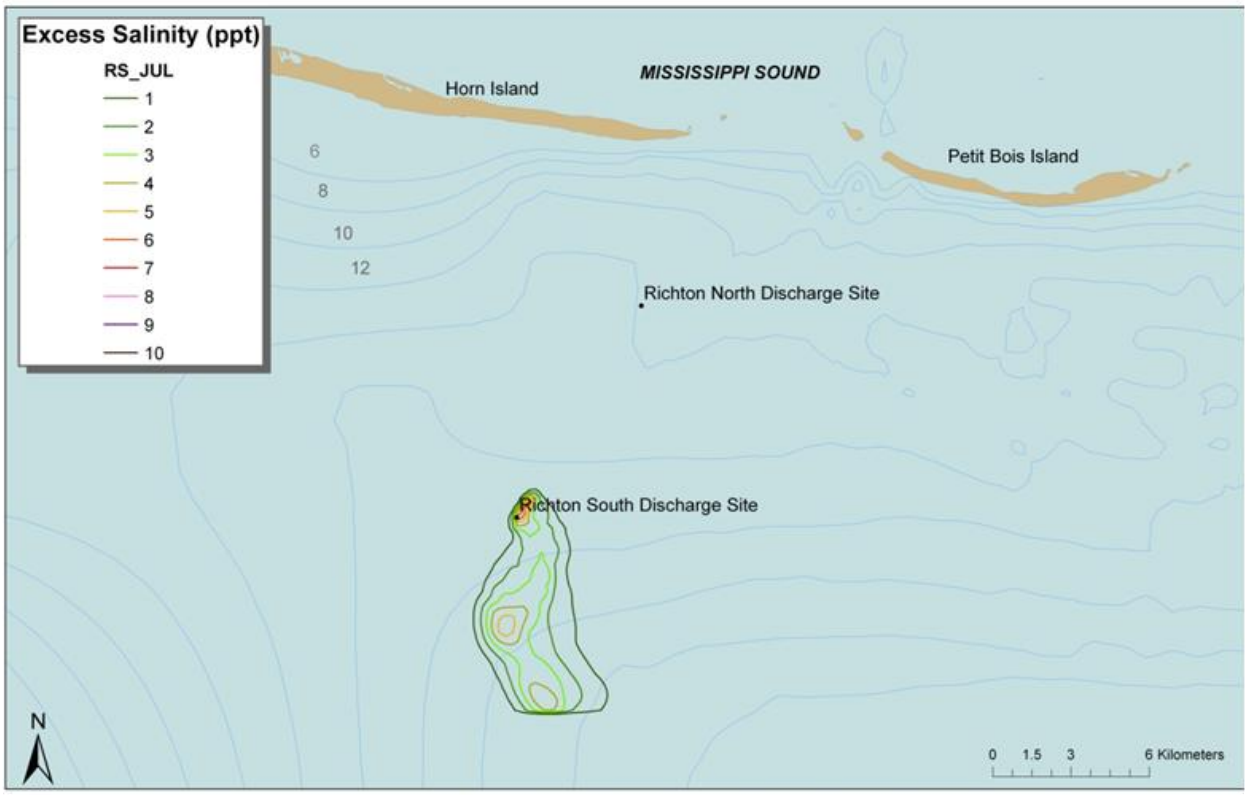

Figure 4.2.2-11. Model-predicted excess salinity of the brine discharge plume from the south discharge site during July 1997. Contours enclose areas of excess salinity.

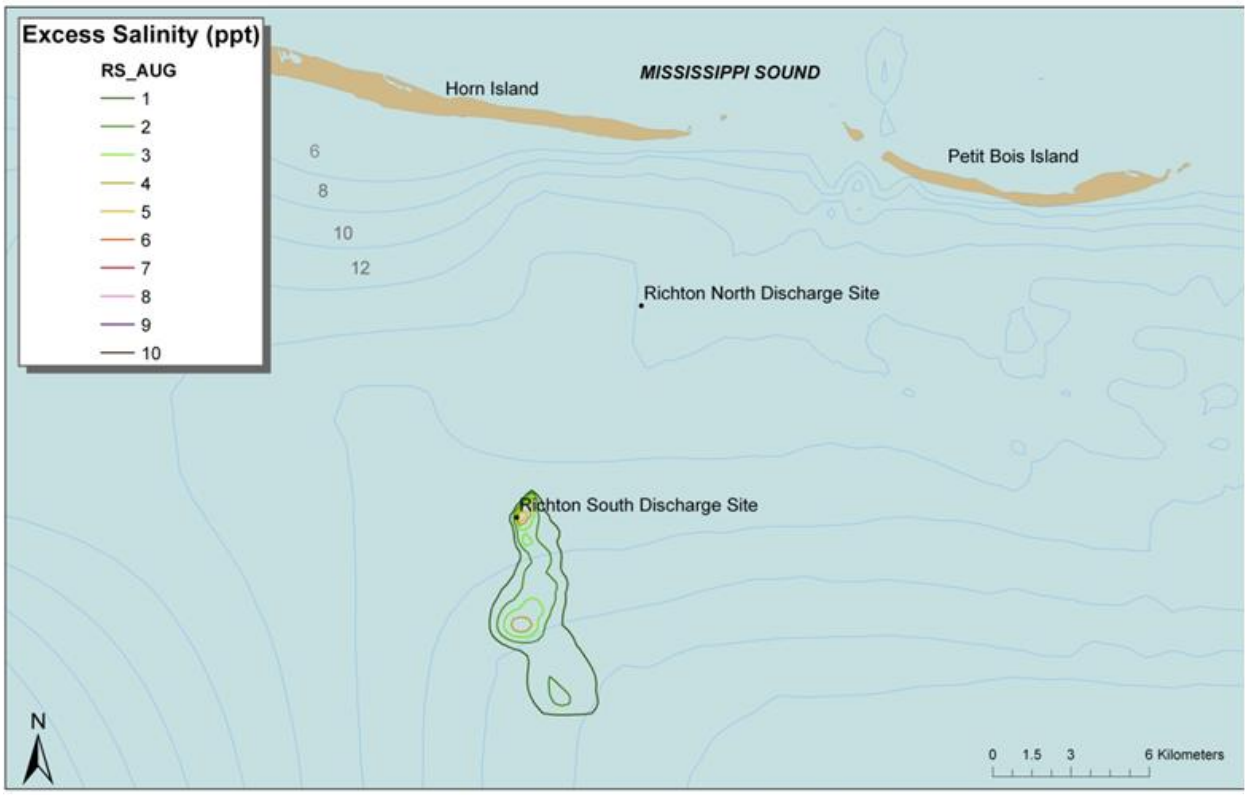

Figure 4.2.2-12. Model-predicted excess salinity of the brine discharge plume from the south discharge site during August 1997. Contours enclose areas of excess salinity.

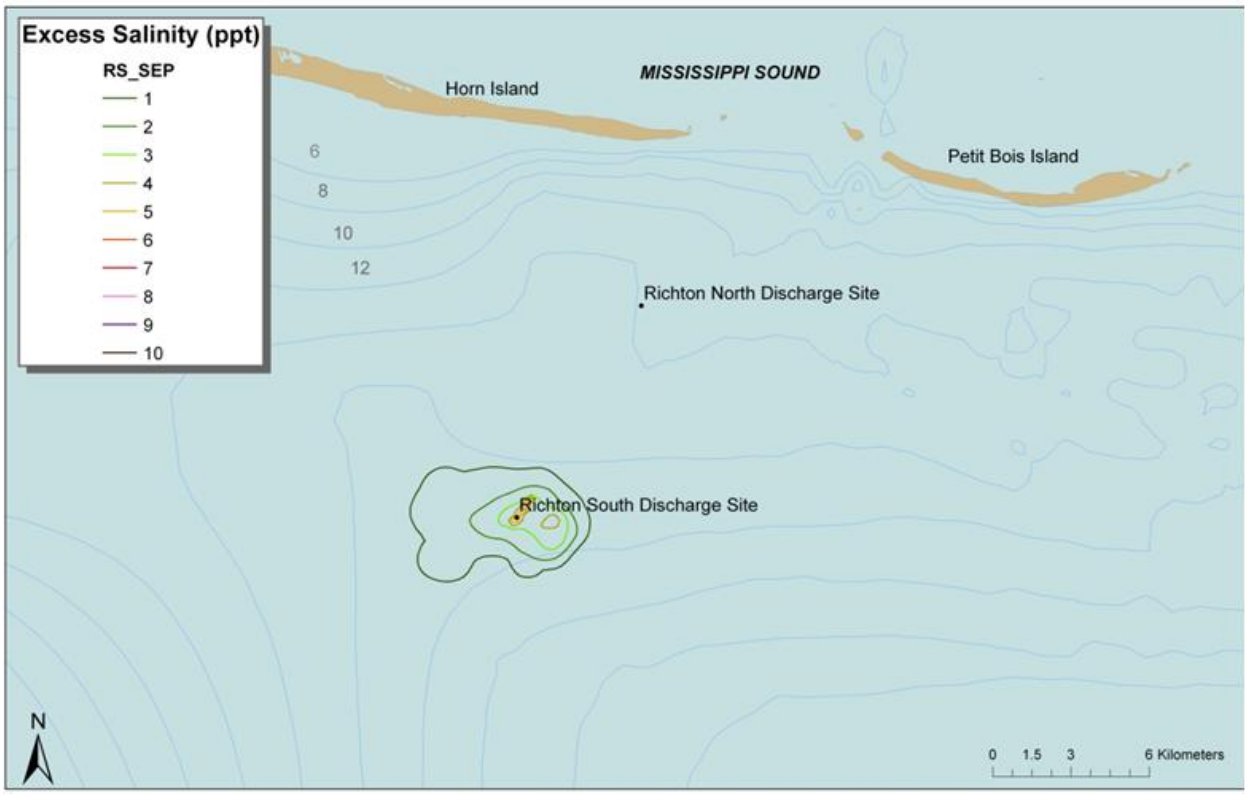

Figure 4.2.2-13. Model-predicted excess salinity of the brine discharge plume from the south discharge site during September 1997. Contours enclose areas of excess salinity.

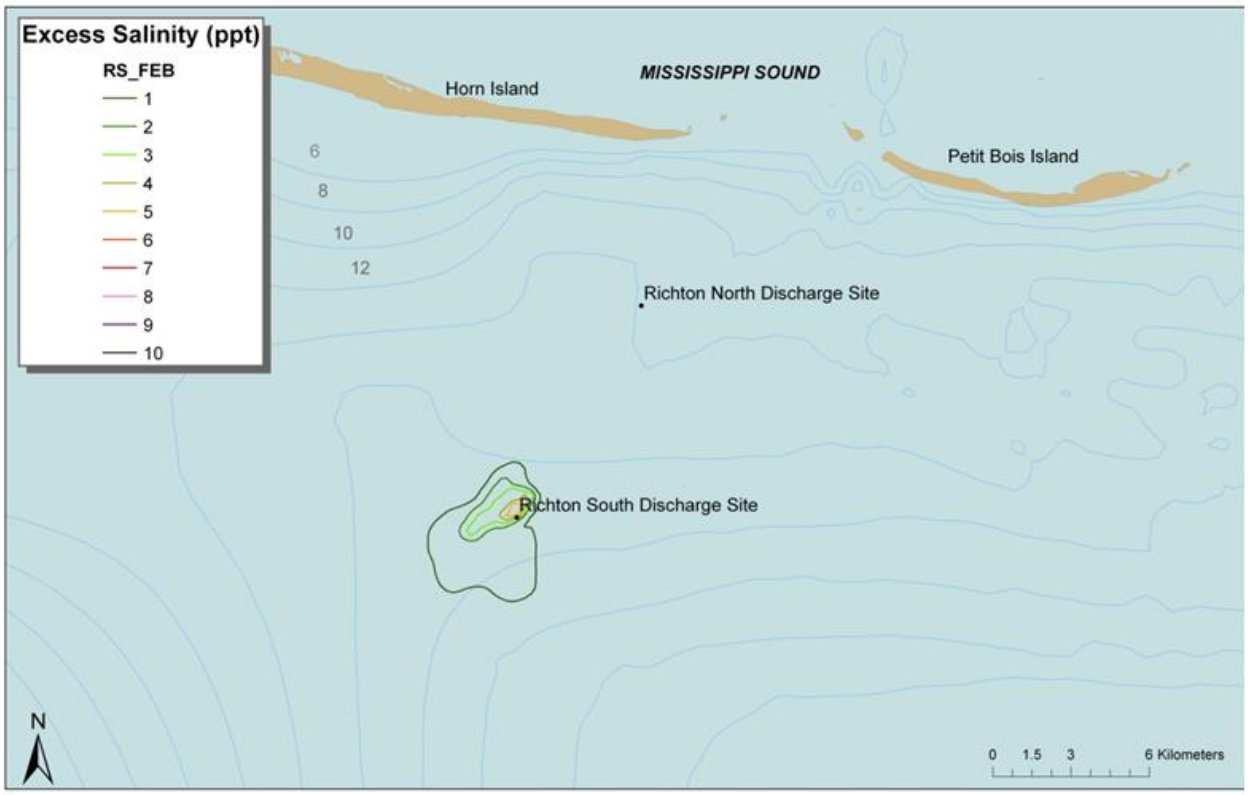

Figure 4.2.2-14. Model-predicted excess salinity of the brine discharge plume from the south discharge site during February 2001. Contours enclose areas of excess salinity.

4.3 Results from Far Field Model Sensitivity Runs

In developing the dense brine plume model, ASA performed a number of sensitivity studies to ensure that the model parameterizations are robust. These studies can help explain the dynamics of the enhanced gravity flow and bound the uncertainty of the model. Model results from the Bryan Mound and Richton sites are presented so that a comparison of the components of the model flow can be easily made. The results from model runs at each location are presented for three conditions: using the full enhanced velocity model, using ambient currents only, and using the gravity-enhanced flow only. By deconstructing the components of the flow in this way, it is more easily seen how each contributes to the solution and to compare their effects at the Bryan Mound and Richton discharge sites.

To further examine the far-field model sensitivity to entrainment, the vertical diffusivity parameterization used in the model is also assessed with model runs using three different constant diffusivity values (0.1, 1, and 10 centimeters squared per second).

4.3.1 Bryan Mound Site

Far-field model simulations were completed at the Bryan Mound site using different flow components. Figure 4.3.1-1 shows the model-predicted excess salinity of the brine discharge from the Bryan Mound site under combined ambient and enhanced flow. Figure 4.3.1-2 shows the model-predicted excess salinity of the brine discharge under ambient flow only, and Figure

4.3.1-3 shows the model-predicted excess salinity of the brine discharge under enhanced flow only.

The impact of the enhanced gravity flow on the plume is apparent. Comparing the combined flow model result (Figure 4.3.1-1) to the ambient-only result (Figure 4.3.1-2), it can be seen that the ambient currents at Bryan Mound are the dominant forcing. With the enhanced-only flow (Figure 4.3.1-3), the plume moves directly down gradient, similar to what happens during periods of low flow at the Bryan Mound site. The comparison here addresses the linear superposition of the two velocity components. At the Bryan Mound site, the strong synoptic (wind-driven) ambient currents appear to overcome the buoyancy forces in the plume.

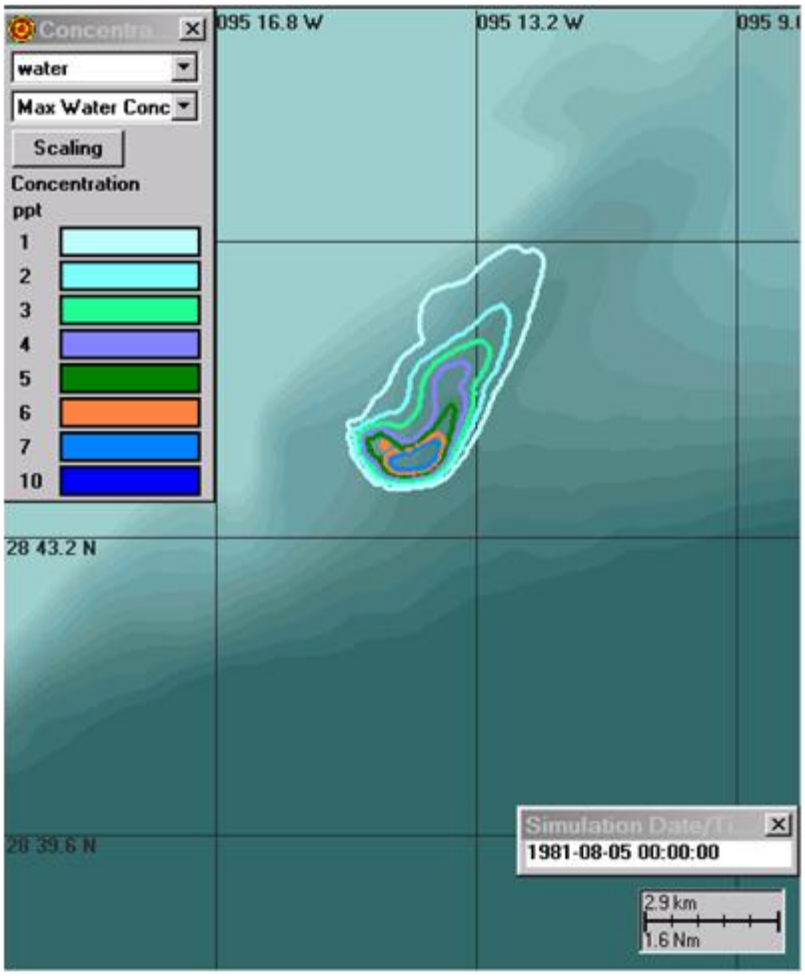

Figure 4.3.1-1. Model-predicted excess salinity of the brine discharge plume from the Bryan Mound discharge site under combined ambient and enhanced-velocity flow. Contours enclose areas of excess salinity at the indicated concentration.

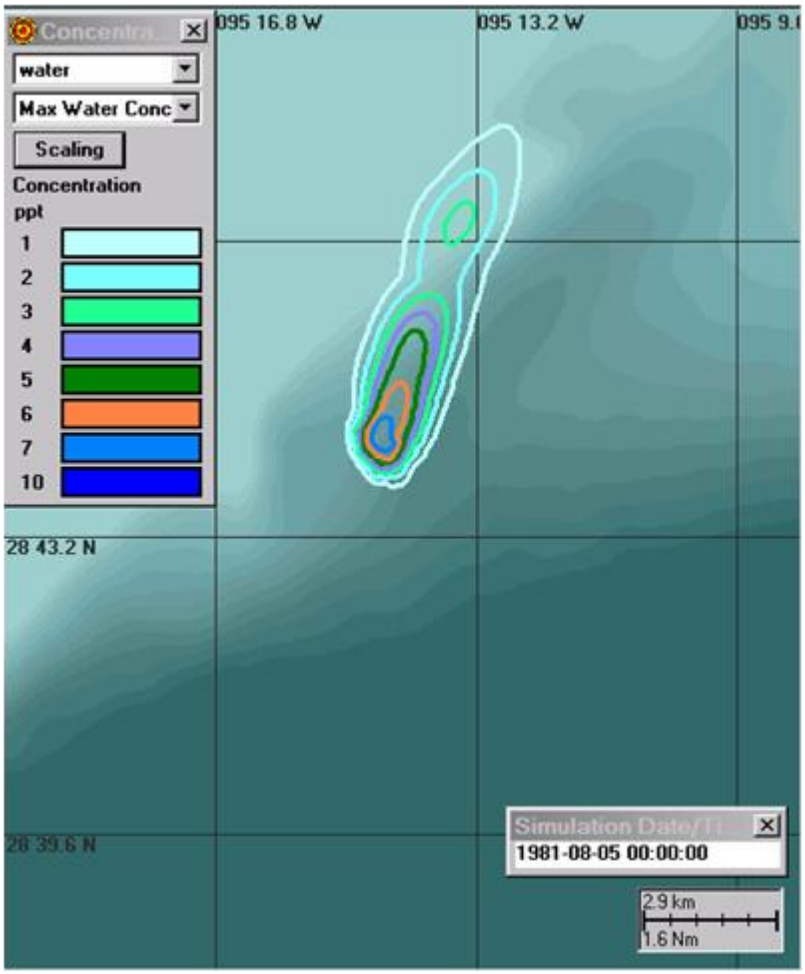

Figure 4.3.1-2. Model-predicted excess salinity of the brine discharge plume from the Bryan Mound discharge site under ambient flow alone. Contours enclose areas of excess salinity at the indicated concentration.

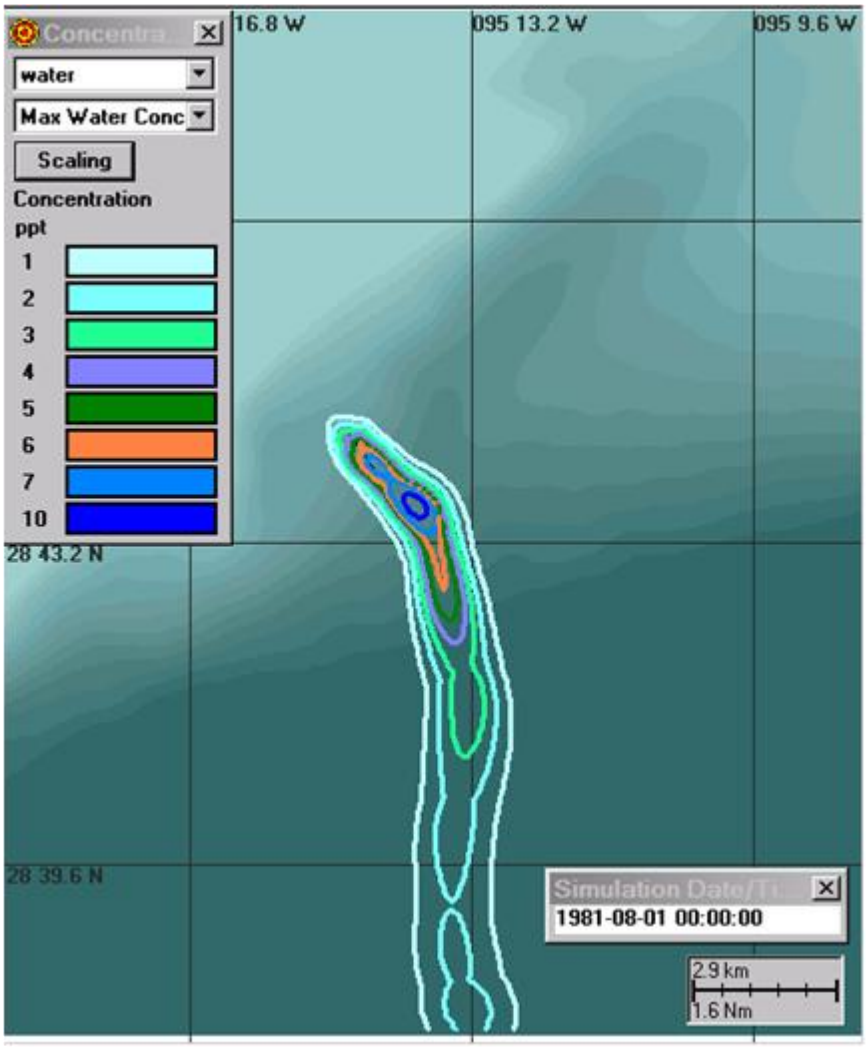

Figure 4.3.1-3. Model-predicted excess salinity of the brine discharge plume from the Bryan Mound discharge site under enhanced velocity alone. Contours enclose areas of excess salinity at the indicated concentration.

Figure 4.3.1-4 shows a model-predicted time series of the area enclosed by contours of 1- and 2-ppt excess salinity from simulations using combined ambient and enhanced flow, ambient flow only, and enhanced flow only. The time series of excess salinity areal extent (Figure 4.3.1-4) shows that the enhanced flow only case provides an upper envelope for the extent of the plume. The ambient currents modulate this maximum through advection and increased diffusivity. During periods when the ambient flow is large, the brine plume is dispersed over a relatively broader area due to advection and vertical diffusion, indicating, in turn, a decrease of the excess salinity in a specific location. Thus, this results in a decrease of the area of excess salinity. When the ambient current speed is low, the plume tends to recover toward the enhanced velocity only result. This demonstrates the dynamic balance between the two influences on the evolution of the plume and the model captures the effect of both the ambient currents and the bottom slope.

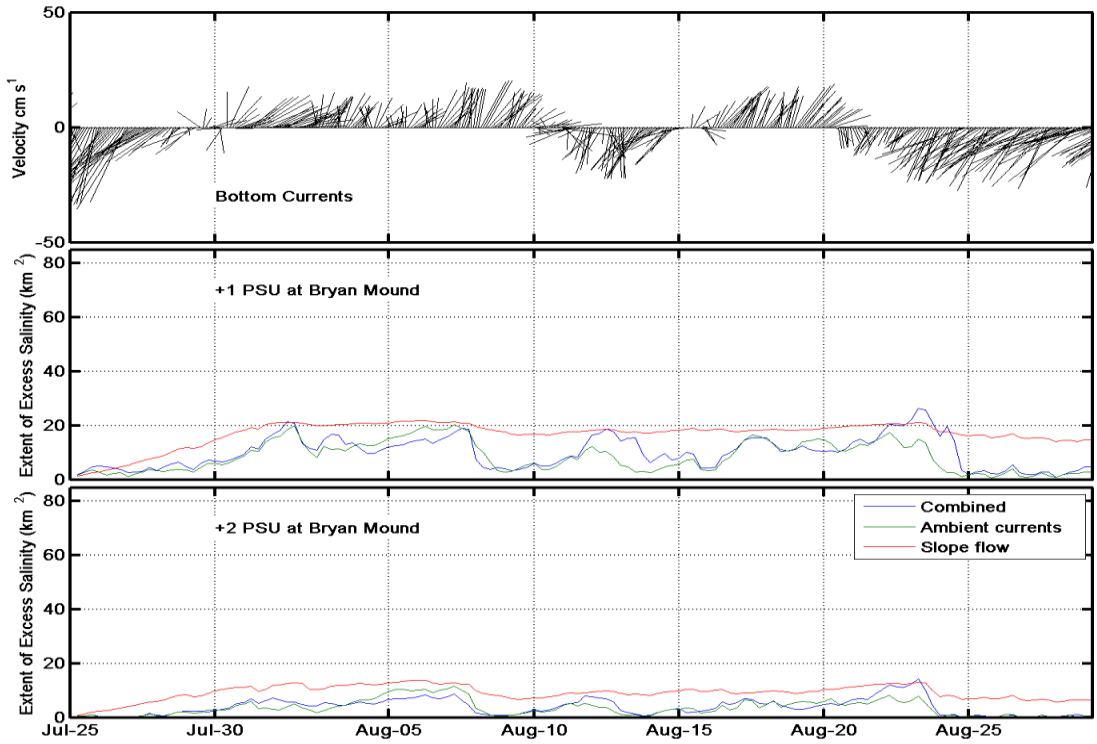

Figure 4.3.1-4. The three panels in this figure show time series from far-field model simulations at the Bryan Mound site. The Top panel is a stick plot of the bottom current speed and direction. The middle panel is the area covered by the 1-ppt excess salinity contour in square kilometers. The lower panel shows the area covered by the 2-ppt excess salinity contour in square kilometers. The middle and bottom panels in the figure compare the area covered by excess salinity for the three flow components as described in the text: enhanced flow only, ambient flow only, and combined ambient and enhanced flow.

4.3.2 Richton Site

Far-field model simulations were also performed at the Richton North and South sites using different flow component combinations. This section presents the results from these simulations. Attachment B presents some additional model results from simulations at the Richton North site using ambient flow without gravity. Figure 4.3.2-1 shows the model-predicted excess salinity of the brine discharge from the Richton North site under combined ambient and enhanced flow. Figure 4.3.2-2 shows the model-predicted excess salinity under ambient flow only, and Figure 4.3.2-3 shows the model-predicted excess salinity under enhanced flow only.

As discussed in Section 3.2.2, Richton is a relatively low energy site with low ambient tidal velocities (i.e., bottom current mostly less than 5 centimeters per second [0.1 knot]) compared to Bryan Mound. The ambient only (Figure 4.3.2-2) and enhanced velocity only results (Figure 4.3.2-3) show very different behavior compared to each other, while the combined model result (Figure 4.3.2-1) clearly has elements of both. The enhanced flow only result shows the down-slope trajectory of the plume and the associated entrainment as the plume dilutes. In the ambient only case, the plume moves east with the current. There is signficant buildup of salinity at the diffuser site, as there is very little mean flow in the ambient currents. With mostly small periodic tidal currents to advect the plume, the salinity concentration around the diffuser tends to build up. When combined with the baroclinic physics of the enhanced velocity flow, there is still

a strong buildup around the diffuser, but the enhanced velocity flow transports the plume away from the diffuser where entrainment and other processes will dilute the plume in deeper water.

Figure 4.3.2-4 shows model-predicted time series of the area enclosed by the 1- and 2-ppt excess salinity contours from simulations at the Richton North site using combined ambient and enhanced flow, ambient flow only, and enhanced flow only. For the first half of the simulation period, the results from the combined flow seem to be correlated well with the gravity-enhanced flow only results, which likely indicates that the dispersion processes are dominated by the gravity-enhanced flow forcing. During the second half of the period, the combined flow case deviates from the gravity-enhanced flow only case and lies somewhere between the ambient only and gravity-enhanced flow only cases, indicating the combined effect of those two forcing mechanisms. The fact that the maximum extent of excess salinity reached approximately 60 square kilometers (23 square miles) for both ambient only and combined flow cases, implies that the brine plume is dispersed to a similar extent under both cases even though it does not happen simultaneously. The gradual increase in areal extent for the ambient flow only case implies this model run does not reach steady state by the end of the simulation.

The time series of excess salinity area and current velocity in Figure 4.3.2-4 helps illustrate the difference between the model results at Bryan Mound and Richton. Comparing the stick plot of currents from Bryan Mound (Figure 4.3.1-4), the ambient flow is clearly dominated by the tidal flow at Richton North site. The magnitude of currents at Richton North are one tenth those observed at Bryan Mound. This results in distinctly different dynamics. The lower velocity at Richton decreases mixing due to diffusion and also reduces the advection of the brine away from the diffuser. The other main difference between the two sites is the influence of the tidal component. While ebb currents may transport the plume to the south, the currents during flood tide will push it to the north again. This dynamic changes dramatically in the combined model because the gravity flow provides a net transport away from the discharge site, while the tidal currents provide increased mixing and entrainment to dilute the plume.

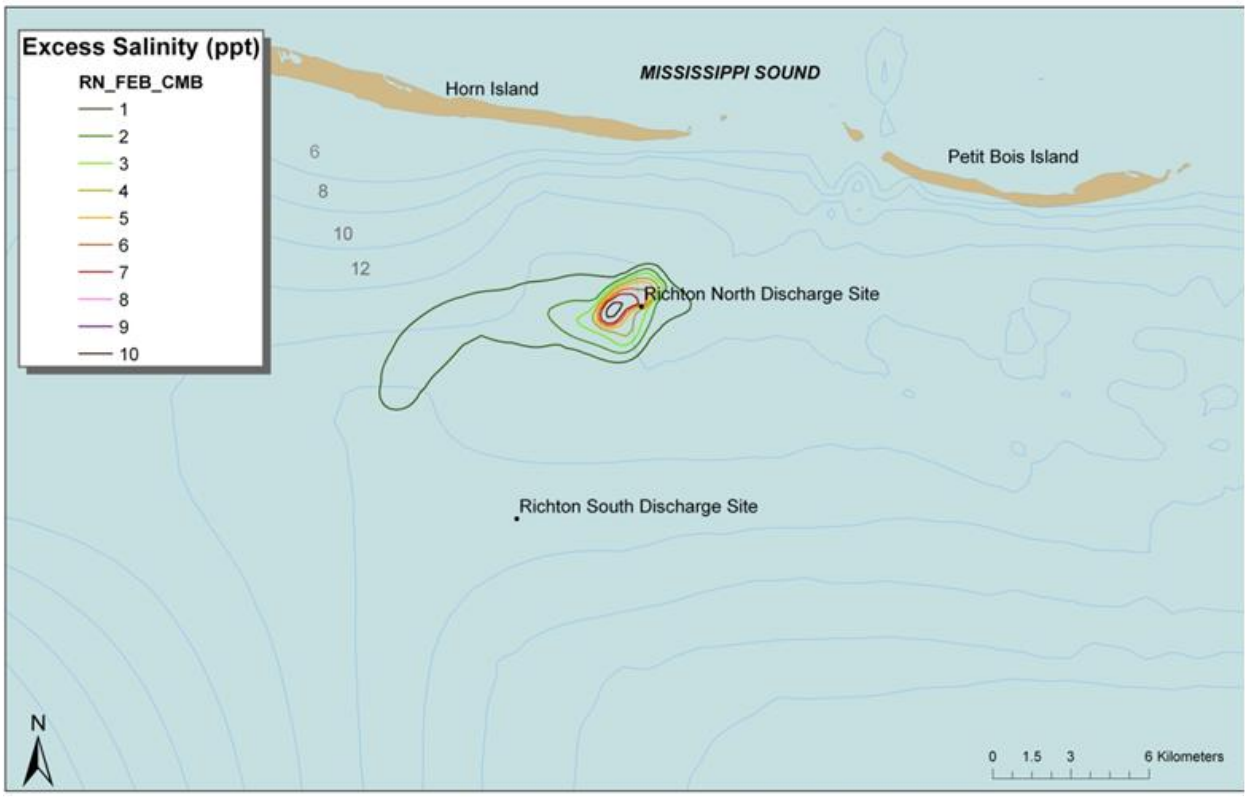

Figure 4.3.2-1. Model-predicted excess salinity of the brine discharge plume from the Richton North discharge site under combined ambient and enhanced velocity flow. Contours enclose areas of excess salinity at the indicated concentration.

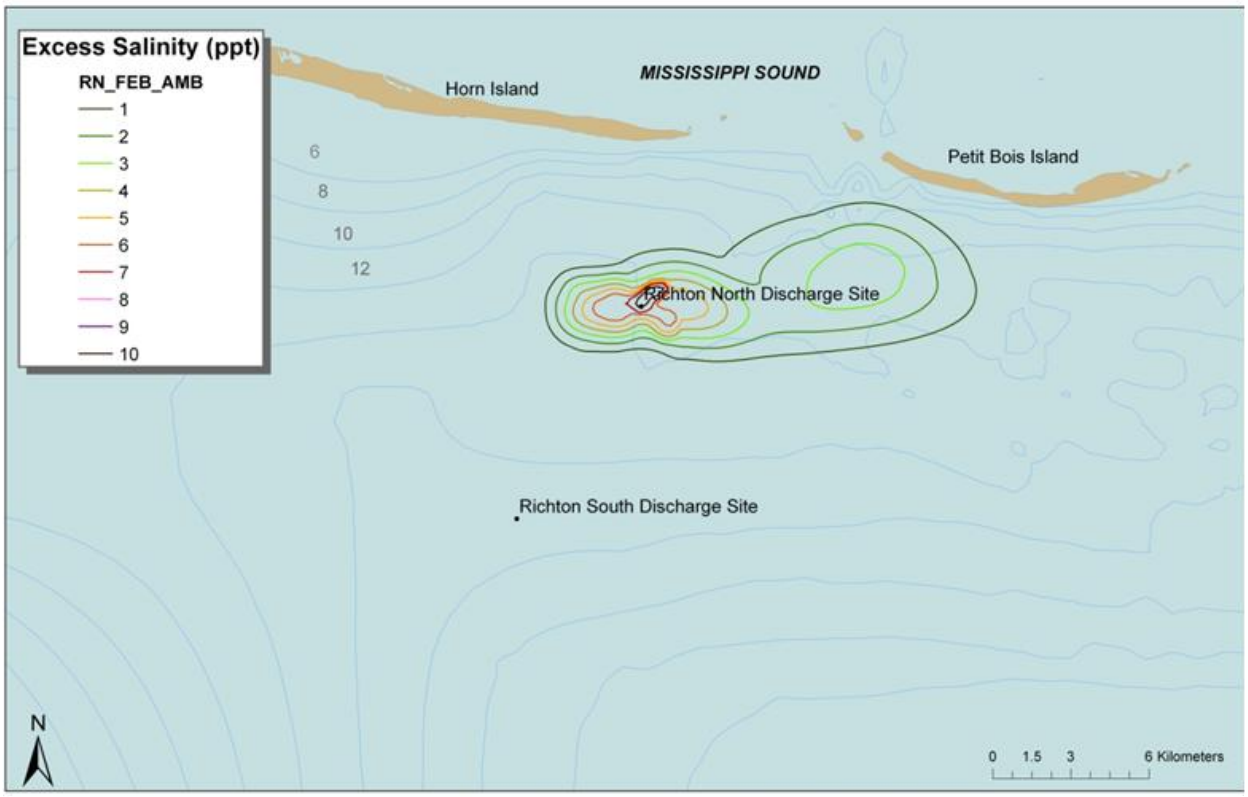

Figure 4.3.2-2. Model-predicted excess salinity of the brine discharge plume from the Richton North discharge site under ambient flow alone. Contours enclose areas of excess salinity at the indicated concentration.

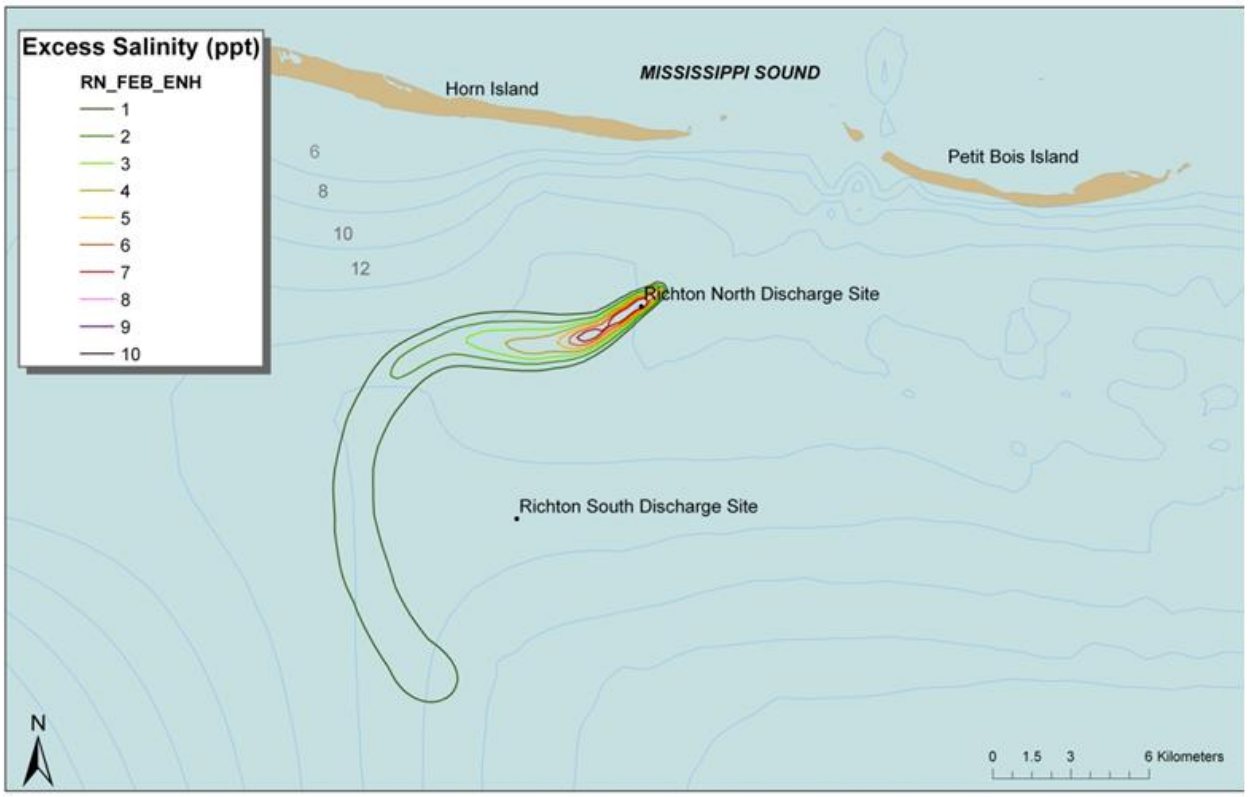

Figure 4.3.2-3. Model-predicted excess salinity of the brine discharge plume from the Richton North discharge site under enhanced velocity flow alone. Contours enclose areas of excess salinity at the indicated concentration.

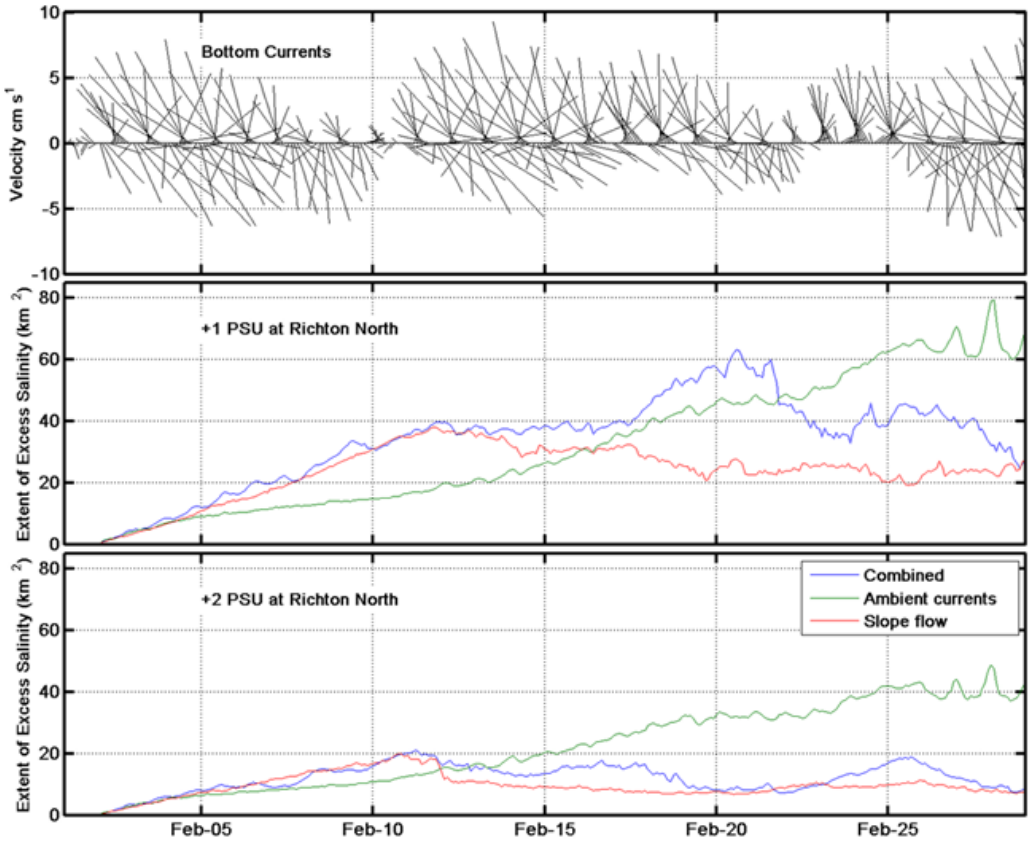

Figure 4.3.2-4. The three panels in this figure show time series from the Richton North model results. The top panel is a stick plot of the currents. The middle panel is the area covered by the 1-ppt excess salinity contour. The lower panel shows the area enclosed by the 2-ppt contour. The model is run with the three parameterizations described above in the contour plots: gravity enhanced flow, ambient flow, and combined.

Figure 4.3.2-5 shows the model-predicted excess salinity of the brine discharge from the Richton South site under combined ambient and enhanced flow. Figure 4.3.2-6 shows the model-predicted excess salinity under ambient flow only, and Figure 4.3.2-7 shows the model-predicted excess salinity under enhanced flow only.

The Richton South site is also a relatively low energy site with low ambient tidal velocities, although with a slightly higher velocity than the Richton North site. The enhanced flow only result (Figure 4.3.2-7) shows the down-slope trajectory of the plume and the associated entrainment as the plume dilutes. The ambient only case shown in Figure 4.3.2-6 indicates the buildup of salinity at the diffuser site, as well as some dispersion toward the east due to the tidal currents at that time. The combined model result (Figure 4.3.2-5) clearly has elements of both. When combined with the gravity forcing, there is still a strong buildup around the diffuser and eastward-directed ambient flow, but the gravity flow transports the plume away from the diffuser resulting in southeast-directed dispersion.

Figure 4.3.2-8 shows a model-predicted time series of the area enclosed by the 1- and 2-ppt excess salinity contours from simulations at the Richton South site using combined ambient and enhanced flow, ambient flow only, and enhanced flow only. For the first half of the simulation period, the brine plume dispersion by the combined flow appears well correlated with the

gravity-enhanced flow only, which likely indicates that the dispersion processes are dominated by the gravity-enhanced flow forcing. During the second half of the period, the combined flow case deviates from the gravity-enhanced flow only case and lies somewhere between the ambient and gravity-enhanced flow only cases, indicating the combined effect of those two forcing mechanisms.

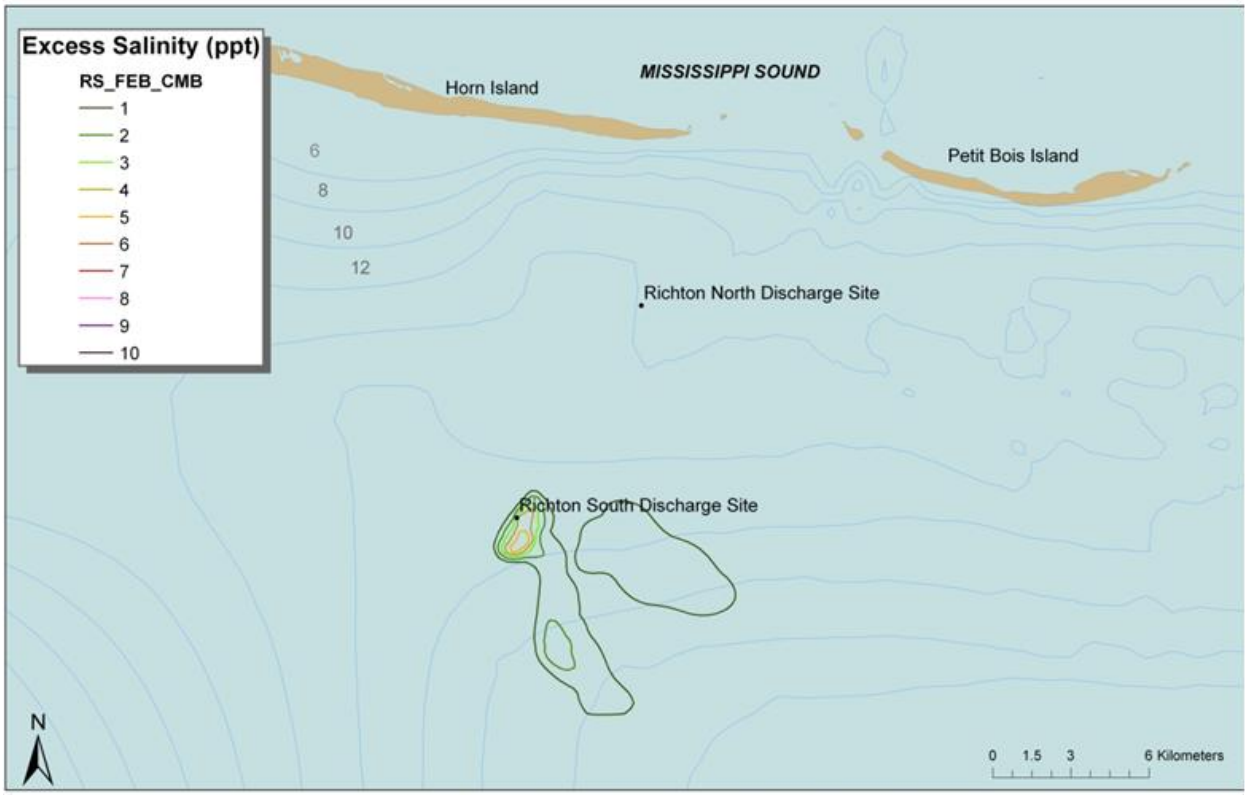

Figure 4.3.2-5. Model-predicted excess salinity of the brine discharge plume from the Richton South discharge site under combined ambient and enhanced velocity flow. Contours enclose areas of excess salinity at the indicated concentration.

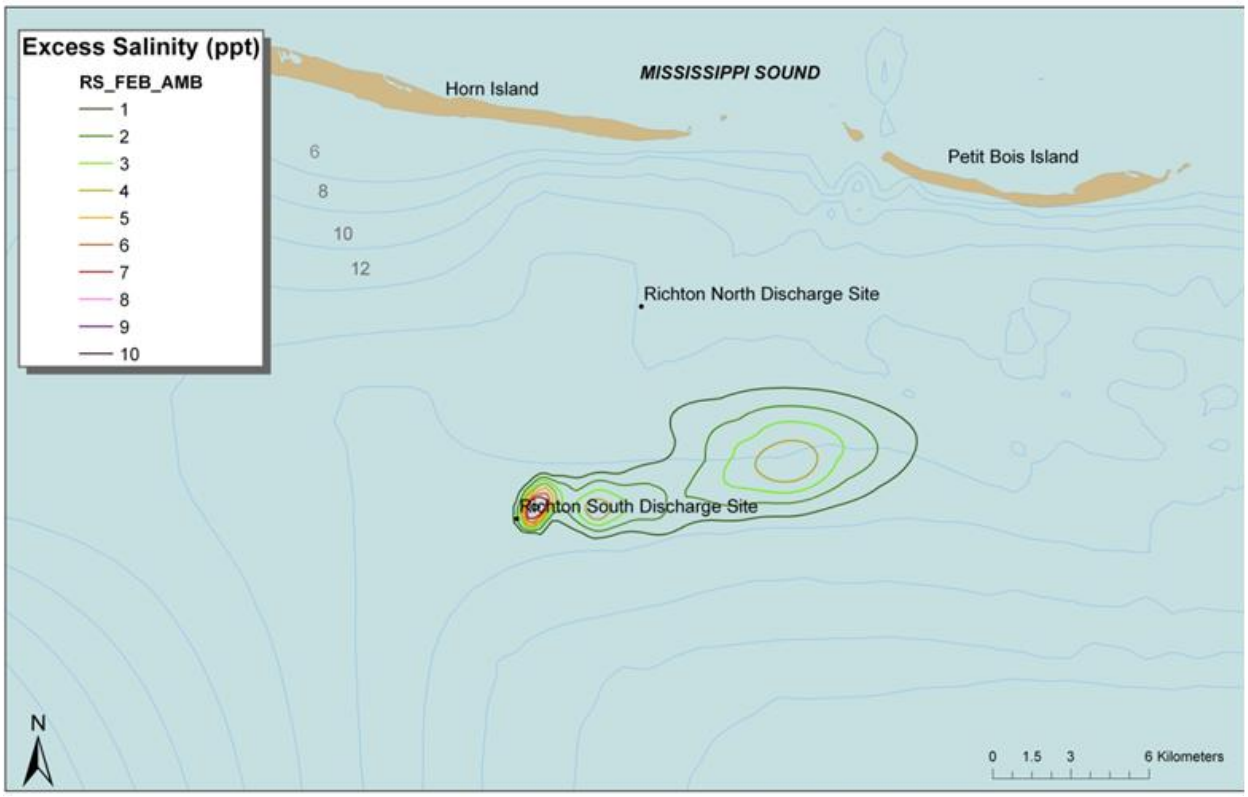

Figure 4.3.2-6. Model-predicted excess salinity of the brine discharge plume from the Richton South discharge site under ambient flow alone. Contours enclose areas of excess salinity at the indicated concentration.

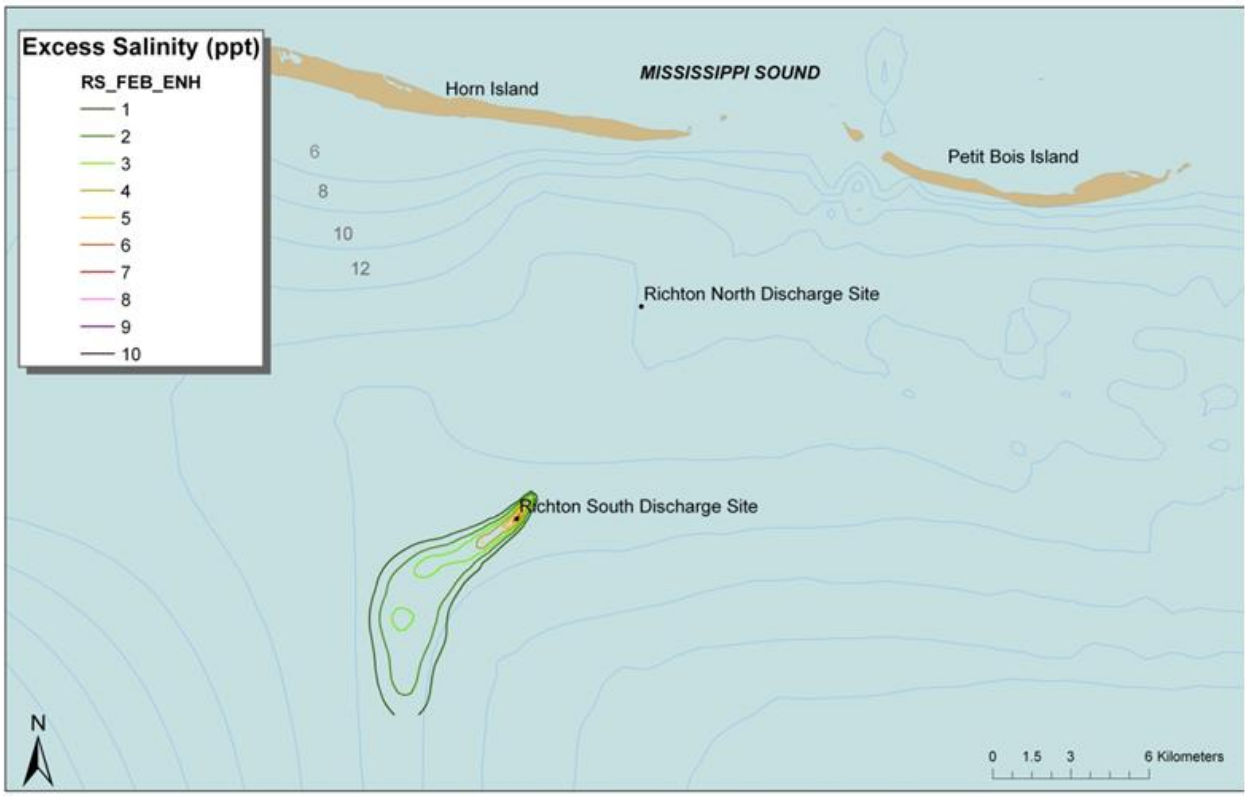

Figure 4.3.2-7. Model-predicted excess salinity of the brine discharge plume from the Richton South discharge site under enhanced velocity flow alone. Contours enclose areas of excess salinity at the indicated concentration.

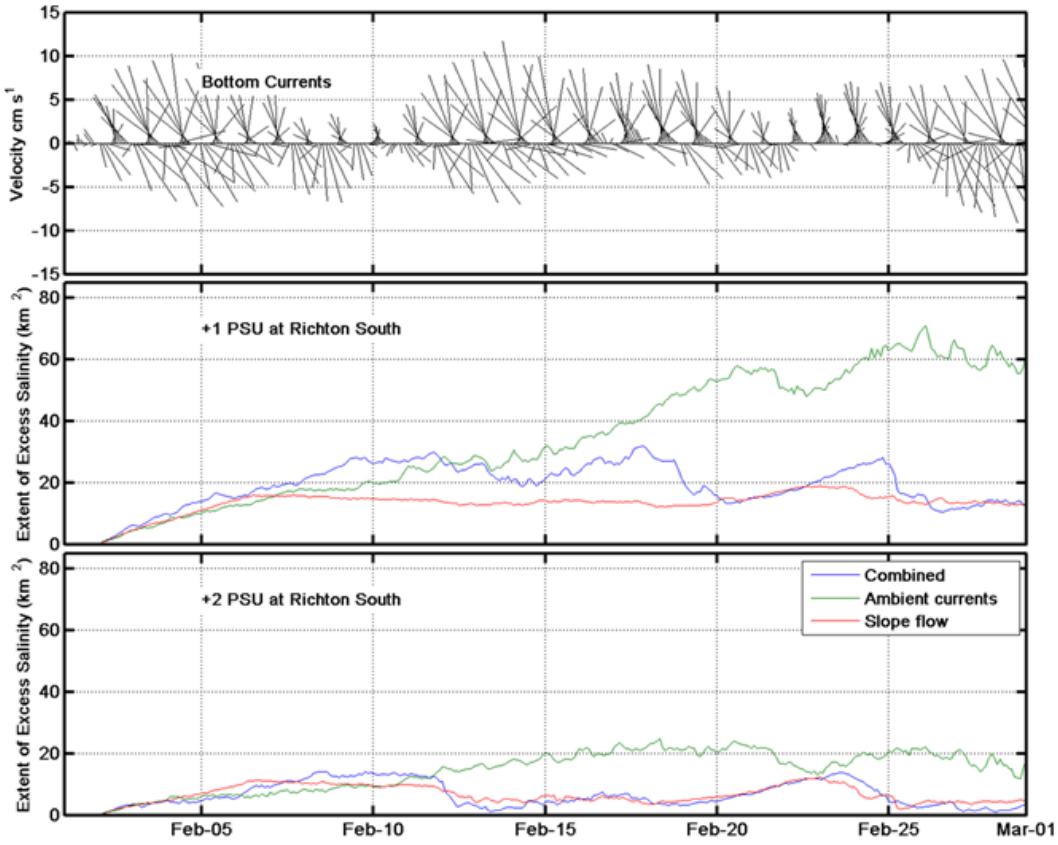

Figure 4.3.2-8. The three panels in this figure show time series from the Richton South model results. The top panel is a stick plot of the currents. The middle panel is the area enclosed by the 1-ppt excess salinity contour. The lower panel shows the area enclosed by the 2-ppt excess salinity contour. The model is run with the three parameterizations described above in the contour plots: gravity enhanced flow, ambient flow, and combined.

Diffusitivity

The vertical diffusivity is a critical parameter controlling model results. The ambient currents cause mixing of the plume with ambient waters through the vertical diffusivity. To examine the sensitivity of the model to this parameter, the winter period Richton North site was run several times, changing only the vertical diffusivity parameterization. Figure 4.3.2-9 shows a stick plot of bottom current speed and direction and a model-predicted time series of the area enclosed by the 1- and 2-ppt excess salinity contours from simulations using three fixed vertical diffusivity values and a Richardson formulation.

The results show that the Richardson number formulation for vertical diffusivity is approximately equivalent to a constant diffusivity of 0.1 centimeter per second (0.002 knot). Based on the entrainment velocity scaling described in Section 2.3.4, this is equivalent to a 0.0005-centimeter per second entrainment rate given a thickness of roughly 200 centimeters. This vertical diffusivity of the plume is low for the coastal ocean and estuaries where values can be as much as 2 orders of magnitude greater. The plume, however, is not a passive tracer because the density of the plume will impede vertical mixing with ambient ocean water, reducing the vertical diffusivity. This finding is well supported in the literature, given the Richardson number of the

plume is roughly 6. From their laboratory studies, Ellison and Turner (1959) set the entrainment rate to zero for a Richadson number greater than 0.8.

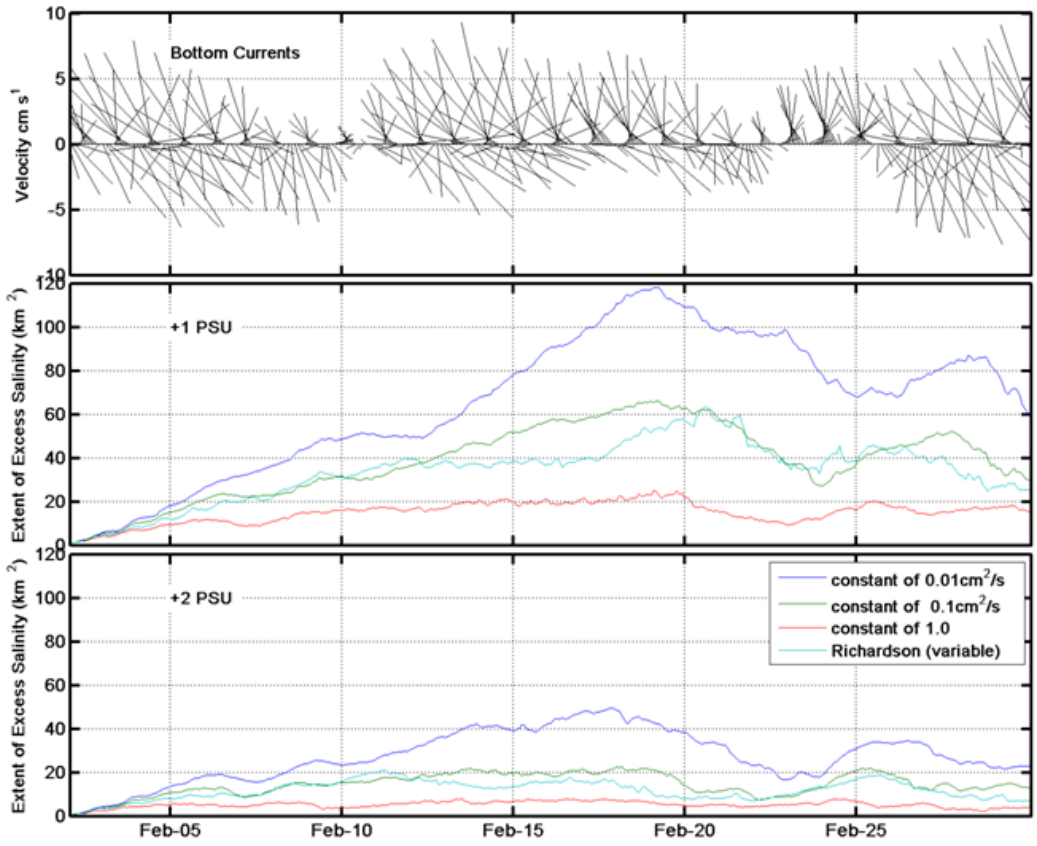

Figure 4.3.2-9. The three panels in this figure present the results of the sensitivity analysis to the vertical diffusion (entrainment) parameterization used in the Lagrangian model. The top panel shows the time series of currents at the diffuser. The middle panel shows the time series of the excess salinity area (1-ppt contour) using each of the four parameterizations. The bottom panel shows the same results for the 2-ppt contour.

To visually examine how the vertical diffusivity parameterizes the entrainment of ambient water in the plume, Figure 4.3.2-10 shows a cross-section plot of contours of salinity and the distribution of Lagrangian particles in the water column. As the plume flows down slope, the contours of constant salinity get thinner because the plume entrains water, thus diluting the salinity. The distribution of particles, on the other hand, becomes thicker as they diffuse vertically, representing the entrainment of ambient water. The thickness of the plume is calculated by the distribution of particles in the vertical, not by the contours of constant salinity. This is dynamically consistent with the enhanced velocity calculation described in Attachment A.

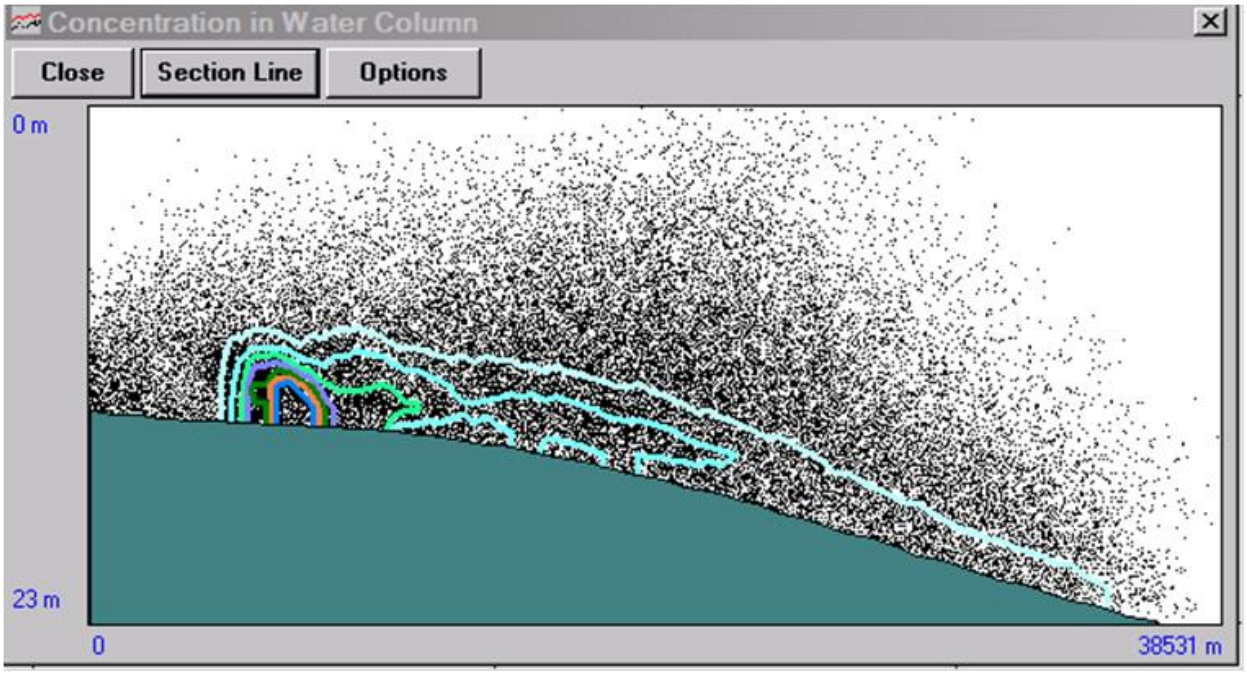

Figure 4.3.2-10. Vertical section of the plume contours with the Lagrangian particle distribution superimposed. The section view shows the thickening of the brine plume as it moves away from the discharge (from left to right).

The sensitivity analysis presented here provides insight into the validation of the plume model at Bryan Mound. By examining the effects of the model components (ambient flow, gravity flow, and diffusivity) separately, the difference between the conditions (water depth and ambient currents) at Bryan Mound and Richton can be sorted out from the model dynamics. The model results at Bryan Mound are different because the flow field is very different. The Lagrangian plume model is a balance of multiple factors in the evolution of the brine plume. Although the dominant factors are different at Richton, the model shows good agreement with the data at Bryan mound, especially in light of the strong variability at the site. While the sensitivity studies do not provide an independent validation of the modeling approach they do demonstrate that the results are robust to the parameters of the model. This is consistent with the scaling analysis, which shows that the baroclinic flow is a first-order term in transporting the plume.

5.0 Conclusions

Measurements of excess salinity at the active Bryan Mound brine discharge site off the coast of Freeport, Texas during the 1980s provide horizontal and vertical dimensions of a brine discharge plume that are useful for comparison with far-field model results. Measurements of the vertical distribution of the brine plume collected directly over the diffuser and at points surrounding the diffuser indicate that the excess salinity from the discharge extended to a maximum of 5.4 meters (17.7 feet) above the seafloor. The maximum excess salinity measured during the entire 1980–1981 monitoring period was 6.9 ppt, even though the maximum discharge salinity was 263 ppt. The relatively low excess salinity maxima measured at Bryan Mound indicate that the brine diluted rapidly at a short distance from the diffuser and/or that the vertical measurements never sampled the highest salinity portion of the discharge. Either way, the measurements indicate that excess salinities above 7 ppt exist within a small volume of water directly surrounding the diffuser.

The UM3 near-field brine plume model was run using a range of current speeds to simulate the near-field dynamics of the discharge plume at the Bryan Mound and Richton North and South discharge sites. Results of near-field modeling show that the discharge plume centerline rises a few meters (a few yards) in the water column and then descends, making contact with the bottom within a few meters (a few yards) from the diffuser. UM3 predicts a rapid dilution (reduction of excess salinity) of approximately 85 percent within a few meters of the diffuser. The near-field model results suggest that salinity measurements taken at the Bryan Mound site were not of sufficient resolution to measure salinity in the brine jet.

ASA has developed a modified Lagrangian model of the far-field evolution of a dense plume of brine on the coastal shelf. There is good agreement between far-field brine plume model results and observation data from Bryan Mound. In a continuous, 45-day model run, the area enclosed by the far-field model-predicted 2-ppt excess salinity contour compares well with the 2-ppt excess salinity contours defined from monitoring data collected on two separate dates in August 1981. The major axis of the 2-ppt excess salinity areas also compare well between the model prediction and the monitoring data at Bryan Mound.

The far-field brine plume model was run to simulate the movement of the brine plume away from the proposed Richton North and South discharge sites under summer and winter current velocity conditions generated from a previously applied hydrodynamic model of the area. The far-field model predicts that the extent of the 2-psu contours is typically 1 to 1.2 kilometers (0.6 to 0.74 mile) wide and between 5.4 and 28 kilometers (3.4 and 17.4 miles) long. The major direction of plume dispersion is toward the south or southwest for most of the simulation period. Discharge plume vertical thickness at the Richton North site averages 5 meters (16 feet) with a maximum of 10 meters (33 feet).

The far-field model predicts that the brine discharge plume at the Richton South discharge site defined by the 1-psu contour is predicted to be smaller compared to that of the Richton North site, typically 2 to 3 kilometers wide and between 5 and 10 kilometers long. The major direction of plume dispersion is also toward the south for the period when the shape of the contour is elongate. Discharge plume vertical thickness at the Richton South site averages 5 meters (16 feet) and has a maximum of 10 meters (33 feet), again similar to the north site.

6.0 References

Baumgartner, D., W. Frick, and P. Roberts. 1994. Dilution Models for Effluent Discharges (3rd Ed). EPA/600/R-94/086, U.S. Environmental Protection Agency, Pacific Ecosystems Branch, Newport, Oregon.

Bunch, B.W., M. Channell, W.D. Corson, B.A. Ebersole, L. Lin, D.J. Mark, J.P. McKinney, S.A. Pranger, P. R. Schroeder, S. J. Smith, D. H. Tillman, B. H. Tracy, M. W. Tubman, and T. L. Welp. 2003. *Evaluation of island and nearshore confined disposal facility alternatives, Pascagoula River Harbor dredged material management plan*. ERDC TR-03-3. Vicksburg, MS: U.S. Army Engineer Research and Development Center.

Bunch, B.W., R.S. Chapman, B.A. Ebersole, P.V. Luong, D.J. Mark, J.P. McKinney, D.H. Tillman, and D.W. Webb. 2005. *Evaluation of proposed improvements to the Gulfport Harbor, Mississippi, Navigation Channel*. Draft technical report for the U.S. Army Engineer District, Mobile by the U.S. Army Engineer Research and Development Center, Vicksburg, MS.

Burns, K.A., S. Codi, M. Furnas, D. Heggie, D. Holdway, B. King, and F. Mcallister. 1999. Dispersion and fate of produced formation water constituents in an Australian northwest shelf shallow water ecosystem. Marine Pollution Bulletin, Volume 38, No. 7. pp 593-603.

Cenedese, C., Whitehead, J.A., Ascarelli, T.A., and Ohiwa, M. 2004. A dense current flowing down a sloping bottom in a rotating fluid. Journal of Physical Oceanography, 34, pages 188-203.

Cenedese, C., May 1, 2009. Personal communication by phone and email regarding an upcoming publication in the Journal of Physical Oceanography.

Chapman, R.S., B.H. Johnson, and S.R. Vemulakonda. 1996. Users guide for the sigma stretched version of CH3D-WES; A three-dimensional numerical hydrodynamic, salinity and temperature model. Technical Report HL-96-21. Vicksburg, MS: U.S. Army Engineer Waterways Experiment Station.

DOE. 2006. Site Selection for the Expansion of the Strategic Petroleum Reserve - Final Environmental Impact Statement. U.S. Department of Energy Office of Petroleum Reserves (FE-47) Washington, DC. Document No. DOE/EIS-0385

Dortch, M.S., Zakikhani, M., Noel, M.R., and Kim, S-C. 2007. Application of a Water Quality Model to Mississippi Sound to Evaluate Impacts of Freshwater Diversions. U.S. Army Engineer Research and Development Center, Environmental Laboratory, Vicksburg, MS, 39180-6199. ERDC/EL TR-07-20.

Ellison, T.H., and Turner, J.S. 1959. Turbulent entrainment in stratified flows. Journal of Fluid Mechanics, Vol. 6, pages 423–448.

French McCay, D.P., 2004a. Oil spill impact modeling: development and validation. Environmental Toxicology and Chemistry 23(10): 2441-2456.

French McCay, D.P., 2003. Development and Application of Damage Assessment Modeling: Example Assessment for the North Cape Oil Spill. Marine Pollution Bulletin, Volume 47, Issues 9-12, September-December 2003, pp. 341-359.

French McCay, D.P. and Isaji, T., 2004b. Evaluation of the consequences of chemical spills using modeling: chemicals used in deepwater oil and gas operations. Environmental Modelling & Software 19(7-8):629-644.

French McCay, D., N. Whittier, M. Ward, and C. Santos, 2006. Spill hazard evaluation for chemicals shipped in bulk using modeling. Environmental Modelling & Software 21(2): 158-171.

Frick, W.E., 2003. Visual Plumes Mixing Zone Modeling Software. Ecosystems Research Division, NERL, ORD, U.S. EPA, 960 College Station Rd, Athens, GA, 30605.

Frick, W. E., P. J. W. Roberts, L. R. Davis, J. Keyes, D. J. Baumgartner, and K. P. George (2003) Dilution models of effluent discharges (4th edition) EPA/600/R-03/025, U. S. Environmental Protection Agency, Ecosystems Research Division, NERL, ORD, Athens, GA.

Garratt, J.R., 1977, Review of drag coefficients over oceans and continents, *Monthly Weather Review*, 105, 915-929.

Hann, R.W. and Randall, R.E., 1982. Evaluation of Brine Disposal from the Bryan Mound Site of the Strategic Petroleum Reserve Program, Final Report of Predisposal Studies to Department of Energy, Strategic Petroleum Reserve Office, Edited by R.W. Hann, Jr. and R.E. Randall, Civil Engineering Dept., Texas A&M University, Volumes 1 and 2, March 1982.

Isaji, T., M. Spaulding, and D. Redford, 1996, Numerical model of sewage sludge transport and deposition from the 106-mile municipal dumpsite, Journal of Marine Environmental Engineering, Vol. 2, p. 141-180.

Johnson, D.R., 2008. Ocean Surface Current Climatology in the Northern Gulf of Mexico. Published by the Gulf Coast Research Laboratory, Ocean Springs, Mississippi, May, 2008.

Munk, W. H., and Anderson, E. R., 1948, Notes on a Theory of the Thermocline, Journal of Marine Research, V7, pp.276- 295.

Özgökmen, T.M., and E.P. Chassignet, 2002: Dynamics of two-dimensional turbulent bottom gravity currents. Journal of Physical Oceanography, 32/5, 1460-1478.

Parker, G., Y. Fukushima, and H. M. Pantin, 1986, Self accelerating turbidity currents. Journal of Fluid Mechanics, 171, 45-181

Randall, R.E., 1982. Tracking of Salinity Plumes Generated by Brine Discharges into the Northwestern Gulf of Mexico. Oceans, Volume 14, pp.1110-1115, September 1982.

Scully, M. E., Friedrichs, C.T., Wright, L. D., 2003. Numerical modeling of gravity-driven sediment transport and deposition on an energetic continental shelf: Eel River, northern California. Journal of Geophyscial Research, Volume 108. pp.17,1-17,14.

Sheng, Y. P. (1986). "A three-dimensional mathematical model of coastal, estuarine and lake currents using boundary fitted grid," Report No. 585, A.R.A.P Group of Titan Systems, Princeton, NJ.

Spaulding, M.L., E.L. Anderson, T. Isaji and E. Howlett, 1993. Simulation of the oil trajectory and fate in the Arabian Gulf from the Mina Al Ahmadi Spill, Marine Environmental Research, Vol. 36, No. 2, p. 79-115.

Spaulding, M.L., V.S. Kolluru, E. Anderson, and E. Howlett, 1994. Application of Three-Dimensional Oil Spill Model (WOSM/OILMAP) to Hindcast the BRAER Spill, Spill Science & Technology Bulletin, Vol. 1, No. 1, September 1994, p. 23-36.

Turner, J.S. 1986 Turbulent entrainment: The development of the entrainment assumption and its application to geophysical flows. Journal of Fluid Mechanics, vol. 170, pages 431-471.

Wright, L.D., 1985. River Deltas. In: Davis, R.A. (Ed), Coastal Sedimentary Environments. Springer, New York, pages 1-76.

Wright, L.D., Friedrichs, C.T., Kim, S.C., and M.E. Scully. Effects of Ambient Currents and Waves on Gravity-Driven Sediment Transport on Continental Shelves. Marine Geology, Volume 175, pages 25-45.